An Internet of Things (IoT) based wide-area Wireless Sensor Network (WSN) platform with mobility support.

A Thesis Submitted to the
College of Graduate and Postdoctoral Studies
In Partial Fulfillment of the Requirements
For the Degree of Doctor of Philosophy
In the Department of Electrical and Computer Engineering
University of Saskatchewan
Saskatoon

By

Gazi Mohammad Ali Ehsan ur Rahman

PERMISSION TO USE

In presenting this thesis in partial fulfillment of the requirements for a Postgraduate degree from the University of Saskatchewan, I agree that the Libraries of this University may make it freely available for inspection. I further agree that permission for copying this thesis in any manner, in whole or in part, for scholarly purposes may be granted by the professor or professors who supervised my thesis work or, in their absence, by the Head of the Department or the Dean of the College in which my thesis work was done. It is understood that any copying or publication or use of this thesis or parts thereof for financial gain shall not be allowed without my written permission. It is also understood that due recognition shall be given to me and to the University of Saskatchewan for any scholarly use which may be made of any material in my thesis.

DISCLAIMER

Reference in this thesis to any specific commercial products, process, or service by trade name, trademark, manufacturer, or otherwise, does not constitute or imply its endorsement, recommendation, or favoring by the University of Saskatchewan. The views and opinions of the author expressed herein do not state or reflect those of the University of Saskatchewan and shall not be used for advertising or product endorsement purposes.

Requests for permission to copy or to make other uses of materials in this thesis in whole or part should be addressed to:

Dean
College of Graduate and Postdoctoral Studies
University of Saskatchewan
116 Thorvaldson Building, 110 Science Place
Saskatoon, SK S7N 5C9 Canada
Or
Head of Department of Electrical and Computer Engineering 57 Campus Drive
University of Saskatchewan,
Saskatoon, SK, S7N 5A9 Canada

ABSTRACT

Wide-area remote monitoring applications use cellular networks or satellite links to transfer sensor data to the central storage. Remote monitoring applications uses Wireless Sensor Networks (WSNs) to accommodate more Sensor Nodes (SNs) and for better management. Internet of Things (IoT) network connects the WSN with the data storage and other application specific services using the existing internet infrastructure. Both cellular networks, such as the Narrow-Band IoT (NB-IoT), and satellite links will not be suitable for point-to-point connections of the SNs due to their lack of coverage, high cost, and energy requirement. Low Power Wireless Area Network (LPWAN) is used to interconnect all the SNs and accumulate the data to a single point, called Gateway, before sending it to the IoT network. WSN implements clustering of the SNs to increase the network coverage and utilizes multiple wireless links between the repeater nodes (called hops) to reach the gateway at a longer distance. Clustered WSN can cover up to a few km using the LPWAN technologies such as Zigbee using multiple hops. Each Zigbee link can be from 200 m to 500 m long. Other LPWAN technologies, such as LoRa, can facilitate an extended range from 1km to 15km. However, the LoRa will not be suitable for the clustered WSN due to its long Time on Air (TOA) which will introduce data transmission delay and become severe with the increase of hop count. Besides, a sensor node will need to increase the antenna height to achieve the long-range benefit of Lora using a single link (hop) instead of using multiple hops to cover the same range. With the increased WSN coverage area, remote monitoring applications such as smart farming may require mobile sensor nodes. This research focuses on the challenges to overcome LoRa's limitations (long TOA and antenna height) and accommodation of mobility in a high-density and wide-area WSN for future remote monitoring applications. Hence, this research proposes lightweight communication protocols and networking algorithms using LoRa to achieve mobility, energy efficiency and wider coverage of up to a few hundred km for the WSN.

This thesis is divided into four parts. It presents two data transmission protocols for LoRa to achieve a higher data rate and wider network coverage, one networking algorithm for wide-area WSN and a channel synchronization algorithm to improve the data rate of LoRa links. Part one presents a lightweight data transmission protocol for LoRa using a mobile data accumulator (called data sink) to increase the monitoring coverage area and data transmission energy efficiency. The proposed Lightweight Dynamic Auto Reconfigurable Protocol (LDAP) utilizes direct or single hop to transmit data from the SNs using one of them as the repeater node. Wide-area remote monitoring applications such as Water Quality Monitoring (WQM) can acquire data from geographically distributed water resources using LDAP, and a mobile Data Sink (DS) mounted on an Unmanned Aerial Vehicle (UAV). The proposed LDAP can acquire data from a minimum of 147 SNs covering 128 km in one direction reducing the DS requirement down to 5% comparing other WSNs using Zigbee for the same coverage area with static DS.

Applications like smart farming and environmental monitoring may require mobile sensor nodes (SN) and data sinks (DS). The WSNs for these applications will require real-time network management algorithms and routing protocols for the dynamic WSN with mobility that is not feasible using static WSN technologies. This part proposes a lightweight clustering algorithm for the dynamic WSN (with mobility) utilizing the proposed LDAP to form clusters in real-time during the data accumulation by the mobile DS. The proposed Lightweight Dynamic Clustering Algorithm (LDCA) can form real-time clusters consisting of mobile or stationary SNs using mobile DS or static GW. WSN using LoRa and LDCA increases network capacity and coverage area reducing the required number of DS. It also reduces clustering energy to 33% and shows clustering efficiency of up to 98% for single-hop clustering covering 100 SNs.

LoRa is not suitable for a clustered WSN with multiple hops due to its long TOA, depending on the LoRa link configurations (bandwidth and spreading factor). This research proposes a channel synchronization algorithm to improve the data rate of the LoRa link by combining multiple LoRa radio channels in a single logical channel. This increased data rate will enhance the capacity of the clusters in the WSN supporting faster clustering with mobile sensor nodes and data sink. Along with the LDCA, the proposed Lightweight Synchronization Algorithm for Quasi-orthogonal LoRa channels (LSAQ) facilitating multi-hop data transfer increases WSN capacity and coverage area. This research investigates quasi-orthogonality features of LoRa in terms of radio channel frequency, spreading factor (SF) and bandwidth. It derived mathematical models to obtain the optimal LoRa parameters for parallel data transmission using multiple SFs and developed a synchronization algorithm for LSAQ. The proposed LSAQ achieves up to a 46% improvement in network capacity and 58% in data rate compared with the WSN using the traditional LoRa Medium Access Control (MAC) layer protocols.

Besides the high-density clustered WSN, remote monitoring applications like plant phenotyping may require transferring image or high-volume data using LoRa links. Wireless data transmission protocols used for high-volume data transmission using the link with a low data rate (like LoRa) requiring multiple packets create a significant amount of packet overload. Besides, the reliability of these data transmission protocols is highly dependent on acknowledgement (ACK) messages creating extra load on overall data transmission and hence reducing the application-specific effective data rate (goodput). This research proposes an application layer protocol to improve the goodput while transferring an image or sequential data over the LoRa links in the WSN. It uses dynamic acknowledgement (DACK) protocol for the LoRa physical layer to reduce the ACK message overhead. DACK uses end-of-transmission ACK messaging and transmits multiple packets as a block. It retransmits missing packets after receiving the ACK message at the end of multiple blocks. The goodput depends on the block size and the number of lossy packets that need to be retransmitted. It shows that the DACK LoRa can reduce the total ACK time 10 to 30 times comparing stop-wait protocol and ten times comparing multi-packet ACK protocol.

The focused wide-area WSN and mobility requires different matrices to be evaluated. The performance evaluation matrices used for the static WSN do not consider the mobility and the related parameters, such as clustering efficiency in the network and hence cannot evaluate the performance of the proposed wide-area WSN platform supporting mobility. Therefore, new, and modified performance matrices are proposed to measure dynamic performance. It can measure the real-time clustering performance using the mobile data sink and sensor nodes, the cluster size, the coverage area of the WSN and more. All required hardware and software design, dimensioning, and performance evaluation models are also presented.

ACKNOWLEDGMENTS

This thesis would not have been possible, or at least not what it looks like now, without the help and guidance of many people. These few lines are not enough to express my gratitude to all of them.

I would like to express my deepest gratitude toward my supervisor, Dr. Khan A. Wahid, for his criticism, patience, invaluable support, and guidance through my research program at the University of Saskatchewan. It has indeed been an honor and rewarding experience to work under his supervision. I have learned important lessons on the skills and values of conducting research.

I would also like to extend my gratitude to my loving wife, my dearest parents, and my caring family members. I am also thankful to my colleagues and lab mates.

My deepest love and gratitude belong to my beloved wife, Noor Fatema, for her tremendous understanding, support, and encouragement during this study. Finally, I wish to express my appreciation to all of those who gave me help when I studied at the University of Saskatchewan

TABLE OF CONTENTS

LIST OF FIGURES

ABBREVIATIONS

ADC	Analog to Digital Converter
ADR	Adaptive Data Rate
AES	Advanced Encryption Standard
AI	Artificial Intelligence
AODV	Ad-Hoc On-demand Distance Vector
BER	Bit Error Rate
BLE	Bluetooth Low Energy
BS	Base Station
BW	Band Width
CAD	Channel Activity Detection
CH	Cluster Head
CIRA	Compression and Image Recovery Algorithm
CR	Code Rate
CRC	Cyclic Redundancy Check
CSMA	Carrier Sense Multiple Access
CSS	Chirp Spread Spectrum
DACK	Dynamic Acknowledgement
DS	Data Sink
DSR	Dynamic Source Routing
ED	End Device
ETA	End of Transmission Acknowledgement
EWS	Exponential Windowing Scheme
FM-RDS	Frequency Modulation Radio Data System
GIS	Geographic Information System
GPRS	General Packet Radio Service
GPS	Global Positioning System
GRP	Geographic Routing Protocol
GW	Gate Way
I2C	Inter Integrated Circuit
ICS	Interleaved Chirp Spreading
IoT	Internet of Things
IP	Internet Protocol
LBT	Listen Before Talk
LC	Logical Channel
LDAP	Lightweight Dynamic Auto-reconfigurable Protocol
LDCA	Lightweight Dynamic Clustering Algorithm

LEACH	Low-Energy Adaptive Clustering Hierarchy
LoWPAN	Low-Power Wireless Personal Area Network
LoRa	Long Range
LOS	Line Of Sight
LPWAN	Low Power WAN
LSAQ	Lightweight Synchronization Algorithm for Quasi-Orthogonal Channels
LTE	Long Term Evolution
MAC	Media Access Control
MCU	Micro Controller Unit
MIMO	Multiple Input Multiple Output
MPLR	Multi-Packet LoRa
NB-IoT	Narrow Band IoT
OLSR	Optimized Link State Routing
OSI	Open Systems Interconnection
PDR	Packet Delivery Rate
PHY	Physical layer
PRR	Packet Reception Ratio
QoS	Quality of Service
RAM	Random Access Memory
RF	Radio Frequency
RN	Repeater Node
ROM	Read Only Memory
RSSI	Received Signal Strength Indicator
RTC	Real Time Clock
SDR	Software Defined Radio
SF	Spreading Factor
SINR	Signal to Interfering Noise Ratio
SN	Sensor Node
SNR	Signal to Noise Ratio
SINR	Signal to Interference Noise Ratio
SPI	Synchronous Peripheral Interface
SSK	Slope Shift Keying
TDMA	Time Division Multiple Access
TOA	Time On Air
TVOC	Total Volatile Organic Compound
UAV	Unmanned Aerial Vehicle
WAN	Wide Area Network
WARM	Wide Area Remote Monitoring
WQM	Water Quality Monitoring
WSN	Wireless Sensor Network

1. Introduction

1.1 Background

1.1.1 Wireless Sensor Network

Remote monitoring applications use various sensors to monitor the resources wirelessly. Wireless Sensor Network (WSN) connects the sensors wirelessly, acquires, transmits, and stores the data in a central storage using the Internet of things (IoT) through the data sinks and gateways. IoT provides transportation and accumulation of data to central storage for further processing by the user. WSN capacity and coverage are increased by clustering the sensor nodes. Clustering is performed by grouping the sensor nodes that are connected to one or more than one sensor nodes by direct wireless links. One of the sensor nodes (or a special node) in the cluster is elected as the Cluster Head (CH), which has direct wireless connection to all the cluster members and accumulates the data from them. CHs of the clusters far from the gateway transfer their data using another CH as the repeater. Communication between the CHs and the gateway through multiple repeater CHs is established by multi-hop short-range links. With the increase of the WSN size data routing (like in a mesh network with multiple hops) becomes complicated and energy inefficient, requires different types of nodes (heterogenous), complex routing algorithm, and becomes difficult to redesign the WSN with the addition of new nodes. Clustering brings controllability, scalability, and homogeneity to the network by introducing the hierarchical structure of the WSN [1]. It also facilitates efficient routing using multiple hops [2]. Clustering is evolving from simple equal clustering [3] to unequal clustering [4], introducing dynamic thresholding [5] and offline optimization algorithms [6]. Recent research works are done by proposing DS relocation [7] and their path planning [8] to increase the WSN capacity and coverage while keeping the network elements (SN, DS, and GW) static.

1.1.2 Low Power Wireless Area Network and LoRa

Low Power Wireless Area Network (LPWAN) technologies are used in a WSN for connectivity. Among the LPWAN, Zigbee is used for short-range links, which limits the WSN coverage to few kms. Cellular LPWAN technologies like Narrow Band IoT (NB-IoT) and satellite links [9] are used for long-range point-to-point connection for remote monitoring applications. However, cellular network and satellite links are not used for WSN to connect the SNs due to the lack of coverage, high cost and energy requirement. Remote monitoring applications that require low data rate can use LoRa for point-to-point and long-range connectivity. LoRa uses Chirp Spread Spectrum (CSS) Modulation [10] to achieve better noise immunity for long-range communication. The range of a LoRa link depends on its Spreading Factor (SF). It ranges from 1 km to 15 km depending on the SF from 7 to 12. Its range also

depends on the height of the antenna and Line of Sight (LOS), and the antenna height h (in m) can be determined by the Fresnel zone (1) at 60% clearance, where, H is the earth curvature, d (in km) is the length of the link and f (in MHz) is the carrier frequency.

$$h = H + 8.657\sqrt{\frac{0.6d}{f}} \qquad (1)$$

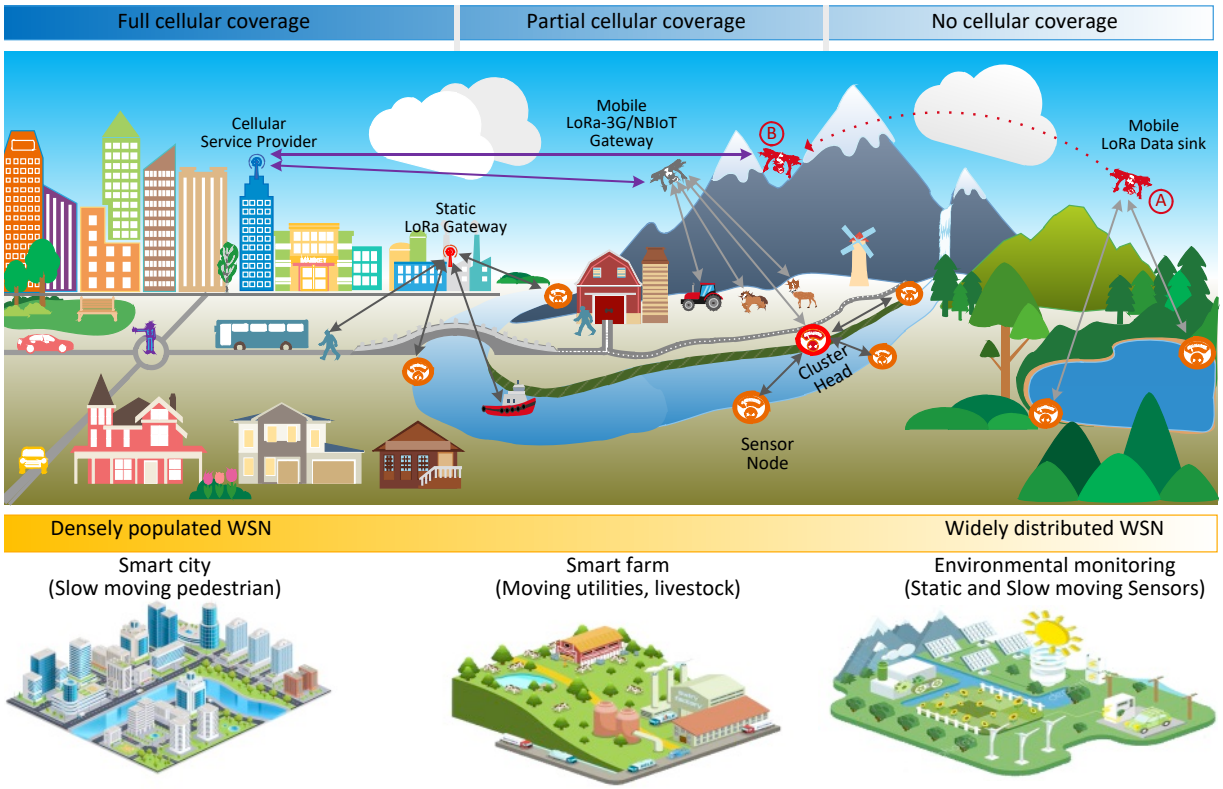

Figure 1-1. Wide-area wireless sensor network using LoRa and UAV with application specific static or mobile SN and DS.

LoRa is orthogonal in terms of radio channel frequency and quasi-orthogonal for some specific combinations of BW and SFs. LoRa's CSS modulation technique makes it immune to interference. LoRa receiver can receive a signal of a very low Received Signal Strength Indicator (RSSI) down to -130 dB and Signal to Noise Ratio (SNR) down to -10. LoRa is also highly immune to the doppler effect, which can be measured [11] by comparing the symbol time of LoRa (T_s) and the coherence time of the doppler shift (T_c). LoRa data losses occur only for $Ts > Tc$, as shown by (2), where BW is the LoRa channel bandwidth (in KHz) and W_d is the angular frequency shift caused by the doppler effect. It appears that the speed of LoRa nodes can increase with the decrease of SF and increase of BW. The node speed can be 38 km/h using

SF = 12, BW = 125 KHz and 76km/h for SF = 12, BW = 250 KHz.

$$T_s > T_c \equiv \frac{2SF}{BW} > \frac{2\pi}{W_d} \quad (2)$$

1.1.3 LoRa-based Wide-area WSN and challenges

Wide-area remote monitoring (WARM) applications, such as environmental, agricultural, and Water Quality Monitoring (WQM), have the resources geographically spread over a wide area. These applications face the challenge of connecting with the IoT network due to little or no cellular network coverage, the high cost and energy requirement of satellite links. Besides, applications like smart farming and smart city with moving sensor nodes mounted on the livestock and slow-moving pedestrian or vehicles may not use the traditional WSN that uses static network elements and offline clustering. Figure 1-1 shows the application-specific wide-area WSN platform using LoRa, mobile DS mounted on Unmanned Aerial Vehicle (UAV) with static and mobile SNs. The mobile DS (position A) acquires sensor data directly from the SNs or the cluster head (position C). Mobile SNs can transfer data directly to the static BS or gateway.

Although LoRa can be used in the WSN for long-range connectivity at a low data rate, it must overcome some challenges [12]. A single LoRa link can cover up to 50 km with LOS. However, a 1km LoRa link requires an antenna height above 8 m, which is not feasible for most WARM applications. Multi-hop LoRa link will introduce a significant amount of delay due to its long TOA. Like, for a 10km link, using ten hops (each of 1km) at SF = 12 (as LoRa range increases with the increase of SF sacrificing data rate), the total TOA will be 36s [13]. A real-time algorithm with this link may have a clustering phase of 720s, which is entirely impractical. For WSN without clustering, only 25 (15x60/36) nodes can be served by that link at a 15 min data acquisition interval. The existing LoRa Wide Area Network (LoRaWAN) is a media access protocol [14] to control channel utilization down to 1% supporting more nodes in the network. This may limit a clustered WSN to transferring aggregated data to the GW.

1.1.4 Research scope and Motivation

The WARM applications may lack accessibility and energy sources or storage. The use of mobile DS mounted on a UAV may overcome these limitations. WARM applications may also have mobile SNs. Considering the mobility and wide-area coverage requirements, the LoRa-based WSN may have the following research scopes.

- LoRa WSN may suffer coverage problems while acquiring sensor data using mobile DS due to its long TOA. For the moving DS, UAV is preferable for its mobility, speed, and ease of recharge or refueling at the base station or charging stations of the WSN. Therefore, LoRa-based WSN may require a lightweight and fast data transmission protocol to acquire data on the fly at a reasonable speed. LoRa BW needs to be more than 250 KHz with the SF from 7 to 10 to meet the speed requirement of a UAV overcoming the doppler effect.

- LoRa-WSN may need multiple clusters to widen its coverage. The traditional clustering schemes use offline optimization keeping the network static. It sometimes requires a heterogenous network for an extended network lifetime (defined as the time the network elements can transfer data to the GW). A lightweight real-time (an event-driven and on-demand basis function) and fast clustering algorithm is required for the mobile network elements in the LoRa-based WSN. This algorithm may utilize RSSI and SNR of the LoRa link to include the environmental effect and doppler effect [15] on the radio channels.

- WARM applications may require an offline (not continuous streaming) image or sequential data transmission. The CHs close to the GW in the clustered WSNs may require sending data at a higher data rate. Synchronous and parallel access of multiple LoRa channels utilizing its quasi-orthogonality may improve the data rate of the LoRa link without changing the modulation technique. Protocols with reduced overhead may improve goodput (effective data rate).

1.2 Literature review

WSN dimension and data transmission capability highly depend on the network architecture and the clustering algorithms. Traditional offline and dynamic threshold-based clustering are not suitable for the wide-area WSN using LoRa that supports mobility. Various autonomous vehicles such as floating boats [16], UAVs [17], and underwater vehicles [18] are used to introduce mobility in the wide-area WSN. Offline BS relocation [19], Fuzzy logic-based [20] offline super CH selection is used to communicate with the mobile DS, which may increase hops in a wide WSN and introduce heterogeneity. The shortest path planning for multiple mobile nodes using ant colony optimization [21] and an optimization solution [22] for delay tolerant SNs introduce mobility in the WSN.

Network capacity improvement using multi-hop routing [23] may suffer a time delay for the long TOA of LoRa. LoRa pseudo-orthogonality is utilized to improve network capacity. Offline SF allocation for subnet [24] of LoRa mesh network improves network coverage. Distance-based SF allocation using Exponential Windowing Scheme (EWS) [25] reduces co-SF interference and improves network capacity by improving the packet delivery rate from 18.2% to 55.25%. However, these algorithms are intended for static networks and require GPS-based

location data or RSSI-based distance calculation. Dynamic SF allocation algorithm [26] utilizes a link capacity-based allocation iterative process. SF superimposed signals [27] using odd SF, and even SF needs to maintain strict synchronization to use the MAC layer that considers all the packets of different SF as a single transmission packet. Cantor [28] calculates the optimized Packet Reception Rate (PRR) for the downlink using Wane and Wax (alternate increase and decrease) optimization algorithm. MIMO (Multiple-Input Multiple-Output)-LoRa [29] uses multiple SFs for parallel transmission to improve BER at higher SF 10, 11, and 12.

In parallel with traditional Chirp Spreading, ICS (Interleaved Chirp Spreading) [30] increases LoRa channel capacity by 42%. Slope Shift Keying (SSK) with ICS [31] used up, down and interleaved up and down chirp modulation to increase the data rate to 28.6%. Time-domain multiplexing is used for LoRa modulation [32] to distribute the bits of a symbol among different SFs, that double the data rate with minor degradation of bit error rate (BER), mainly at the lower SF (SF=7).

1.3 Research objective

This research addresses the challenges of wide-area WSN coverage using LoRa and mobile nodes by developing simple data transmission protocols and lightweight networking algorithms. The objectives of this research are:

- To develop a direct or single-hop data transfer protocol in a LoRa-based WSN for wide-area coverage using homogenous SNs. All the SNs need to be capable of working as a sensor node and as a repeater node as required by the data sink. This research proposes a lightweight dynamic auto-reconfigurable protocol (LDAP) utilizing mobile DS mounted on a UAV for wide-area remote monitoring applications.

- To develop a Real-time clustering algorithm for mobile SNs and DSs in a LoRa-based WSN. This algorithm focuses on the resource constrained SNs and is fast enough to reduce the total clustering time to maximize mobility in the network.

- To develop a data rate improvement scheme for LoRa links. It utilizes the LoRa's quasi-orthogonality in Spreading Factor (SF) for parallel transmission over multiple physical channels. To develop a mathematical model for optimum SF selection and a synchronization algorithm to maximize the data rate.

- To develop a dynamic acknowledgement protocol to improve data goodput for image and sequential data transmission over the LoRa link. It reduces the packet overhead by utilizing the end-of-transmission acknowledgement for a block of LoRa packets determined dynamically.

1.4 Organization of the thesis

This thesis is organized in a manuscript-based style. The first chapter of the thesis presents the technical background, an overview, the importance, and the challenges of wide-area WSNs using LoRa. It also includes the motivation and research objectives with related literature. The main content and contribution of the thesis are included in the form of published or under-review manuscripts.

Chapter 2 presents a data transmission protocol called LDAP for wide-area WSNs using LoRa and mobile data sink. It utilizes UAVs to increase the WSN coverage above 100 km. Considering the TOA limitation, it determines the maximum network capacity for a high-speed UAV carrying the data accumulator. It evaluates the performance of the proposed protocol in terms of coverage and mobility.

The manuscript in chapter 3 describes the development of a clustering algorithm for the LoRa-based WSN to increase network coverage and accommodate the mobility of the SNs using the data transmission protocol as described in chapter 2. The algorithm focuses on the resource constrained SNs that will participate with the DS for cluster formation and cluster head (CH) election in real time. It evaluates the clustering performance by clustering time using LoRa compared with other LPWAN (Low Power Wireless Area Network) technologies.

Chapter 4 presents a synchronization algorithm required for parallel data transmission using multiple LoRa physical channels. It shows the effectiveness and limitations of different orthogonality of LoRa, such as radio channel frequency, bandwidth, and SF. It derives the mathematical model from determining the perfect combination of SFs in different ways for the application-specific requirement in terms of network capacity, coverage, and data rate. It compares the performance of other LoRa data rate improvement schemes and algorithms.

Chapter 5 focuses on the goodput improvement of the LoRa link to transfer image and sequential data reducing the packet overhead. It presents the development and performance analysis of an application layer protocol that utilizes dynamic acknowledgement. Finally, the summary of accomplishments and future research scopes are presented in chapter 6.

1.5 References

1. Z. Sun, L. Wei, C. Xu, T. Wang, Y. Nie, X. Xing, and J. Lu, "An Energy-Efficient Cross-Layer-Sensing Clustering Method Based on Intelligent Fog Computing in WSNs," *IEEE Access*, vol. 7, pp. 144165-144177, 2019, doi: 10.1109/ACCESS.2019.2944858.
2. N. Gharaei, Y. D. Al-Otaibi, S. A. Butt, G. Sahar and S. Rahim, "Energy-Efficient and Coverage-Guaranteed Unequal-Sized Clustering for Wireless Sensor Networks," in *IEEE Access*, vol. 7, pp. 157883-157891, 2019, doi: 10.1109/ACCESS.2019.2950237.
3. S. K. Singh, P. Kumar, and J. P. Singh, "A Survey on Successors of LEACH Protocol," in *IEEE Access,* vol. 5, pp. 4298-4328, 2017, doi: 10.1109/ACCESS.2017.2666082.
4. S. Arjunan and S. Pothula "A survey on unequal clustering protocols in Wireless Sensor Networks," *J. of KSU- Comput. Info. Sci*., vol. 31, no. 3, pp. 304-317, 2019, doi: 31. 10.1016/j.jksuci.2017.03.006.
5. J. Wang, X. Gu, W. Liu, A. Kumar, H. Kim, and Hye-Jin. "An empower hamilton loop based data collection algorithm with mobile agent for WSNs", *Hum. Cent. Comput. Inf. Sci*., vol. 9, no. 18, May 2019, doi: 10.1186/s13673-019-0179-4.
6. H. Bagci, and A. Yazici, An energy aware fuzzy unequal clustering algorithm for wireless sensor networks. IEEE Int. Conf. Fuzzy Syst. 2010, 1–8, doi:10.1109/FUZZY.2010.5584580.
7. A. Verma, S. Kumar, P. R. Gautam, T. Rashid and A. Kumar, "Fuzzy Logic Based Effective Clustering of Homogeneous Wireless Sensor Networks for Mobile Sink," in *IEEE Sensors*, vol. 20, no. 10, pp. 5615- 5623, 15 May15, 2020, doi: 10.1109/JSEN.2020.2969697.
8. H. K. Srivastava and R. K. Dwivedi, "Energy Efficiency in Sensor Based IoT using Mobile Agents: A Review," in 2020 Int. Conf. Power Electron. IoT Appl. Renewable Energy and its Control (PARC), India, Feb. 2020, pp. 314-319, doi: 10.1109/PARC49193.2020.236617.
9. J. Morón-López et al., "Implementation of Smart Buoys and Satellite-Based Systems for the Remote Monitoring of Harmful Algae Bloom in Inland Waters," in *IEEE Sensors J*, vol. 21, no. 5, pp. 6990-6997, 2021, doi: 10.1109/JSEN.2020.3040139.
10. Semtech SX1278, Accessed: Sep. 30, 2020. [Online]. Available: https://www.semtech.com/products/wireless- rf/lora-transceivers/sx1278 .
11. J. Petajajarvi, K. Mikhaylov, M. Pettissalo, J. Janhunen, J. Iinatti, "Performance of a low-power wide-area network based on LoRa technology: Doppler robustness, scalability, and coverage," in *IJDSN*, vol. 13, pp. 1-16, 2017, doi: 10.1177/1550147717699412.
12. G.M.E. Rahman, K.A. Wahid, and A. Dinh, "IoT enabled Low power and Wide range WSN platform for environment monitoring application", 2020 IEEE Region 10 Symposium (TENSYMP), Dhaka, Bangladesh, 2020, pp. 908-911, doi: 10.1109/TENSYMP50017.2020.9230959.
13. LoRa airtime calculator, Accessed: Sep. 30, 2020. [Online]. Available: https://www.loratools.nl/#/airtime.
14. T. Bouguera, J. Diouris, J. Chaillout, R. Jaouadi, G. Andrieux, "Energy Consumption Model for Sensor Nodes Based on LoRa and LoRaWAN," in *MDPI Sensors, vol.* 18, pp. 2104–2126, 2018, doi: 10.3390/s18072104.
15. A. P. A. Torres, C. B. D. Silva and H. T. Filho, "An Experimental Study on the Use of LoRa Technology in Vehicle Communication," in *IEEE Access*, vol. 9, pp. 26633-26640, 2021, doi: 10.1109/ACCESS.2021.3057602.

16. H. Cao, Z. Guo, S. Wang, H. Cheng, C. Zhan, “Intelligent Wide-Area Water Quality Monitoring and Analysis System Exploiting Unmanned Surface Vehicles and Ensemble Learning,” in *MDPI* W*ater*, vol. *12*, pp. 681–695, 2020, doi: 10.3390/w12030681.
17. C. Koparan, A.B. Koc, C.V. Privette, C.B. Sawyer, J.L. Sharp, “Evaluation of a UAV-Assisted Autonomous Water Sampling,” in *MDPI Water*, vol. 10, pp. 655–670, 2018, doi: 10.3390/w10050655.
18. R.L.P. Lima, F.C. Boogaard, R.E. Dinther, “Innovative Water Quality and Ecology Monitoring Using Underwater Unmanned Vehicles: Field Applications, Challenges and Feedback from Water Managers,” in *MDPI Water*, vol. *12*, pp. 1196–1215, 2020, doi: 10.3390/w12041196.
19. J. Wang, Y. Gao, W. Liu, A. Kumar, and H. Kim, "Energy Efficient Routing Algorithm with Mobile Sink Support for Wireless Sensor Networks", *MDPI Sensors*, vol. 19, no. 7, p. 1494, Mar. 2019, doi: 10.3390/s19071494.
20. A. Verma, S. Kumar, P. R. Gautam, T. Rashid and A. Kumar, "Fuzzy Logic Based Effective Clustering of Homogeneous Wireless Sensor Networks for Mobile Sink," in *IEEE Sensors Journal*, vol. 20, no. 10, pp. 5615-5623, 15 May15, 2020, doi: 10.1109/JSEN.2020.2969697.
21. A. Pang, F. Chao, H. Zhou and J. Zhang, "The Method of Data Collection Based on Multiple Mobile Nodes for Wireless Sensor Network,"in *IEEE Access*, vol. 8, pp. 14704-14713, 2020, doi: 10.1109/ACCESS.2020.2966652.
22. Y. Yun and Y. Xia, "Maximizing the Lifetime of Wireless Sensor Networks with Mobile Sink in Delay-Tolerant Applications," in *IEEE Transactions on Mobile Computing*, vol. 9, no. 9, pp. 1308-1318, Sept. 2010, doi: 10.1109/TMC.2010.76.
23. H.C. Lee, K.H. Ke, “Monitoring of Large-Area IoT Sensors Using a LoRa Wireless Mesh Network System-Design and Evaluation,” in *IEEE Transactions on Instrumentation and Measurement*, vol. 67, no. 9, pp. 2177-2187, Sept. 2018, doi: 10.1109/TIM.2018.2814082.
24. G. Zhu, C. -H. Liao, T. Sakdejayont, I. -W. Lai, Y. Narusue and H. Morikawa, "Improving the Capacity of a Mesh LoRa Network by Spreading-Factor-Based Network Clustering," in *IEEE Access*, vol. 7, pp. 21584-21596, 2019, doi: 10.1109/ACCESS.2019.2898239.
25. D. Saluja, R. Singh, S. Gautam and S. Kumar, "EWS: Exponential Windowing Scheme to Improve LoRa Scalability," in *IEEE Transactions on Industrial Informatics*, vol. 18, no. 1, pp. 252-265, Jan. 2022, doi: 10.1109/TII.2021.3074377.
26. G. Zhu, C. -H. Liao, T. Sakdejayont, I. -W. Lai, Y. Narusue and H. Morikawa, "Improving the Capacity of a Mesh LoRa Network by Spreading-Factor-Based Network Clustering," in *IEEE Access*, vol. 7, pp. 21584-21596, 2019, doi: 10.1109/ACCESS.2019.2898239.
27. Y. Hou, Z. Liu and D. Sun, "A novel MAC protocol exploiting concurrent transmissions for massive LoRa connectivity," in *Journal of Communications and Networks*, vol. 22, no. 2, pp. 108-117, April 2020, doi: 10.1109/JCN.2020.000005.
28. D. Xu et al., "Cantor: Improving Goodput in LoRa Concurrent Transmission," in *IEEE Internet of Things Journal,* vol. 8, no. 3, pp. 1519-1532, 1 Feb.1, 2021, doi: 10.1109/JIOT.2020.3013315.
29. J. -M. Kang, "MIMO-LoRa for High-Data-Rate IoT: Concept and Precoding Design," in *IEEE Internet of Things Journal*, doi: 10.1109/JIOT.2022.3143516.
30. P. Edward, M. El-Aasser, M. Ashour and T. Elshabrawy, "Interleaved Chirp Spreading LoRa as a Parallel Network to Enhance LoRa Capacity," in *IEEE Internet of Things Journal,* vol. 8, no. 5, pp. 3864-3874, 1 March1, 2021, doi: 10.1109/JIOT.2020.3027100.

31. A. Mondal, M. Hanif and H. H. Nguyen, "SSK-ICS LoRa: A LoRa-Based Modulation Scheme with Constant Envelope and Enhanced Data Rate," in *IEEE Communications Letters,* doi: 10.1109/LCOMM.2022.3150666.
32. S. An, H. Wang, Y. Sun, Z. Lu and Q. Yu, "Time Domain Multiplexed LoRa Modulation Waveform Design for IoT Communication," in *IEEE Communications Letters*, vol. 26, no. 4, pp. 838-842, April 2022, doi: 10.1109/LCOMM.2022.3146511.

2. LDAP: Lightweight Dynamic Auto-Reconfigurable Protocol in an IoT-Enabled WSN for Wide-Area Remote Monitoring

This chapter describes the proposed data transmission protocol for LoRa to enhance the coverage, capacity, and energy efficiency of the wireless network used for remote monitoring applications. Wide-area remote monitoring applications like Water Quality Monitoring (WQM) may require monitoring the geographically spread water resources using distributed sensor nodes. The cellular network or satellite link-based communication technologies may not be suitable to connect all these sensor nodes to the Internet of Things Network (IoT) due to its lack of coverage, high cost and energy requirement. Short-range Low-Power Wireless Area Network (LPWAN) technologies such as Zigbee may require a larger number of SNs to cover these distributed water resources. LoRa can be used to increase the coverage area, network capacity and energy efficiency. LoRa range depends on the antenna height, higher Spreading Factor (SF) and Line of Sight (LOS). However, antenna height and LOS may not be attained for all the sensor nodes due to their location and terrain. Focusing on all these challenges, this research proposes a data transmission protocol for a mobile data sink to acquire data while maintaining LOS reducing the distance between the sensor nodes and the data sink. The proposed Lightweight Dynamic Auto Reconfigurable Protocol (LDAP) uses mobile data sink mounted on Unmanned Aerial Vehicle (UAV) to extend the coverage area. The long Time on Air (TOA) of LoRa, which increases with higher SF may suffer the Doppler effect or reduce the speed of the mobile data sink. Therefore, LDAP uses lower SF decreasing the TOA and direct or single-hop data transmission to overcome the Doppler effect achieving higher UAV speed and higher data rate, hence increasing monitoring area coverage.

The proposed LDAP configures sensor nodes as the repeater node dynamically for single-hop transmission. The use of the Received Signal Strength Indicator (RSSI), and Signal to Noise Ratio (SNR) makes LDAP immune to the environmental effect on the LoRa radio signal. This research derives a mathematical model to calculate the WSN capacity depending on the UAV speed and altitude. The experimental results and the mathematical model show a significant reduction (up to 80%) in the number of data sinks while using the proposed LDAP. We also evaluated the energy consumption of the SNs and the repeater nodes to determine the lifetime of the WSN using the LDAP algorithm. Data transfer performance is measured in packet drop while acquiring sensor data in the field using LOS and no LOS.

The development work, analysis and findings of this chapter is reported in the below mentioned published journal manuscript. The student contributed to the main idea, implementing code, writing the original draft, evaluation and revision of the manuscript.

G.M.E. Rahman and K.A. Wahid, LDAP: Lightweight Dynamic Auto-Reconfigurable Protocol in an IoT-Enabled WSN for Wide-Area Remote Monitoring. Remote Sens. 2020, 12, 3131. https://doi.org/10.3390/rs12193131.

Funding: This research is supported by a grant from the Natural Sciences and Engineering Research Council of Canada (NSERC).

Acknowledgments: Our thanks to Rakibul Chowdhury, Hanif Sohag, Rinku Basak, and Mohammad Habibullah for helping us in the field trial.

LDAP: Lightweight Dynamic Auto-Reconfigurable Protocol in an IoT-Enabled WSN for Wide-Area Remote Monitoring

Gazi M. E. Rahman * and Khan A. Wahid

Department of Electrical and Computer Engineering, University of Saskatchewan, Saskatoon, SK S7N 5A9, Canada; khan.wahid@usask.ca

* Correspondence: ehsan.rahman@usask.ca

Received: 7 August 2020; Accepted: 16 September 2020; Published: 24 September 2020

Abstract: IoT (Internet of Things)-based remote monitoring and controlling applications are increasing in dimensions and domains day by day. Sensor-based remote monitoring using a Wireless Sensor Network (WSN) becomes challenging for applications when both temporal and spatial data from widely spread sources are acquired in real time. In applications such as environmental, agricultural, and water quality monitoring, the data sources are geographically distributed, and have little or no cellular connectivity. These applications require long-distance wireless or satellite connections for IoT connectivity. Present WSNs are better suited for densely populated applications and require a large number of sensor nodes and base stations for wider coverage but at the cost of added complexity in routing and network organization. As a result, real time data acquisition using an IoT connected WSN is a challenge in terms of coverage, network lifetime, and wireless connectivity. This paper proposes a lightweight, dynamic, and auto-reconfigurable communication protocol (LDAP) for Wide-Area Remote Monitoring (WARM) applications. It has a mobile data sink for wider WSN coverage, and auto-reconfiguration capability to cope with the dynamic network topology required for device mobility. The WSN coverage and lifetime are further improved by using a Long-Range (LoRa) wireless interface. We evaluated the performance of the proposed LDAP in the field in terms of the data delivery rate, Received Signal Strength (RSS), and Signal to Noise Ratio (SNR). All experiments were conducted in a field trial for a water quality monitoring application as a case study. We have used both static and mobile data sinks with static sensor nodes in an IoT-connected environment. The experimental results show a significant reduction (up to 80%) of the number of data sinks while using the proposed LDAP. We also evaluated the energy consumption to determine the lifetime of the WSN using the LDAP algorithm.

Keywords: distributed wireless sensor network; wide- area remote monitoring; lightweight protocol; internet of things; dynamic protocol; water quality monitoring

2.1 Introduction

Remote monitoring of various environmental parameters and resources is a major area of interest in the planning of future initiatives and control methods. The Internet of Things (IoT) and wireless technologies make it simple to accommodate a large number of sensing devices

and gradually extend their coverage over the monitoring area. The IoT is the extension of the internet from our personal computers and smartphones to various types of devices, ranging from wristwatches to large industrial machines. It facilitates the flow of information from these devices to the end-user through the internet for monitoring and controlling purposes. Wireless communication plays a primary role in connecting most edge devices with the IoT network, and the Wireless Sensor Network (WSN) connects sensors in a network to collect various physical parameters of different systems and accumulate them in central storage.

A traditional WSN connects the sensor nodes (SNs) in a clustered network [1] with static network topologies using multiple base stations (BSs) or a data sink (DS) and transfers the sensor data using multiple repeater nodes [2] to increase the monitoring coverage area. This type of WSN is used mainly for densely populated sensor networks and is not suitable for wide-area remote monitoring (WARM) applications, where both temporal and spatial data is acquired in real time. The clustering procedure in WSNs uses various optimization methods [3] to improve the energy requirement and WSN lifetime. This clustering process may not be suitable for the battery-powered and resource-constraint nodes that are used in remote locations with less accessibility. A WSN also uses multiple special nodes as a hop that retransmits the sensor data to the BS in order to increase the WSN coverage, and also to distribute the energy load over the SNs. In doing so, a WSN implements complex routing algorithms which generate extra processing loads for the repeater nodes and the SNs, and hence, energy consumption is increased.

Many WARM applications, such as environmental, agricultural, and water quality monitoring (WQM), where the resources are geographically spread over a wide area, have little or no cellular data coverage, and face the challenge of connecting with the IoT network. Present WARM applications are implemented using (a) point-to-point or point-to-multi-point connectivity, mainly through satellite links [4], (b) multi-hop wireless communication for long-distance connectivity with the BS, and (c) vehicular mobile SNs [5]. Each of these implementations has limitations in terms of cost, energy consumption, and real-time data acquisition.

Water quality monitoring (WQM) is chosen in this work as a useful case for a WARM application. Water resources are widely distributed over the globe and requires both spatial and temporal monitoring. Eighty percent of our daily consumption comes from surface water [6], of which less than 3% is usable (97.2% of surface water is ocean water and is highly saline). Usable surface water mainly comes from glaciers, rivers, and lakes. A natural solvent, surface water carries contaminating substances while traveling on the ground surface and underground. Through the hydrologic cycle, where surface water travels through the air and comes back again, it also becomes contaminated by air pollution from urbanization [7] and other environmental factors [8,9]. WQM also helps the planning and management of the restoration of water

resources and transboundary water distribution [10]. Long-term WQM facilitates the study of ecological changes [11], agricultural conservation practices [12], and long-term changes in water quality parameters. Present WARM is mainly performed by satellite imaging [13], which combines in situ data acquisition with the GIS (Geographic Information System) [14]. On-site digital-color [15], unmanned aerial vehicle (UAV)-based hyperspectral [16], multispectral, thermal, and optical imaging [17] are also used.

To monitor agriculture, the environment, or water resources, using sensors deployed remotely at the site, we need to acquire the data wirelessly using a WSN. The available wireless connectivity systems, such as Zigbee, BLE (Bluetooth Low Energy), and WiFi, have very short range [18] compared to the geographical distributions of the water resources. Long-range wireless connectivity based on cellular networks, such as GPRS (General Packet Radio Service), 3G, WiMax, LTE (Long-Term Evolution), and NB-IoT (Narrow Band-IoT), lacks geographical coverage of most of the water resources due to large power requirements and infrastructural and operational costs. On the other hand, the long-range and low-power wireless technologies, such as LoRa (Long-Range), Sigfox, and Ingenu, are not capable of image-based monitoring. Lastly, the network topology to be used for the WSN depends on the geographical distribution and locations of the resources and the parameter to be monitored.

Therefore, considering the limitations of wireless technologies, the need for various on-site sensors over the widely spread resources, and the lack of accessibility, this research proposes a lightweight dynamic auto-reconfigurable protocol (LDAP) to facilitate the implementation of the sensor network for real-time and long-term WARM applications. Some sensor-based solutions, including the presently available WSNs used for WARM applications, are described in the following section, followed in Section 2.4 by the problem formulation and the detailed description of the proposed LDAP. Section 2.5 describes the field trial of the LDAP for a WQM application, followed by Section 2.6, describing the performance of the LDAP in terms of features and WSN implementation. Section 2.7 concludes the paper with the future scope of LDAP applications.

2.2 Related Work

Research work related to WSN implementation for WARM applications are studied for this paper. WSN coverage can be improved by using multiple hops, long-range wireless links, or by introducing mobility to the WSN elements, such as SNs or a DS. Multiple hops in a WSN require network-specific routing protocols. For a WARM application such as WQM, various underwater routing protocols [19] have been proposed that use multiple transmission paths, a layered network, the creation pf a cylindrical path, the fragmentation of the packet to multiple forwarder nodes, multiple mobile data sinks, and mobile repeater nodes. However, because of

the underwater noise, multipath delay, low bandwidth, and the limited mobility of the nodes, these routing protocols are not suitable for above surface WARM applications which require wide-area coverage. In another study, the lifetime of the WSN is improved by event-driven data transmission [20]. This type of WSN is ideal for a static WSN with clustering, but lacks coverage. Compressed sensing is proposed in [21] to reduce the total energy consumption of the WSN where most of the sensors are used to measure very similar parameters. This may suffer spatial relations of the data for a WARM application where different types of parameters need to be acquired. In [22] base-station relocation using various local or global optimization algorithms are used to achieve wider coverage and energy balance in a densely populated WSN, which is not capable of continuous relocation to cover large geographical areas required for WARM. An analysis of the relocation or positioning of a mobile DS in a pre-clustered WSN using various optimization algorithms is presented in [23]; however, it is only suitable for static and densely populated clustered WSN.

LoRaWAN (LoRa Wide Area Network) is a MAC (Media Access Control) layer protocol [24] on the LoRa physical (LoRa-PHY) layer used to control channel access and reduce collision and channel congestion. The LoRaWAN protocol stack is described in Section 4.1. A secure device-to-device communication using the LoRaWAN-IP (Internet Protocol) gateway is proposed in [25] to increase security, but it also increases energy consumption by 5%. Therefore, it is not efficient for WARM applications in terms of power consumption and bandwidth requirement, since the data travels inefficiently over the node to the gateway link. The LoRaWAN-based ADR (Adaptive Data Rate) scheme in [26] is implemented with link-check and acknowledgment features. This algorithm is dependent on criteria that may cause an unnecessary delay while establishing the links, and may also cause unseen data loss for a densely populated mesh network. Another option with the LoRa-PHY-based multi-hop routing [27] to the LoRa-IoT gateway also may suffer a time delay for a long TOA (Time On Air). It may not support topology-independent routing that is essential for a WSN in WARM applications. In [28], a WSN with the LoRa interface is implemented using a random-number-based clustering algorithm, which is suitable for static star topology. In [29], allocation of a specific spreading factor for each subnet is used for a LoRa static mesh WSN to improve coverage efficiency. Both these algorithms [28,29], may not be suitable for a mobile DS, because they cause topological changes in the network. A low-power data reduction technique is implemented in [30], using dynamic sub-sampling to reduce LoRa traffic for an environmental monitoring application. Given the above drawbacks of LoRaWAN and multi-hop transmission using LoRa-PHY, only a single-hop LoRa link was considered for WARM applications for the proposed LDAP.

UAVs are also used to provide mobility for remote data acquisition, in which dedicated SNs are mounted on the UAV, or UAV-based networking is implemented. However, UAV-based network communication suffers connection disruption, causing data loss due to its

frequent mobility and dynamic routing [31]. To overcome this issue, there are various routing protocols, such as the Ad-Hoc on-demand distance vector (AODV), dynamic source routing (DSR), optimized link state routing (OLSR), and geographic routing protocol (GRP) currently being developed [32]. An energy-efficient UAV-routing protocol for a WSN is proposed in [33], where the energy efficiency of the SNs and the dynamic distance with a traveling DS is considered to determine the shortest routing path. This type of optimization may perform better in a densely populated WSN and may not be suitable for a WARM application where the SNs are widely distributed. An UAV-WSN routing protocol is implemented in [34] based on the shortest total path, using multiple UAVs as agents, which is mainly suitable for a clustered WSN.

Besides the WSN, there is some off-line or point-to-point data acquisition performed for WARM applications. Many mobile sensor nodes are implemented by being mounted on autonomous vehicles such as floating boats [35], amphibious vehicles [36], UAVs [37], and underwater vehicles [38]. All of these require a considerable amount of electric energy for their mobility. These vehicles may not be capable of traveling the long range required for a WARM application. Moreover, static SNs powered by a solar panel [39], wireless power transmission [40], and network-connected sensors using ZigBee [41] need a large number of BSs for wider coverage. Satellite-based wireless data transmission is used in [42] for remote locations, but it is cost-intensive when using a large number of SNs. Community-based learning and data gathering [43] using smartphone apps [44] are being studied for their cultural acceptance, accessibility, and cellular network coverage requirements.

2.3 Problem Formulation

The limitations of currently used WSN technologies for WARM applications are:

- A satellite-based solution requires considerable power and is very expensive due to image data acquisition and processing.
- Satellite-based sensor data acquisition is a high-cost and high-energy solution and therefore, is used only to acquire data from a few locations or those of concern.
- Present WSN technology using a short-range wireless link, such as ZigBee or Wi-Fi, requires a large number of sensor nodes for extensive coverage.
- A WSN with a long-range wireless link, such as LoRa and Sigfox, may reduce the sensor node count. However, this requires a large number of base stations, as most of the water resources have no or inadequate cellular coverage. This will eventually increase the cost.
- A large number of sensor nodes and base stations will require complicated multi-hop data

routing. It is not cost effective in terms of energy cost effective or resource requirements, and may induce latency for some wireless technology, such as LoRa.

- Finally, the lack of or poor unavailability of cellular data coverage, including the NB-IoT for widely distributed water resources, is a bottleneck for IoT connectivity.

Along with the above technical limitations, WARM requires a considerable volume of data acquisition for its distributed resources and a wide range of quality parameters. This requirement is further intensified because of the randomness and fuzziness of acquired data [45], the spatial and temporal variation of the parameters [46], and its dynamics [47]. The WSN for a WARM application, such as WQM, also demands an IoT connectivity to utilize its cloud-based data processing [45] for various reporting and modeling types. Therefore, an IoT-connected WSN is a preferable choice for this type of WARM application.

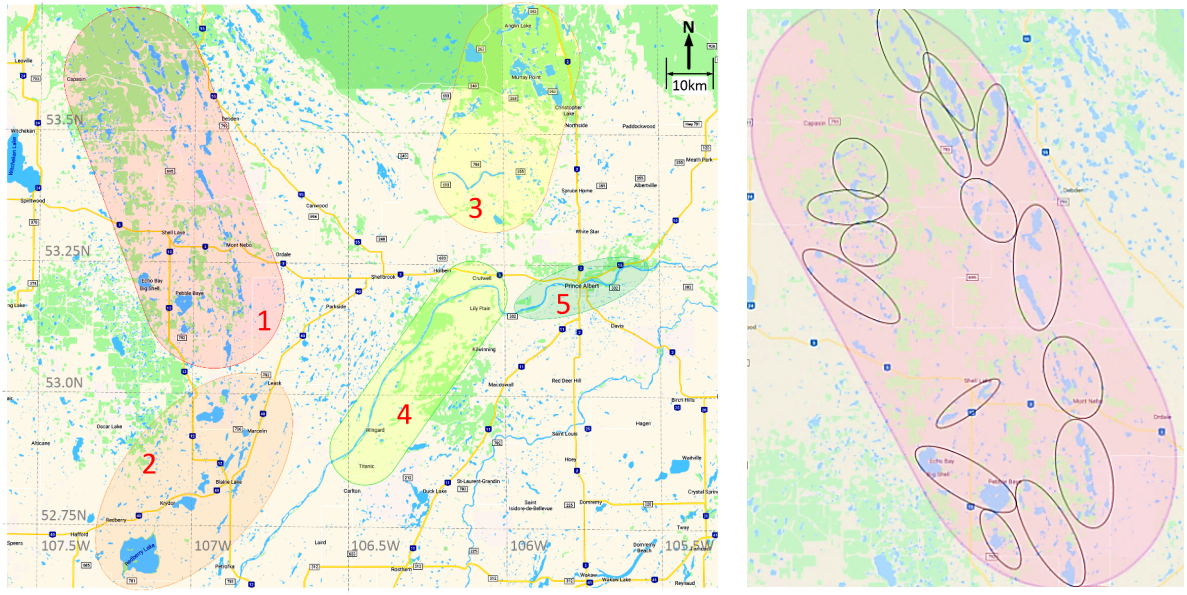

(**a**) (**b**)

Figure 2-1. (**a**): Water resource distribution in Northern Saskatchewan with five different zones, (**b**): Wide Wireless Sensor Network (WSN) for water quality monitoring (WQM) for Zone 1.

Figure 2-1(a) shows the water resource distribution in lower Northern Saskatchewan in Canada with five different zones based on their distribution and cellular network coverage availability. Table 2-1 summarizes the area covered by each zone with its IoT-WSN size measured by visual estimation and also shows the required number of SNs, the BS, and the highest number of hops using the presently available technology. The dimensions of the zones mentioned here is the measure of length and width. This WSN deployment is done using the short-range link ZigBee, commonly used for various clustered WSNs [1], and the long-range link LoRa, used for wide-area coverage [30]. The short-range link is of 500 m and the long-

range link 1 km to 5 km. Figure 2-1(b) shows a probable WSN deployment in zone 1 to monitor almost 80% of the water resources. The rest of the zones can be distributed similarly. There are 16 WSNs in zone 1; each one has at least one BS, and the number of SNs under every BS depends on the range of the wireless link used and the preferable number of hops. IoT connectivity can be implemented using the available cellular data network coverage close to the urban area and long-range point-to-point wireless links for the remote area.

Table 2-1. WSN requirements for the water resources shown in Figure 2-1(a). LDAP: lightweight dynamic auto-reconfigurable protocol.

Zone	Dimension L × W (km × km)	Number of BSs Required			Number of SNs Required			Number of Hops Required			Energy Efficiency * (%)		
		Short-Range [1]	Long-Range [30]	LDAP	Short-Range [1]	Long-Range [30]	LDAP	Short-Range [1]	Long-Range [30]	LDAP	Short-Range [1]	Long-Range [30]	LDAP
1	30 × 80	60	16	3	3000+	480	480	8	5	1	94.2	95.0	99.7
2	30 × 55	30	8	2	1000+	150	150	5	4	1	96.5	94.7	99.3
3	50 × 25	40	12	3	2000+	300	300	8	5	1	94.2	94.0	99.5
4	15 × 55	15	4	1	150+	50	50	8	5	1	71.2	88.5	99.0
5	10 × 25	6	2	1	100+	25	25	5	3	1	92.9	95.4	98.0

**Explained later in Section 2.6.3*

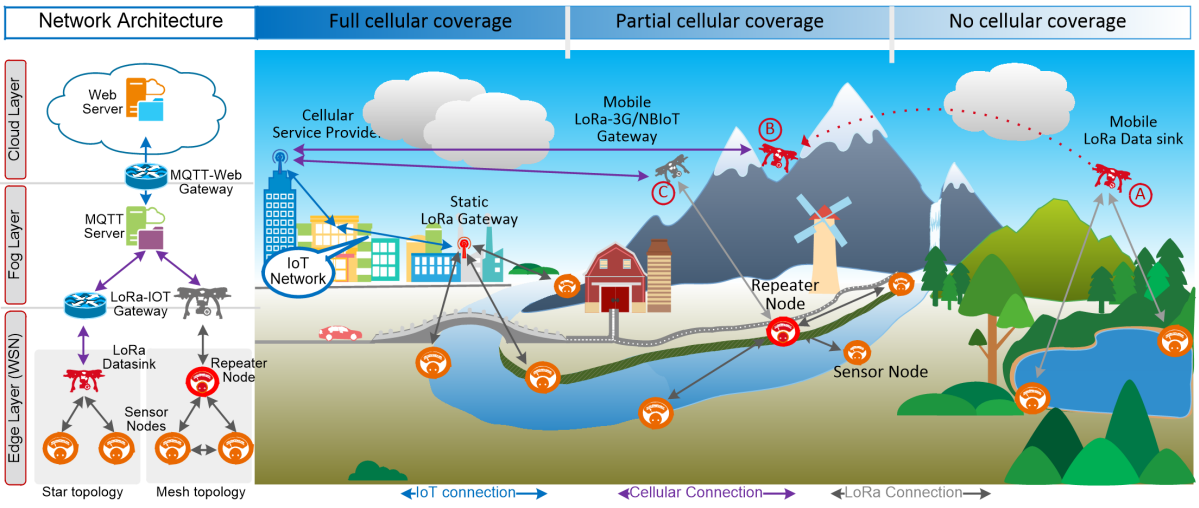

Figure 2-2. A Wide-Area Remote Monitoring (WARM) application focusing the WQM with dynamic network configuration.

From Table 2-1, it can be seen that the WSN dimension is not directly related to the geographical area but to the distribution of the water resources, the technology used, the availability of wireless connectivity, and the network topology to be used. A large number of SNs increases the network topological complexity, which can be reduced using long-range SNs and a larger number of BSs. However, it still suffers from the network routing complexity, the

increased energy requirement for the repeater nodes introducing heterogeneity, and the requirement for various optimization algorithms [48] or a layered protocol [49]. Considering the above limitations and complexity of the available WSN technologies, this paper proposes a lightweight, dynamic, and auto-reconfigurable WSN protocol (LDAP) for the resource and energy-constrained SNs. This LDAP uses a homogeneous network with both static and mobile data sinks instead of static or relocatable base stations [23]. The improvements due to the proposed LDAP are also evident in Table 2-1, in terms of the number of BSs, number of hops, and energy efficiency of the WARM network, which will be described in the performance analysis section. Implementation of the proposed LDAP using an UAV where ground mobility is limited and the WQM application are described in Section 2.5.

2.4 Proposed Solution

Figure 2-2 shows the geographically distributed water resources with partial or no cellular coverage for connecting the SNs with the IoT network. Here, the WSN is based on LoRa, and the IoT connectivity is achieved using a LoRa-IoT gateway. It also shows different types of WSN topologies, where a sensor node is acting as a repeater and communicating with a mobile data sink under partial cellular coverage. The mobile DS is mounted on an UAV to access the remote SNs when other means of vehicular movement may not be possible. A mobile DS, under partial cellular coverage, can also act as a LoRa-IoT gateway. On the other hand, an offline mobile DS (position A) stores the sensor data from the water resources with no cellular coverage and uploads the data to the IoT server when it comes to cellular coverage (position B). While designing the proposed dynamic protocol and the SN's auto self-reconfigurable capability for WARM, our primary focus is on the following:

1. Selection of wireless communication technology; and
2. Lightweight dynamic communication protocol.

2.4.1 Selection of Wireless Communication Technology

The requirements of the wireless network are: low power and long-range wireless technology for the WARM-specific WSN, and other wireless technology with higher bandwidth and with a low-power requirement for IoT connectivity. Cellular networks are constantly in transition, deploying newer generation technology such as 3G to LTE, or LTE to 5G. As the entire service provider still to deploy 5G with NB-IoT capability, 3G or LTE is a better option than any other technologies to connect the WSN with the IoT network wirelessly, depending on the bandwidth requirement and availability. However, all cellular networks need an infrastructure with considerably more power compared with SNs. Depending on the WSN

dimensions and network topology, it may generate very little to moderate traffic for cellular data networks such as LTE and 3G. Moreover, to provide and maintain cellular coverage for all the water resources, which are mainly in rural areas for WARM, is not feasible either commercially or technologically due to a lack of accessibility. Therefore, we need a non-cellular wireless network for the WSN in some areas and the existing cellular network depending on its availability.

Table 2-2. Low-Power Wireless Area Network technologies basic features. LoRa: Long-range.

Technology	Standard	Data Rate (bit/s)	Range (km)	Required Power
NB-IoT	3GPP Cellular	250 k	Urban 8, Rural >25	Low
LoRa	Proprietary	<50 k	Urban 5, Rural >15	Very Low
Sigfox	Proprietary	100	Urban 10, Rural 50	Very Low
Ingenu	Proprietary	20	Urban 3, Rural 15	Very Low
Dash7	ISO/IEC 18000–7	13 k, 55 k, 200 k	1–2	Very Low
6LoWPAN	IEEE 802.15.4	Less than 250 k	<0.1	Low
ZigBee	IEEE 802.15.4	20 k, 40 k, 250 k	<1	Low
Wi-Fi	IEEE 802.15.11	Up to 54 M	0.2	High
New Wi-Fi	IEEE 802.15.11ah	>150 k, <7.8 M	1	Low

Table 2-2 summarizes the basic features of Low-Power Wireless Area Network (LPWAN) technologies [50–52], such as LoRa, Sigfox, Dash7, Ingenu, ZigBee, 6LoWPAN, Bluetooth, and Wi-Fi. Although NB-IoT is a cellular technology, it is included in Table 2-2 as it is designed for IoT connectivity for SNs. Among these LPWAN technologies, LoRa was chosen for its low-power, long-range connectivity, and performance evaluation in several recent works [51]. Table 2-2 shows that LoRa falls in the third position in terms of range and the second position in terms of data-rate. However, because of the requirement of the cellular infrastructure and the related high operational cost of NB-IoT, LoRa can be chosen for the WSN connectivity for WARM as a low-cost option. Unlike LoRaWAN, LoRa-PHY can be used to achieve more flexibility to configure the WSN topology as star, tree, or mesh by implementing a custom network layer on it. Moreover, LoRaWAN supports three types (A, B, and C) [53] of channel acquisition. In contrast, custom channel acquisition can be achieved using the proposed layer on top of LoRa-PHY; Figure 2-3a shows the protocol stack used with LoRa-PHY in this paper relating with the OSI layers. Figure 2-3b shows the LoRa-WAN stack compared with the proposed stack. The basic three layers are shown in this stack, which are the LoRa-PHY, proposed, and application layers. The proposed layer corresponds to the network, transport, and session layers of the OSI (Open Systems Interconnection) reference model. In the network layer, it uses the physical IDs of the SNs and the DS to select the logical route. In the session and transport layers, it forms the LoRa payload packet for the sensor data along with some headers to maintain the connectivity for the logical route. To keep the protocol lightweight for the SNs all these OSI layers are implemented together as a single function, as described in the following subsection.

2.4.2 Lightweight Dynamic Communication Protocol

Along with the LoRa interface, the WSN coverage can be further enhanced by introducing a mobile DS. However, mobility in the WSN makes the topology dynamic; hence, the communication protocol becomes complicated, demanding more processing resources and energy. Therefore, a lightweight and dynamic protocol is crucial to cope with the dynamic topology while maintaining a long WSN lifetime. This protocol involves both the SNs and DS to keep the WSN homogenous (in terms of energy consumption of the SNs) and to make it dynamic for the mobile DS. The SN needs to have the capability to reconfigure itself for the different network topologies, such as star and tree topology. In the star topology, all the SNs will communicate directly with the DS. In the tree or mesh type, most SNs communicate with another SN called the repeater node (RN) which maintains the DS's connectivity. A lightweight algorithm for the SN is also developed to reconfigure it as an edge SN or RN dynamically, depending on the direct or single-hop routing requirement for the proposed LDAP. As the proposed LDAP is based on the LoRa-PHY layer, unlike LoRaWAN, a DS-controlled channel access scheme is implemented along with pre-configured addressing for the SNs. The main assumptions are:

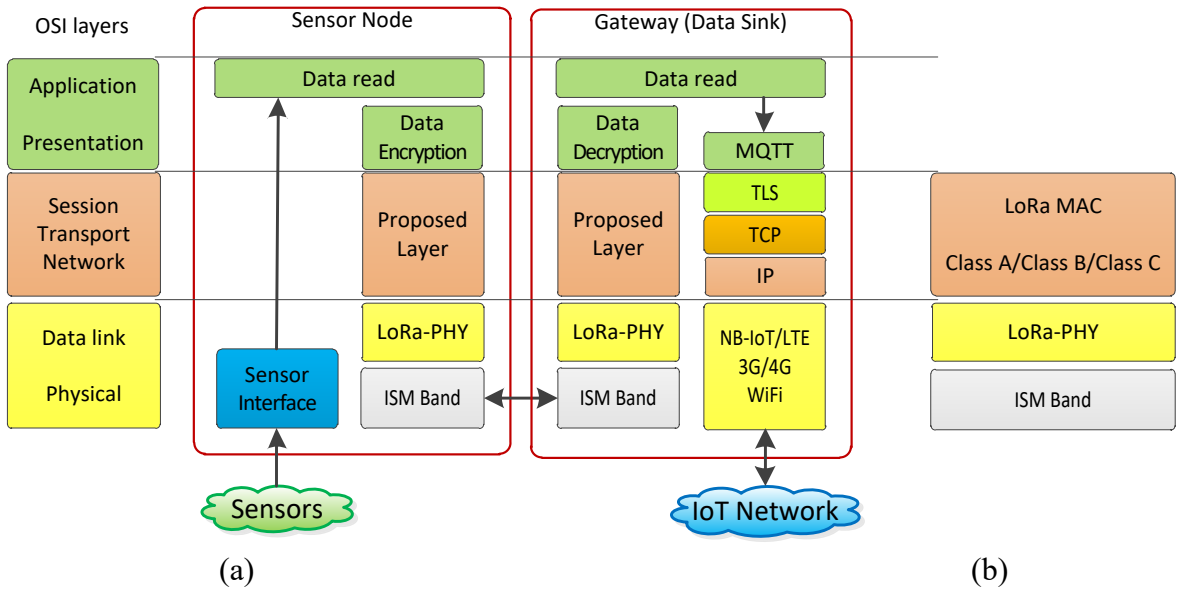

Figure 2-3. (a): LoRa network protocol for the WARM system, (b): LoRaWAN protocol stack.

- Each SN and DS has its unique fixed ID;
- All the SNs are homogeneous in terms of resource and residual energy;
- The SN is static, and the DS is static or mobile;

- All SNs and the DS transmit their signals at a fixed transmit power; and
- The mobile DS travel path is well planned prior to data acquisition.

This proposed protocol is a master-initiated communication protocol to keep better synchronization in the WSN. Figure 2-4 shows the message format without the LoRa packet header. A single packet can be 12 to 256 bytes. Packet transmitter and receiver types (ST, RT) can be any of the DS, RN, or SN. Table 2-3 describes all the fields of the LDAP packet with example values. ST and RT facilitate the SN and DS to configure the WSN dynamically as a star or tree topology according to the WARM requirement. SQN keeps track of the link between the data request to data received in order to cope with the multi-node transmission, mainly in a tree network. PLT and EOM facilitate a multi-packet data transfer for a payload larger than 245 bytes. A multi-packet data transfer can be implemented for offline data acquisition by the mobile DS or for sensor data acquisition at a very high rate, such as multiple samples for every transfer interval. The payload consists of the sensor data, measured parameter unit, and timestamp. It also includes the node ID to implement the message transfer by the repeater node.

Tag	RT	RID	ST	SID	MID	SQN	PLT	PLL	PL	EOM
Size (byte)	1	2	1	2	1	1	1	1	1 to 245	1

Figure 2-4. Implemented message format of LDAP.

Table 2-3. IoT-WARM Communication packet description of LDAP.

Tag	Full Name	Values	Example
RT	Receiver Type	1/2/3	1: sink, 2: RN, 3: node
RID	Receiver ID	0001 to FFFF	Device ID (1 to 65535)
ST	Sender Type	1/2/3	1: sink, 2: RN, 3: node
SID	Sender ID	0001 to FFFF	Device ID (1 to 65535)
MID	Message ID	1–4	1: Req., 2: Ack., 3: Data, 4: Conf., 5: Init.
SQN	Msg. seq. number	1	0–255 (binary)
PLT	Payload Type	0/1	0: last block, 1: multi-block
PLL	Payload Length	1–245	8bit data stream
PL	Payload	Binary/ASCII	Sensor data with date-time
EOM	End of message	0/1	0: Last packet, 1: Continuous packet

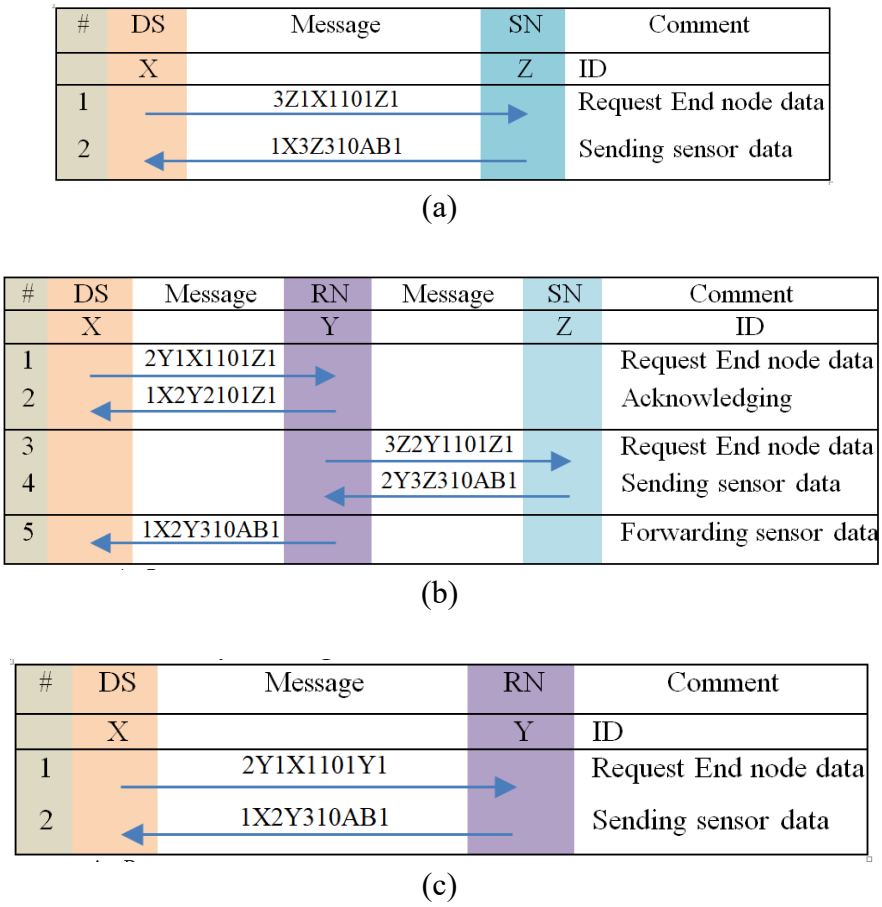

Figure 2-5. Date transfer protocol (**a**): from the SN to DS, (**b**): from the SN to DS through the RN, (**c**): from the SN to RN.

The LDAP has three phases: initialization, configuration, and routing. In the initialization phase, the SN configures itself automatically with the sensors connected. The parameters need to be acquired, including the interval for data acquisition and the node's initial energy state. This configuration can also be done at the beginning of the WSN deployment or at any time required by using the configuration message (MID = 5). For the mobility of at DS, both configuration and routing phases are performed simultaneously in the data transfer request message (MID = 1). The WARM configuration message (MID = 4) is also implemented for a fixed topology while using a static DS. The acknowledgment message (MID = 2) is implemented for the synchronization of the data transmission message (MID = 3) to enable sensor data transmission from the edge SN to the DS or RN, and from the RN to the DS. Figure 2-5a shows the direct DS to SN data transfer protocol. Figure 2-5b shows the configuration and data transmission from the DS to SN through the RN, and Figure 2-5c shows the data transfer protocol between the SN and RN. Every data transfer from the SN to DS through the RN ensures a single-hop data transmission to reduce data transfer energy consumption. The selection of a different SN

as the RN for every round of non-direct data transfer helps to maintain the energy balance in the WSN, thus keeping the WSN homogeneous, which is very important for dynamic network topology. This dynamic RN selection can be performed by proper DS travel route planning, using an offline optimization algorithm.

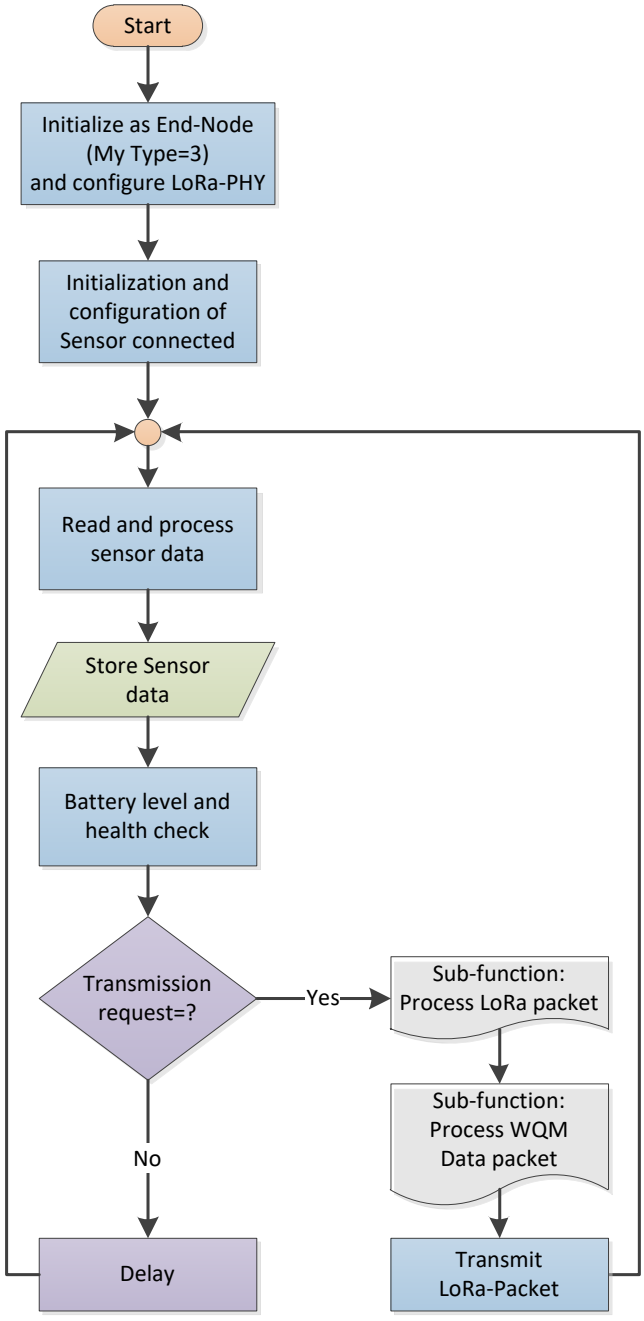

Figure 2-6. (**a**) Software algorithm for the SN

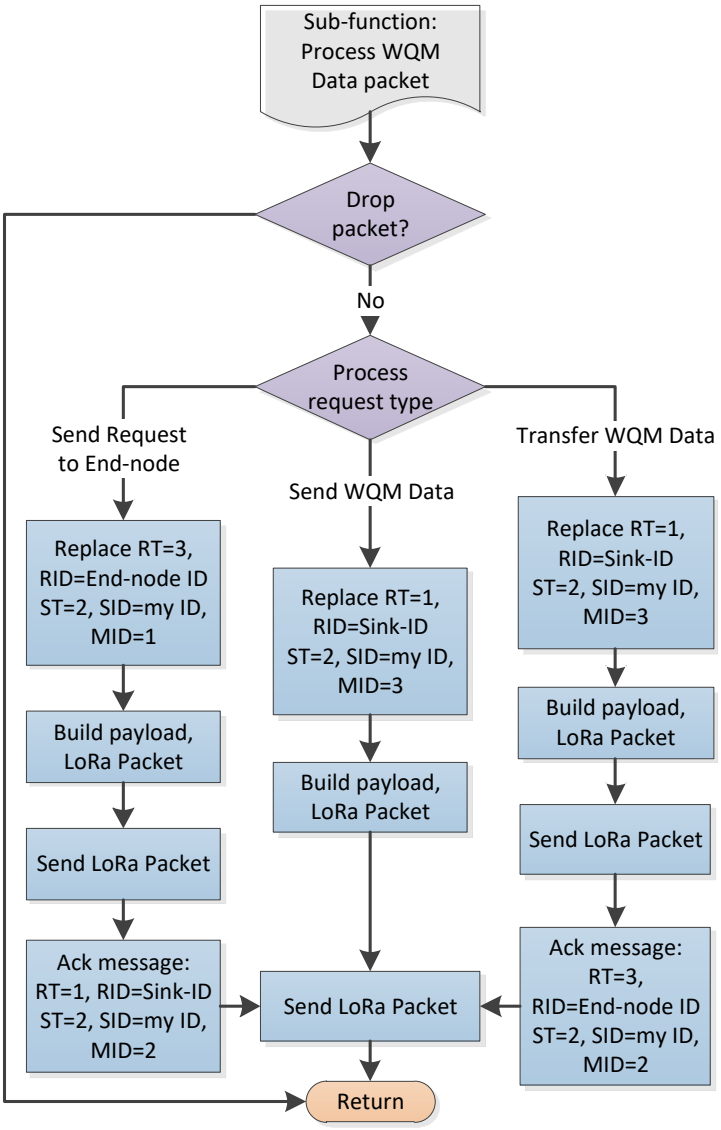

Figure 2-6 (**b**) SN dynamic routing algorithm

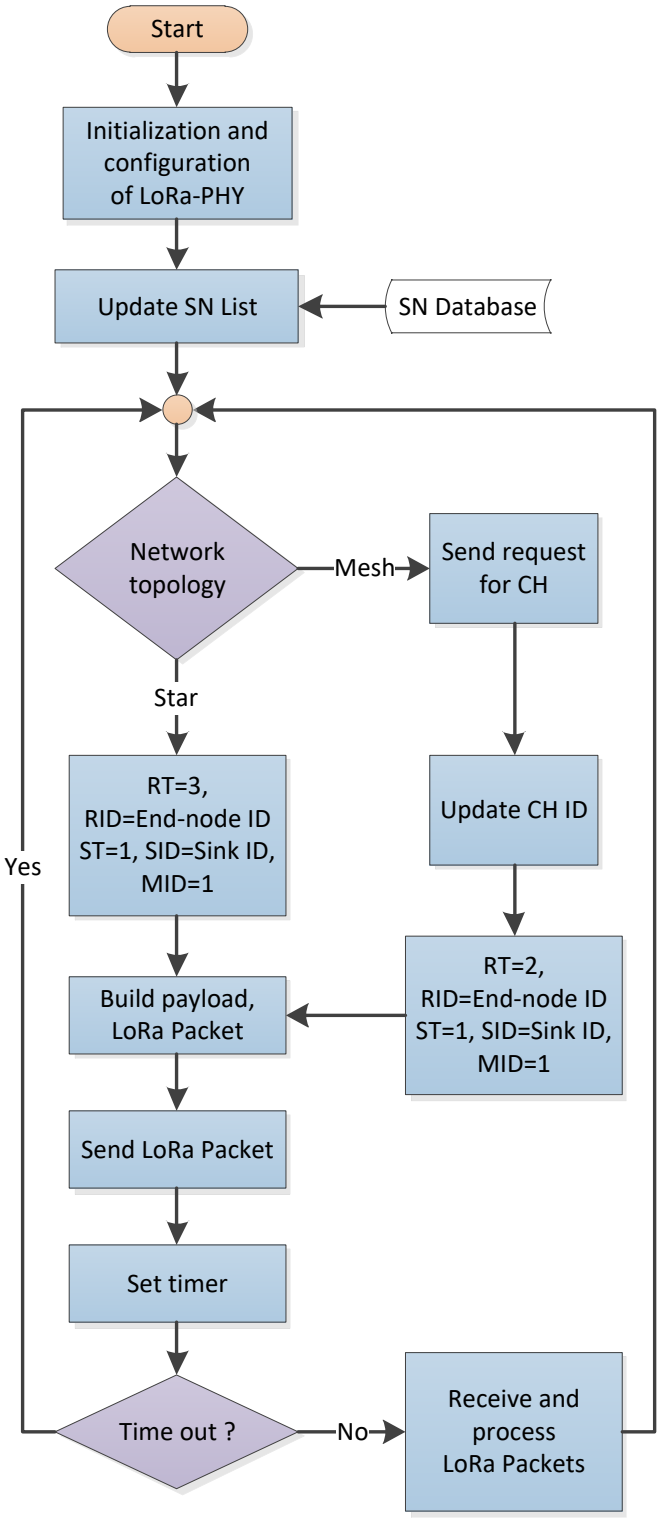

Figure 2-6 (**c**) software algorithm for the DS.

An algorithm to perform LoRa wireless link configuration, packet construction, data processing, and synchronization functionality for the LDAP is implemented both in the SN and the DS. Figure 2-6 shows the software algorithms implemented in the SN and DS. In Figure 2-6(a), the SN performs the initialization and configuration at the start, then reads the sensor and waits for a message from the DS for data upload to the DS. After the initialization phase, the DS starts communication with the SN in a loop and tries to acquire sensor data from the SN database, as shown in Figure 2-6(c). If no SN responds in a specific time, it requests a SN with the lowest RSSI (Received Signal Strength Indicator) and highest energy level to relay the missing SN's data. Figure 2-6(b) shows the dynamic RN implementation algorithm for the SN. Dimensioning of the WSN and planning the DS travel path depends on the WARM implementation, network configuration, and LoRa link quality described in Section 2.6.

2.4.3 Timing Model

The number of SNs covered by a mobile DS depends significantly both on the data acquisition interval and the LoRa Time On Air (TOA). Because LoRa uses Chirp Spread Spectrum (CSS) modulation, its TOA is highly dependent on the bandwidth (BW), and the spreading factor (SF) used, as shown in Equation (1). This equation is derived from the equation given in the manufacturer data sheet [54] and uses a set of nominal values for the parameters given in Table 2-4. It was validated using the online tool [55]. Therefore, network coverage by a mobile DS also depends on the BW and packet length used. The total time for data acquisition depends on the routing from the SN to the DS, as shown in Figure 2-5. For direct SN to DS data transmission, the total time T_{AQSN} can be calculated using Equation (2). The total time of data transmission from the SN through the RN, T_{AQRN}, will be the sum of several data requests, acknowledgement, and data transmission messages, as shown in Equation (3).

$$TOA = \left(20.25 + \text{ceil}\left[\left(\frac{2PL - SF + 7}{SF}\right)\right] \times 5\right)\left(\frac{2^{\text{SF}}}{BW}\right) \quad (1)$$

$$T_{AQSN} = T_{RDS} + T_{DSN} \quad (2)$$

$$T_{AQRN} = T_{RDS} + T_{ARN} + T_{RRN} + T_{DSN} + T_{DRN} + T_{ADS} \quad (3)$$

Where T_{RDS} is the TOA of the data request message from the DS, T_{ARN} is the TOA of the acknowledgment message; T_{RRN} is the TOA of the data request message from the RN; T_{DSN} is the TOA of the data message from the SN; T_{DRN} is the TOA of the data message from the RN; and T_{ADS} is TOA of the acknowledgment message from the DS. For simplicity, all the requests

and acknowledgement messages are considered to generate a 16-byte LoRa payload, and the data transmission and retransmission messages are 256 bytes. Therefore, $T_{RDS} = T_{ARN} = T_{RRN} = T_{ADS} = \text{TOA}_{\text{min}}$, and $T_{DSN} = T_{DRN} = \text{TOA}_{\text{max}}$. Then equation (3) can be written as Equation (4), and the time can be calculated using the values given in Table 2-4.

$$T_{AQRN} = 4TOA_{min} + 2TOA_{max} = 4x197.25 + 2x33.41 = 855.82ms \quad (4)$$

$$N_{max} = \text{ceil}\left(\frac{\text{Duty Cycle}}{\text{T}} \times U_{CH} \times R_{OH}\right) \quad (5)$$

Table 2-4. LoRa parameters with their default and calculated values.

Symbol	Description	Value
SF	Spreading Factor	7
BW	Bandwidth (KHz)	250
CR	Code Rate	1
nPR	Preamble length	8
H	Explicit Header Enable (0: enable)	1
CRC	Cyclic Redundancy Check Enable (1: enable)	0
D	Low data-rate enable (0: disable)	0
U_{CH}	LoRa channel utilization	10%
TOA_{max}	Time On Air (TOA) at maximum payload size of 245 bytes	197.25 ms
TOA_{min}	TOA at minimum payload size of 16 bytes	33.41 ms

The last acknowledgment message from the DS is an optional message for event-sensitive data transmission (hence, $T_{ADS} = 0$ and $T_{AQ} = 822.41$ ms). The maximum number of SNs covered by a single DS can be calculated using Equation (5). U_{CH} and R_{OH} stand for wireless channel utilization over the whole WSN and the SN's processing overhead ratio, respectively. Given a data acquisition interval of 15 min and 20% processing overhead (which depends on the SN hardware design and is obtained from the experimental data for the implemented SN), the maximum number of SNs (N_{max}) under one DS is found to be 142 for the given LoRa parameters.

2.4.4 Energy Model

The total energy consumption for a message or data transmission by the SN is the sum of event-specific energy consumption and calculated using Equation (6). The power and timing

measurements were performed during the lab experiments, as described in Section 6.3, where P_{AC}, P_{RX}, and P_{TX} are the power requirements at active, LoRa-receive, and LoRa-transmit events, respectively, and T_{AC}, T_{RX}, and T_{TX} are the times required for those activities. This total energy requirement is highly dependent on the hardware design of the SN. For complete data transmission using the LDAP, the total energy consumption of a SN can be given by Equation (7), where E_{A1} is the energy consumption for request and acknowledgment messages (T_{TX} = TOA_{min}) and E_{A2} is the maximum energy consumption for a data transfer message (T_{TX} = TOA_{max}). Similarly, the total energy consumption of the RN, for data transmission through it, can be provided by Equation (8). Therefore, the total WSN energy consumption can be calculated using Equation (9). The average per node energy requirement (E_{AV}) per cycle can be given by Equation (10), where k is the number of data transmissions through the RN. Energy efficiency (η) for the proposed LDAP can be calculated using Equation (11). From this equation, it is shown that the energy performance of the proposed LDAP depends on the number of hop or repeater nodes used in the WSN. Energy consumption calculation values are given in Table 2-5, using the experimental values of T_{TX}.

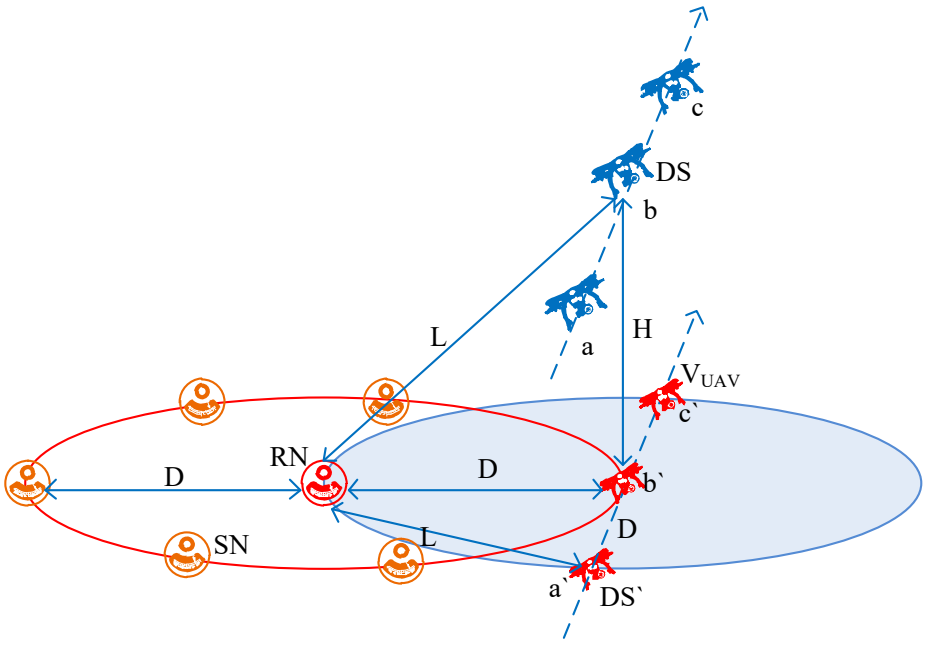

Figure 2-7. Data transmission from the SN to the mobile DS mounted on an unmanned aerial vehicle (UAV).

$$E_A = P_{AC}T_{AC} + P_{RX}T_{RX} + P_{TX}T_{TX} \quad (6)$$

$$E_{SN} = E_{A1} + E_{A2} \quad (7)$$

$$E_{RN} = 4E_{A1} + 2E_{A2} \quad (8)$$

$$E_{WSN} = N_{max}E_{SN} + kE_{RN} \quad (9)$$

$$E_{AV} = E_{SN} + \left(\frac{k}{N_{max}}\right)E_{RN} \quad (10)$$

$$\eta = 1 - \frac{k}{N_{max}} \quad (11)$$

2.4.5 Mobility Model

The proposed LDAP can be implemented using any type of ground or over-the-ground vehicle depending on the WARM applications. However, most of the WARM applications may require remote connectivity where the SNs are difficult to access using ground vehicles. Therefore, for the WARM case, an UAV-mounted DS is considered. Figure 2-7 shows an UAV-mounted DS, which is moving from its initial position, a, to b and then to c, at a ground speed of V_{UAV}, at an altitude of H, and with the LoRa link distance from the RN represented by L. The projected position of the DS is shown as DS` at different times (at a`, b`, and c`). The projected distance between the RN and the DS` is D, which is considered equal to H for optimized altitude vs. the wireless link coverage condition, so that $D = H = 0.7\ L$. An UAV-mounted DS needs to perform two tasks; link establishment and data transfer. To keep the proposed LDAP lightweight, these two tasks are designed to meet the UAV speed and the LoRa TOA. According to the experimental setup used for the WQM case, we calculated a data transfer time through the repeater node (T_{AQRN}) as 856 ms for the maximum sensor data size of 245 bytes. We can calculate the number of SNs data messages to be transferred using a low to medium height UAV, such as the Zephyr 7 [56], with the following conditions:

- UAV altitude is 3.5 km for a 5 km LoRa link;
- UAV maximum ground speed = 50 km/hr = 13.8 m/s = 833 m/min; and
- The data transfer ratio through the repeater node = 100%.

With the above conditions where the minimum distance between the DS and SN (L) is very high compared with the distance traveled per second (or the time of T_{AQRN}) by the UAV, the DS can be considered static for the period of T_{AQRN}. As shown in Figure 2-7, when all the SNs are distributed at a minimum distance of 3.5 km (0.7 L) from the RN, they will communicate with the DS through the RN only in the worst case scenario. The DS can travel half of the SN-DS distance (3.5 km) in 126 seconds without losing the connection with the RN, and during this time it can receive data from at least 147 SNs. Table 2-1 shows that with the LDAP, the SNs

are much more distributed or the number of SNs within the 3.5 km range is lower than the number of SNs that the UAV-mounted DS can acquire data through the RN. The maximum number of SN density can be calculated as 56 (3.5* 480/30) for zone 1. Therefore, the UAV-mounted mobile DS with the LDAP can easily be implemented for the WQM case as described in Section 2.3. Similarly, using the proposed LDAP, the mobile DS mounted on a specific UAV, traveling at an altitude of H (= 0.7 L), can acquire data from the number of SNs (SN_{UAV}) which can be calculated using Equation (12).

$$SN_{UAV} = \left(\frac{0.7L}{V_{UAV}}\right)\left(\frac{1}{2T_{AQRN}}\right) \tag{12}$$

2.4.6 WSN Dimensioning

Dimensioning of a WSN mainly depends on various application-specific requirements and can be done using automated network dimensioning tools. Dimensioning of a widely distributed WSN depends on several factors, such as the number of SNs, maximum and minimum link distances. The data acquisition interval, the number of BSs/DSs, and, mostly, the distribution of the data sources from which the parameters' variability can be acquired. Given all these factors, using the timing model of the LDAP described in Section 4.3 and based on visual inspection, a WSN can be dimensioned for a given area as shown in Figure 2-1a. Table 2-1 shows the dimension of a WSN using the LDAP, while keeping the number of SNs unchanged for better differentiation between them in terms of the number of BSs/DSs. For zone 4 and zone 5, the number of SNs is very low to get the benefit of a mobile DS; hence, the WSN with a mobile DS is more efficient with widely distributed SNs than with the densely populated SNs.

2.5 Field trial and Validation

The field trial consists of the hardware implementation of the SNs, the WSN implementation in the field near the water resources, and lab experiments for SN performance measurement.

2.5.1 Hardware Implementation

A low-power SN is designed to implement and test the proposed LDAP using an 8-bit microcontroller (MCU), namely the ATMega328, with only 32 kB of ROM (Read Only Memory), 4 kB of RAM (Random Access Memory), and running at 16 MHz. Figure 2-8(a)

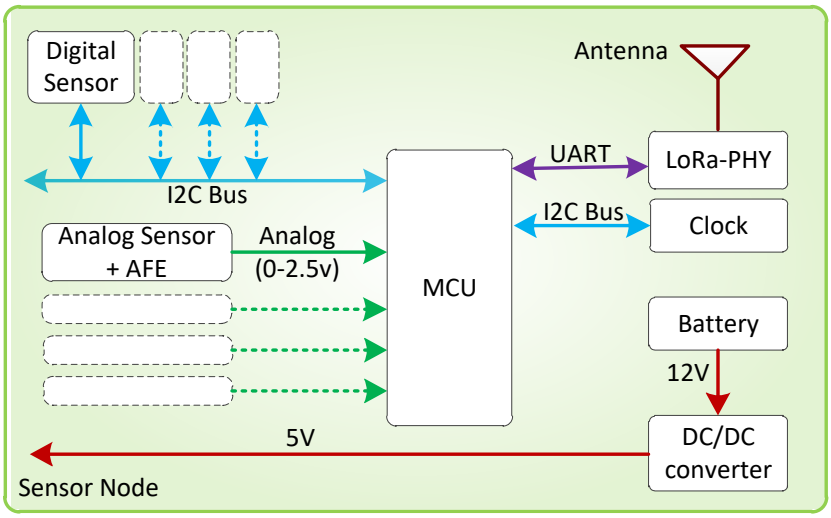

(a)

(a)

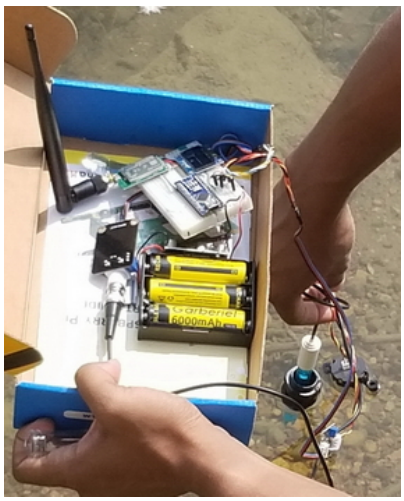

(c)

Figure 2-8. (**a**): Hardware block of SN, (**b**): RN with air-quality sensors, and (**c**): SN with pH and turbidity sensors.

shows the hardware block diagram of the SN with LoRa and sensor connections. With the SX1276 LoRa module at 915 MHz, the MCU is capable of interfacing four analog sensors and four digital sensors simultaneously through the built-in ADC (Analog to Digital Converter) and I2C (Inter Integrated Circuit) interface, respectively. The MCU used in the SN is powered by a 12 V to 5 V voltage converters, and the sensors connected with it also need to operate at 5 V. The total SN is powered by three 18,650 Li-Ion batteries, each of 6000 mAH, providing 10.8 V to 12 V, which can also be replaced by a 12 V lead-acid battery with a 12 V solar panel for external charging for lengthy remote operations. Figure 2-8b, and figure 2-8c show two SNs connected with a LoRa wireless module, battery, and the different types of sensors used in the

field trial. The DS and LoRa-IoT gateway are implemented using a Raspberry-Pi with LoRa, Wi-Fi, and a dedicated LTE-Wi-Fi access point.

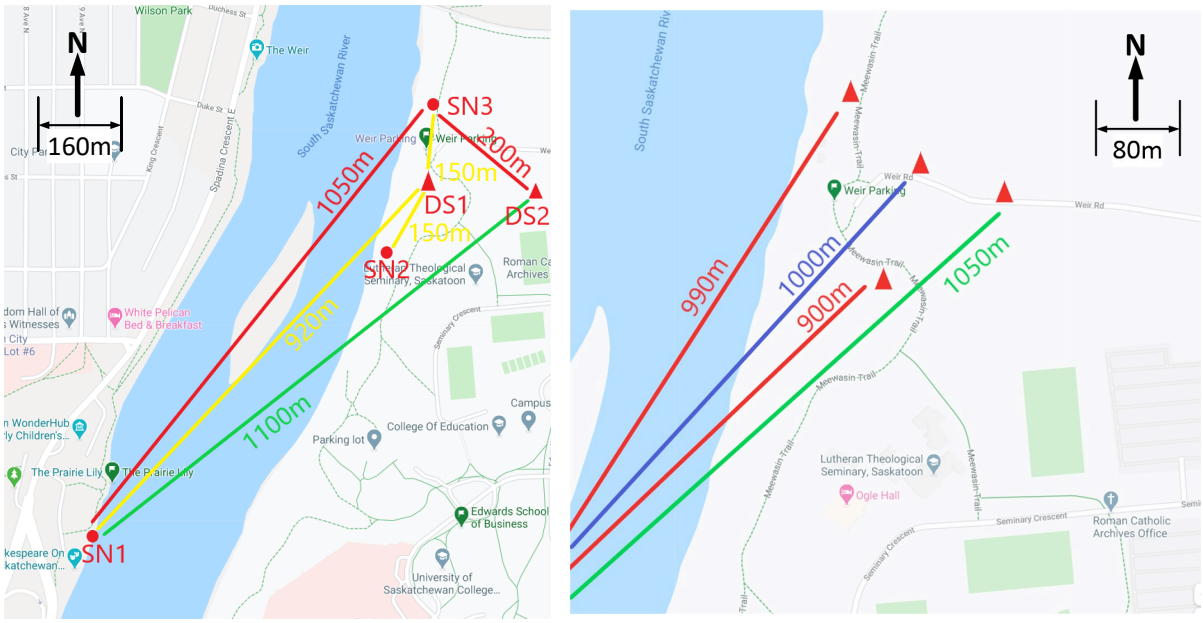

(**a**) (**b**)

Figure 2-9. Google Map view of (**a**): WQM field trial setup of Sensor Nodes SN1, SN2, SN3, and Data Sinks DS1, DS2, DS3; (**b**): different positions of the mobile data sinks.

2.5.2 Experimental Setup

As WQM is used here to show the performance of the proposed LDAP algorithm, we used different types of sensors with the SNs mainly to collect various water quality parameters such as pH, turbidity, and temperature, and air parameters such as temperature, pressure, and humidity. In Figure 2-9a, a Google map view of one field trial is shown, where three SNs (red dots) were installed with one static DS (red triangle) and one mobile DS; lines of different color show the LoRa links. In the first phase, we collected sensor data using the static DS1 from SN1, SN2, and SN3 directly, and then we collected data from SN1 via the SN3 as the RN using DS2 (red lines). SN1 has no line of sight (LOS) with DS2 (the green line shows the link with no line of sight). In the second phase, we collected data from SN1 using a mobile DS. Figure 2-9b shows the map view of some positions of the mobile DS. We also measured the energy performance of the SNs using an energy monitoring and logging setup in the laboratory.

2.6 Performance Analysis

We evaluated the performance of the proposed protocol by measuring the SN's functionality as a RN in terms of the data delivery rate through the RN, the LoRa performance with the mobile DS, and the energy performance of the SN in different functional modes.

2.6.1 Functional Performance

We evaluated the functional performance of the SNs in a fully configured IoT network. We used seven SNs to collect data from different types of sensors and send them to the IoT server through two data sinks. The system was also configured to form the network in two different ways: star networks (SN to DS direct link) and tree networks with the DS using any one SN as the RN, where one SN does not have direct wireless connectivity with the DS. Data from a SN were acquired at three-second intervals, which is a very high rate compared to 15-min intervals; thus, more than 800 packets were collected during the two-day experiment. Figure 2-10a shows the pH and turbidity data taken from the South Saskatchewan River gathered directly from two different SNs to the DS and via the RN, respectively. Figure 2-10b shows the air-quality data received from the temperature, pressure, uncalibrated TVOC (total volatile organic compound measure), and humidity sensor on the river bank. Data delivery success rate between the SN and DS was 100%, and through the RN was 99%.

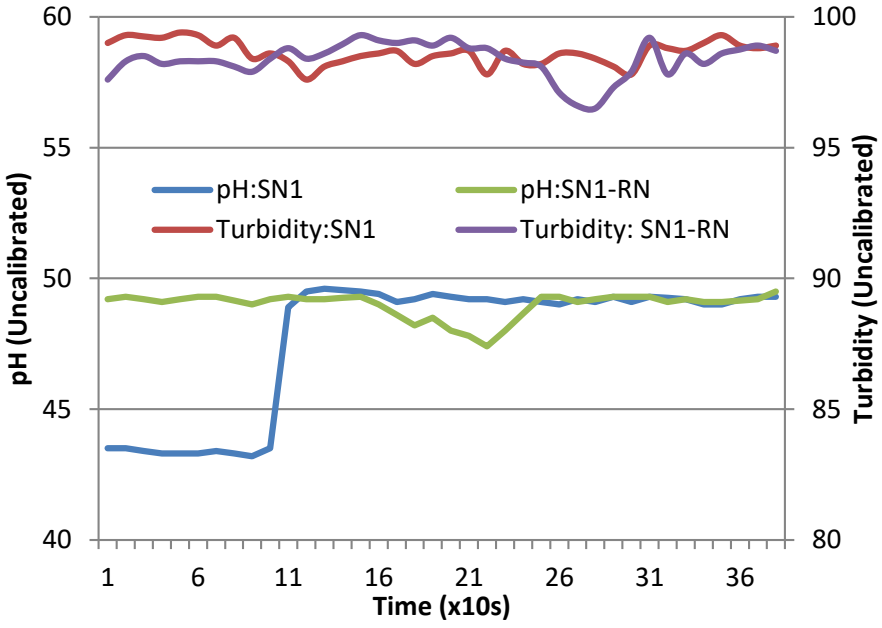

(a)

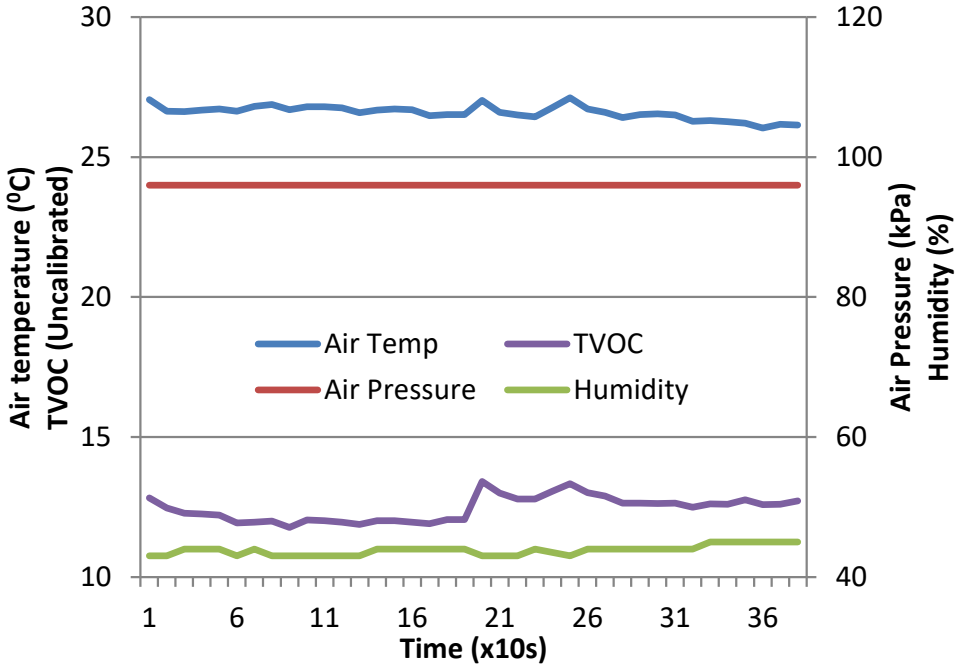

(b)

Figure 2-10. WQM parameters (**a**): pH and turbidity from two different SNs, (**b**): Temperature, humidity, pressure, and uncalibrated total volatile organic compound measure (TVOC) from different SNs.

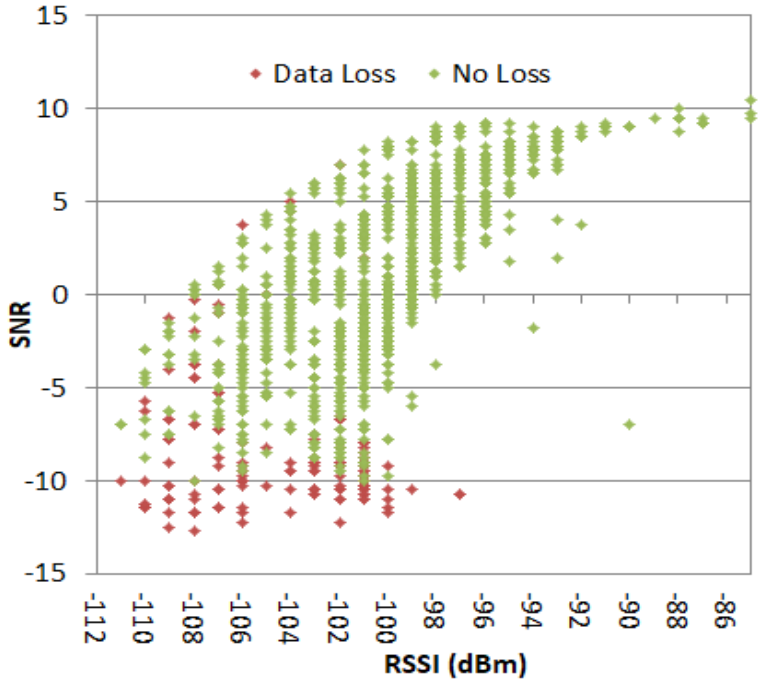

(a)

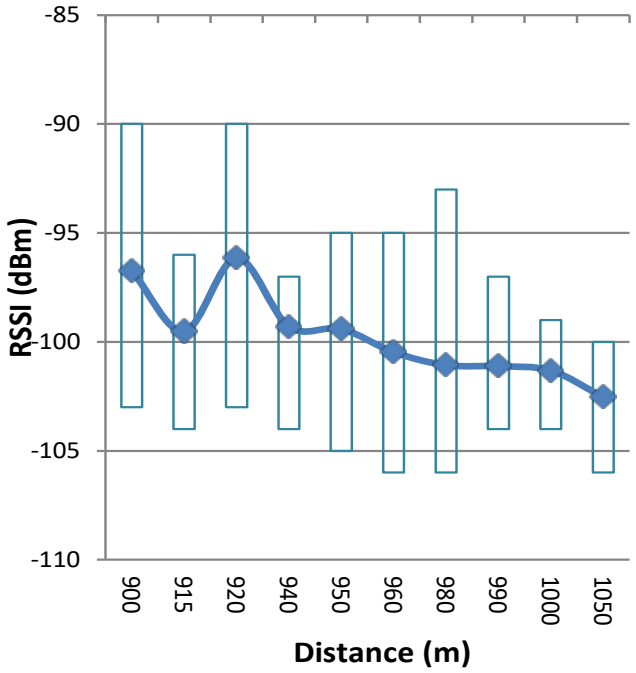

(b)

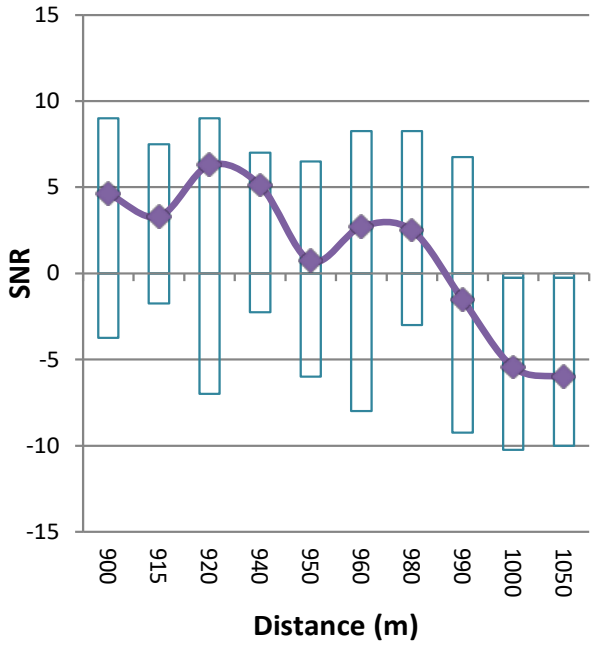

(c)

Figure 2-11. (**a**): Data loss at different RSSIs and SNRs, (**b**): RSSI and (**c**): SNR changes with the distance between the SN and DS.

2.6.2 Network Performance

Network performance was measured in terms of RSSI (Received Signal Strength Indicator), SNR (Signal to Noise Ratio), and data loss from the SN received by the DS. For the WARM application in some remote locations using a mobile DS radio signal, the quality depends on various environmental parameters along with the distance between the SN and the DS. With varying distances, data loss is the primary performance indicator, and when measured was found to depend on both the RSSI and SNR. Figure 2-11a shows that data loss becomes significant when the RSSI goes below −95 dBm with the SNR below 0. Increasing data loss was observed with a decrease of the SNR and RSSI, mainly above a 1000 m distance and without a line of sight. Figure 2-11b, c show the relationship between the RSSI and SNR with the distance between the SN and DS, respectively; the line curve is for the median values, and the box graphs show the ranges of RSSI and SNR values at different distances. These results can also be used by the mobile DS to improve the data delivery rate by using a RN or by changing the transmit power or the travel path.

2.6.3 Energy Performance

The SN's energy performance is one of the first parameters to measure the SN's life in the field and the lifetime of the WSN. The SN has three main components for measuring energy consumption: the MCU, the LoRa module, and the sensors. Irrespective of the components used, the total power consumption of the SN varies at the different events performed by the SN. These events mainly depend on the software algorithm and transmission time required for the protocol used. The events used to measure the SN's energy performance are startup-mode (the MCU is initializing), active mode (the MCU is running the normal functions such as housekeeping and sensor reading), sleep mode (the MCU is not running, and only the RTC (Real Time Clock) and sensor are functional), LoRa data receive mode, and LoRa transmission mode. We use a DC energy measuring unit and log the data to monitor the input voltage, current, and power consumption of the SN, at a resolution of 1 mV and 1 mA. The voltage is measured at the input of the sensor node as shown in Figure 2-8a and after the DC-DC converter. The DC-DC converter efficiency is considered to be 85% to calculate the lifetime of a node with the power supply used. The SN is configured to transmit data at three-second intervals to measure the energy consumption of the SN at different events, and the MCU operates at 16 MHz without any sleep mode. In the beginning, the MCU is re-started to begin the initialization event; it then moves to the active mode followed by the LoRa reception and transmission activities. The entire event's duration and power requirement are measured using an energy meter and data logger. Table 2-5 summarizes the event duration, voltage, current, power, and energy consumption, including energy consumption for a complete cycle. In this experiment, LoRa transmission time is kept close to the TOA_{max} by using a data packet size of 165 bytes. For the field operation with

a data transfer interval of 15 min, the MCU can be in sleep mode most of the time other than when it is active, and during LoRa transmission events. In this configuration, the LoRa transmission channel utilization was calculated as only 0.015%, which is very low compared with the LoRaWAN channel utilization ratios of 0.1% and 1.0%. Therefore, using LoRaPHY can increase the LoRa channel capacity, and hence, can accommodate more SNs in a specific WSN. SN lifetime using three 18,650 Li-Ion battery of 3.6 V and 6000 mAH, can be calculated as 681 days, which is a rough estimate and may depend on the working temperature of the sensor node itself.

Table 2-5. Event-wise energy calculation of the SN with a 3-sec cycle using the LDAP.

Event	Duration (mS)	Voltage (V)	Current (mA)	Power (mW)	Energy (mJ)
Active	T_{AC} = 2,407	5.01	31	P_{AC} = 155.31	E_{AC} = 373.83
LoRa Rx	T_{RX} = 336	5.01	44	P_{RX} = 220.44	E_{RX} = 74.07
LoRa Tx	T_{TX} = 135	5.00	148	P_{TX} = 740.00	E_{TX} = 99.90
Full cycle	2,878				547.80

The overall energy efficiency of the WSN using the proposed LDAP can easily be calculated using Equation (11). One method to measure the energy efficiency of a specific WSN algorithm or protocol is to express it in terms of the ratio of the energy required without implementing that algorithm or protocol and the total WSN energy required with the algorithm or protocol implemented. As the energy required for the algorithm or protocol is highly dependent on the method of implementation (software algorithm or methodology), the energy efficiency of the LDAP is not comparable with other routing protocols or algorithms using their proposed implementation. However, a comparison in terms of the energy efficiency is shown in Table 2-1 based on the general concept and Equation (11), where k is calculated using the number of hops (h) and the data relay factor (μ), as shown in Equation (13).

$$k = \quad \mu\left\{\frac{h}{2}(h+1)\right\} \tag{13}$$

Therefore, k is highly dependent on μ, which is highly dependent on the WSN topology used, and μ is variable over the whole WSN. It is lower for the higher hops than the lower ones. For a WSN with a short-range wireless link and a higher number of hops, μ will be very low. If the same values of μ are used for both the WSN with short-range [1] and long-range [30] wireless links it will have very low (50% to 70%) energy efficiency, which is not practical. To improve the energy efficiency of traditional WSNs, various clustering and optimization algorithms are implemented with the added costs of SN hardware resources and processing

energy. Therefore, the energy efficiency shown in Table 2-1 is calculated using different values for μ; $\mu = 0.1$ for a WSN with a long-range wireless link. For a WSN with a short-range wireless link with hops fewer than 5, $\mu = 0.1$, and with hops greater than 5, $\mu = 0.05$. As the proposed LDAP is designed considering only one hop, $\mu = 0.5$ is used for the WQM case. Even after optimization is applied to the traditional WSNs, the proposed LDAP shows an improvement in terms of energy efficiency.

2.6.4 Timing Performance

Timing performance of a routing protocol can be measured in terms of the time required for the data to be received by the DS from the SN after sending the data request message. The data request message has two main components: processing time (including message decoding, data encryption, and data packet processing) required for the specific protocol and the TOA of the wireless technology used. For the LoRa wireless network used with the proposed LDAP, the processing time (around 7 mS as measured for the prototype SN) is around 5% compared with the LoRa TOA (135 mS).

2.6.5 Features and Comparison

The proposed LDAP achieved the objectives of the WSN coverage in terms of the number of SNs and its geographical coverage, as well as meeting the long lifetime requirement. Table 2-1 shows a significant reduction (50%) in data sinks in zone 5 with cellular coverage, and is significantly reduced (81%) in zone 1 with poor cellular coverage. Moreover, other main features of the proposed LDAP are as follows:

- Unlike the UAV-mounted SNs or multi-hop static WSN, a mobile DS can increase the monitoring area coverage significantly. The proposed LDAP can acquire the sensor data using the mobile DS mounted on an UAV for most of the WARM applications where ground mobility may not be possible. UAV-based mobility is not possible for the SNs with short-range wireless links [1], as described in Section 2.3, due to the required altitude of the UAV; hence, long-range wireless connectivity is required. Moreover, multi-hop routing used for the traditional WSN may not be suitable for the mobile DS due to the routing complexity of the dynamic network topology.

- A mobile data sink is more energy efficient than a mobile sensor node, as the number of DSs is much lower than that of the SNs that would be required to cover the same area being monitored. The energy required to facilitate mobility to the SN or DS depends highly on the type of vehicle (or other means) used is not considered. However, for the same type of

mobility, a WSN using a mobile DS requires significantly lower energy compared with the WSN with a mobile SN. For a static SN with a static BS, there is no energy required for mobility; however, it may incur other costs due to the high number of BSs. Unlike image-based data acquisition, WARM applications do not require continuous streaming and the SNs can store data over time. The stored data can be transmitted when a wireless link is established with the DS, and in this way, the SN can acquire sensor data at a rate as high as 1-minute intervals and transmit it at 60-minute intervals using the proposed LDAP.

Table 2-6. Features of the proposed protocol and comparison with other technologies.

	Proposed LDAP	**Remote node [42]**	**Vehicle-mounted [35–38]**	**Conventional WSN [39–41]**
SN type	Static	Static	Mobile	Static
Network topology	Dynamic	Static star	Static Star	Static Star/tree
DS type	Static/mobile	Static	Static	Static/relocatable BS
Routing hop	Direct, single hop	Direct	Direct	Single/multi-hop
Energy consumption	Low	Low	High	Medium
Wireless interface	LoRa	Satellite	-	ZigBee and other
Coverage	Wider coverage using UAV mounted DS	Small coverage for static SN	Limited coverage using only mobile SNs	Wider coverage using a large number of nodes
Processing overhead	Very low	NA	NA	Moderate to High
Deployment complexity	Low	Moderate	Moderate	Moderate to High
Features	Low cost, low power	Low cost, less coverage	High cost,	Need network planning or optimization

- In terms of coverage, the number of mobile SNs is reduced compared to the static SNs; however, it may lose data coherence over time, which can be overcome by using static SNs associated with a mobile DS.

- Most of the routing optimization, clustering, and cluster head election in the WSN is performed using the residual energy and location of the SNs to keep the energy consumption of the SNs uniform (using a smaller cluster size closer to the DS) over the WSN. However, most of these procedures do not consider the environmental impact on the wireless signal quality, and require high processing resources and energy for the SNs, or use heterogeneous nodes (special nodes with higher energy consumption and capacity). The proposed LDAP can select direct RN-based data transmission, based on the residual energy, RSSI, and SNR

of the SNs. Therefore, it is more immune to the environmental impact on the wireless signal quality and can maintain the energy balance among the SNs with very low energy consumption due to its light weight.

- Moreover, most of the present cluster based WSNs use multiple hops for data transfer, which require maintaining a static network topology or a complex routing optimization for any changes of topology due to the relocation of the BS. In contrast, the proposed LDAP does not depend on the network topology, as it uses direct or single-hop data transmission from the SNs to the mobile DS.

- Present WSNs require complex clustering and routing algorithms to improve the efficiency of overall energy consumption. The complexity and processing load of this type of algorithm demand an additional resource (such as a high-speed processor and extra memory), which introduces energy overhead and cost. It makes the deployment of the WSN complicated and reduces scalability. On the other hand, the proposed LDAP uses only direct and single-hop data transfer, which is lightweight and suitable for resource-constrained sensor nodes. In addition, it reduces the deployment and expansion overhead in WSN implementations.

Some features of the proposed LDAP and other available technologies are summarized in Table 2-6. Unlike vehicle mounted mobile SNs, the LDAP uses static SNs to reduce energy consumption and the complexity of WSN deployment. It also helps to implement mobile DSs over the wide WSN, which is not used in any type of existing solutions. The use of mobile DSs requires support for network topology changes, which is achieved easily by avoiding multi-hop data transmission as done in most of the conventional WSNs. Unlike the satellite link and other wireless technologies such as Zigbee, the LDAP is optimized for LoRa (higher TOA than non-CSS technologies), which makes it consumes less energy and capable of wider geographical coverage.

2.7 Conclusion and Future Scope

This paper has addressed the main challenge of an IoT-based WARM system, where real-time data acquisition is required for the distributed resources. We have proposed a lightweight dynamic auto-reconfigurable protocol (LDAP) for the SNs using a mobile DS to increase the WSN coverage geographically and to maintain a long WSN lifetime. The proposed LDAP also focused on minimizing the number of hops for data transmission, which also reduced the routing complexity, and the DS-based control further reduced the processing load of the SN, thus increasing its lifetime. It is shown that the efficiency of the proposed protocol is highly dependent on the geographical distribution of the SN, and maximum benefit can be achieved for two-dimensional (over both the length and width of the monitoring area) SN distribution.

Maximum coverage and energy balance of the WSN also depend on proper path planning for the DS, which can be achieved offline by implementing various path optimization schemes. For future study, an offline or real-time path planning algorithm for the mobile DS could be developed to achieve the energy balance of the proposed LDAP. The coverage of the WSN for some applications, such as smart farming, where the sensor nodes are distributed both longitudinally and laterally with the direction of the moving DS, could be improved. A minimal clustering algorithm with a single-hop transmission could be implemented for a mobile DS.

Author Contributions: Conceptualization, G.R. and K.W.; methodology, G.R.; software, G.R.; validation, G.R.; formal analysis, G.R.; investigation, G.R.; resources, K.W.; data curation, G.R.; writing—original draft preparation, G.R.; writing—review and editing, K.W.; visualization, G.R.; supervision, K.W.; project administration, K.W.; funding acquisition, K.W. All authors have read and agreed to the published version of the manuscript.

2.8 References

1. Arjunan, S.; Sujatha, P. A survey on unequal clustering protocols in Wireless Sensor Networks. *J. KSU Comput. Inf. Sci.* **2019**, *31*, 304–317.
2. Gharaei, N.; Al-Otaibi, Y.; Butt, S.; Sahar, G.; Rahim, S. Energy-Efficient and Coverage-Guaranteed Unequal-Sized Clustering for Wireless Sensor Networks. *IEEE Access* **2019**, *7*, 1–9.
3. Bagci, H.; Yazici, A. An energy aware fuzzy unequal clustering algorithm for wireless sensor networks. *IEEE Int. Conf. Fuzzy Syst.* **2010**, 1–8, doi:10.1109/FUZZY.2010.5584580.
4. Mugo, R.; Waswa, R.; Nyaga, J.W.; Ndubi, A.; Adams, E.C.; Flores-Anderson, A.I. Quantifying Land Use Land Cover Changes in the Lake Victoria Basin Using Satellite Remote Sensing: The Trends and Drivers between 1985 and 2014. *Remote Sens*. **2020**, *12*, 2829.
5. Feng, Q.; Yang, J.; Liu, Y.; Ou, C.; Zhu, D.; Niu, B.; Liu, J.; Li, B. Multi-Temporal Unmanned Aerial Vehicle Remote Sensing for Vegetable Mapping Using an Attention-Based Recurrent Convolutional Neural Network. *Remote Sens.* **2020**, *12*, 1668.
6. Kimberly Mullen, C.P.G. "Information on Earth's water", National Ground Water Association. Available online: https://www.ngwa.org/what-is-groundwater/About-groundwater/information-on-earths-water (accessed on). 18th September 2020
7. Szumińska, D.; Czapiewski, S.; Goszczyński, J. Changes in Hydromorphological Conditions in an Endorheic Lake Influenced by Climate and Increasing Water Consumption, and Potential Effects on Water Quality. *Water* **2020**, *12*, 1348–1373.
8. Liu, S.; Ye, Q.; Wu, S.; Stive, M.J.F. Wind Effects on the Water Age in a Large Shallow Lake. *Water* **2020**, *12*, 1246–1262.
9. Magnússona, R.; Cammeraata, E.; Lückeb, A.; Jansena, B.; Zimmerc, A.; Rechartec, J. Influence of glacial sediments on the chemical quality of surface water in the Ulta valley, Cordillera Blanca, Peru. *Elsevier J. Hydrol.* **2020**, *587*, 1–16.
10. Kim, S.U.; Yu, X. Analysis of Dam Inflow Variation Using the Hydrological Sensitivity Method in a Trans-Boundary River Basin: Case Study in the Korean Peninsula. *Water* **2019**, *11*, 395–409.

11. Mena-Rivera, L.; Vásquez-Bolaños, O.; Gómez-Castro, C.; Fonseca-Sánchez, A.; Rodríguez-Rodríguez, A.; Sánchez-Gutiérrez, R. Ecosystemic Assessment of Surface Water Quality in the Virilla River: Towards Sanitation Processes in Costa Rica. *Water* **2018**, *10*, 845–860.
12. Singh, G.; Saraswat, D.; Sharpley, A. A Sensitivity Analysis of Impacts of Conservation Practices on Water Quality in L'Anguille River Watershed, Arkansas. *Water* **2018**, *10*, 443–464.
13. Caballero, I.; Stumpf, R.P.; Meredith, A. Preliminary Assessment of Turbidity and Chlorophyll Impact on Bathymetry Derived from Sentinel-2A and Sentinel-3A Satellites in South Florida. *Remote Sens.* **2019**, *11*, 645–664.
14. Carstens, D.; Amer, D. Spatio-temporal analysis of urban changes and surface water quality: Use of in-situ, GIS and satellite images for WQM. *Elsevier J. Hydrol.* **2019**, *569*, 720–734.
15. Kabir, S.M.I.; Ahmari, H. Evaluating the effect of sediment color on water radiance and suspended sediment concentration using digital imagery. *Elsevier J. Hydrol.* **2020**, *589*, 1–11.
16. Wei, L.; Huang, C.; Wang, Z.; Wang, Z.; Zhou, X.; Cao, L. Monitoring of Urban Black-Odor Water Based on Nemerow Index and Gradient Boosting Decision Tree Regression Using UAV-Borne Hyperspectral Imagery. *Remote Sens.* **2019**, *11*, 2402–2428.
17. Judah, A.; Hu, B. The Integration of Multi-source Remotely-Sensed Data in Support of the Classification of Wetlands. *Remote Sens.* **2019**, *11*, 1537–1564.
18. Olatinwo, S.O.; Joubert, T.H. Enabling Communication Networks for Water Quality Monitoring Applications—A Survey. *IEEE Access* **2019**, *7*, 100332–100362.
19. Khan, A.; Ali, I.; Ghani, A.; Khan, N.; Alsaqer, M.; Rahman, A.U.; Mahmood, H. Routing Protocols for Underwater Wireless Sensor Networks: Taxonomy, Research Challenges, Routing Strategies and Future Directions. *Sensors* **2018**, *18*, 1619–1648.
20. Wang, X.; Cheng, G.; Sun, Q.; Xu, J.; Zhang, H.; Yu, J.; Wang, L. An event-driven energy-efficient routing protocol for water quality sensor networks. *Wirel. Netw.* **2020**, 1–12. doi:10.1007/s11276-020-02320-4.
21. Du, R.; Gkatzikis, L.; Fischione, C.; Xiao, M. Energy Efficient Sensor Activation for Water Distribution Networks Based on Compressive Sensing. *IEEE J. Sel. Areas Commun.* **2015**, *33*, 2997–3010.
22. Wang, J.; Gao, Y.; Liu, W.; Sangaiah, A.; Kim, H. Energy Efficient Routing Algorithm with Mobile Sink Support for Wireless Sensor Networks. *Sensors* **2019**, *19*, 1494–1512.
23. Thiruchelvi, A.; Karthikeyan, N. Pair-based sink relocation and route adjustment in mobile sink WSN integrated IoT. *IET Commun.* **2020**, *14*, 365–375.
24. Bouguera, T.; Diouris, J.-F.; Chaillout, J.-J.; Jaouadi, R.; Andrieux, G. Energy Consumption Model for Sensor Nodes Based on LoRa and LoRaWAN. *Sensors* **2018**, *18*, 2104–2126.
25. Kim, J.; Song, J. A Secure Device-to-Device Link Establishment Scheme for LoRaWAN. *IEEE Sens. J.* **2018**, *18*, 2153–2160.
26. Marais, J.M.; Malekian, R.; Mahfouz, A.M.A. Evaluating the LoRaWAN Protocol Using a Permanent Outdoor Testbed. *IEEE Sens. J.* **2019**, *19*, 4726–4733.
27. Lee, H.C.; Ke, K.H. Monitoring of Large-Area IoT Sensors Using a LoRa Wireless Mesh Network System-Design and Evaluation. *IEEE Trans. Instrum. Meas.* **2018**, *67*, 2177–2187.
28. Qin, Z.; Liu, Y.; Li, G.Y.; McCann, J.A. Performance Analysis of Clustered LoRa Networks. *IEEE Trans. Veh. Tech.* **2019**, *68*, 7616–7629.

29. Zhu, G.; Liao, C.; Sakdejayont, T.; Lai, I.; Narusue, Y.; Morikawa, H. Improving the Capacity of a Mesh LoRa Network by Spreading-Factor Based Network Clustering. *IEEE Access* **2019**, *7*, 21584–21596.
30. Valencia, J.B.; Londono, L.C.; Viloria, D.M.; Garcia, M.R. Data Reduction in a Low-Cost Environmental Monitoring System Based on LoRa for WSN. *IEEE Internet Things J*. **2019**, *6*, 3024–3030.
31. Lee, J.Y.; Lee, W.; Kim, H.; Kim, H. Adaptive TCP Transmission Adjustment for UAV Network Infrastructure. *Appl. Sci.* **2020**, *10*, 1161–1174.
32. Tan, X.; Zuo, Z.; Su, S.; Guo, X.; Sun, X.; Jiang, D. Performance Analysis of Routing Protocols for UAV Communication Networks. *IEEE Access* **2020**, *8*, doi:10.1109/ACCESS.2020.2995040.
33. Baek, J.; Han, S.; Han, Y. Energy-Efficient UAV Routing for Wireless Sensor Networks. *IEEE Trans. Veh. Technol.* **2019**, *69*, 1741–1750.
34. Popescu, D.; Dragana, C.; Stoican, F.; Ichim, L.; Stamatescu, G. A Collaborative UAV-WSN Network for Monitoring Large Areas. *Sensors* **2018**, *18*, 4202.
35. Cao, H.; Guo, Z.; Wang, S.; Cheng, H.; Zhan, C. Intelligent Wide-Area Water Quality Monitoring and Analysis System Exploiting Unmanned Surface Vehicles and Ensemble Learning. *Water* **2020**, *12*, 681–695.
36. Esakki, B.; Ganesan, S.; Mathiyazhagan, S.; Ramasubramanian, K.; Gnanasekaran, B.; Son, B.; Park, S.W.; Choi, J.S. Design of Amphibious Vehicle for Unmanned Mission in Water Quality Monitoring Using Internet of Things. *Sensors***2018**, *18*, 3318–3340.
37. Koparan, C.; Koc, A.B.; Privette, C.V.; Sawyer, C.B.; Sharp, J.L. Evaluation of a UAV-Assisted Autonomous Water Sampling. *Water* **2018**, *10*, 655–670.
38. Lima, R.L.P.; Boogaard, F.C.; de Graaf-van Dinther, R.E. Innovative Water Quality and Ecology Monitoring Using Underwater Unmanned Vehicles: Field Applications, Challenges and Feedback from Water Managers. *Water* **2020**, *12*, 1196–1215.
39. Pham, T.N.; Ho, A.P.H.; Nguyen, T.V.; Nguyen, H.M.; Truong, N.H.; Huynh, N.D.; Nguyen, T.H.; Dung, L.T. Development of a Solar-Powered IoT-Based Instrument for Automatic Measurement of Water Clarity. *Sensors* **2020**, *20*, 2051–2066.
40. Mirzavand, R.; Honari, M.M.; Laribi, B.; Khorshidi, B.; Sadrzadeh, M.; Mousavi, P. An Unpowered Sensor Node for Real-Time Water Quality Assessment (Humic Acid Detection). *Electronics* **2018**, *7*, 231–241.
41. Demetillo, A.T.; Japitana, M.V.; Taboada, E.B. A system for monitoring water quality in a large aquatic area using wireless sensor network technology. *Springer Sustain. Environ. Res.* **2019**, *29*, 12–21.
42. Bisio, I.; Marchese, M. Efficient Satellite-Based Sensor Networks for Information Retrieval. *IEEE Syst. J.* **2008**, *2*, 464–475.
43. Flores-Díaz, A.C.; Quevedo Chacón, A.; Páez Bistrain, R.; Ramírez, M.I.; Larrazábal, A. Community-Based Monitoring in Response to Local Concerns: Creating Usable Knowledge for Water Management in Rural Land. *Water* **2018**, *10*, 542–556.
44. Thatoe Nwe Win, T.; Bogaard, T.; van de Giesen, N. A Low-Cost Water Quality Monitoring System for the Ayeyarwady River in Myanmar Using a Participatory Approach. *Water* **2019**, *11*, 1984–1999.
45. Yang, B.; Lai, C.; Chen, X.; Wu, X.; He, Y. Surface Water Quality Evaluation Based on a Game Theory-Based Cloud Model. *Water* **2018**, *10*, 510–524.

46. Grzywna, A.; Bronowicka-Mielniczuk, U. Spatial and Temporal Variability of Water Quality in the Bystrzyca River Basin, Poland. *Water* **2020**, *12*, 190–206.
47. Bhatti, E.-U.-H.; Khan, M.M.; Shah, S.A.R.; Raza, S.S.; Shoaib, M.; Adnan, M. Dynamics of Water Quality: Impact Assessment Process for Water Resource Management. *Processes* **2019**, *7*, 102–115.
48. Sackey, S.H.; Ansere, J.A.; Anajemba, J.H.; Kamal, M.; Iwendi, C. Energy Efficient Clustering Based Routing Technique in WSN Using Brain Storm Optimization. In Proceedings of the 15th International Conference on Emerging Technologies (ICET), Peshawar, Pakistan, 2–3 December 2019.
49. Lee, J.; Kao, T. An Improved Three-Layer Low-Energy Adaptive Clustering Hierarchy for Wireless Sensor Networks. *IEEE Internet Things J.* **2016**, *3*, 951–958.
50. Popli, S.; Jha, R.K.; Jain, S. A Survey on Energy Efficient Narrowband Internet of things (NBIoT): Architecture, Application and Challenges. *IEEE Access* **2018**, *7*, 16739–16776.
51. Ayoub, W.; Samhat, A.E.; Nouvel, F.; Mroue, M.; Prévotet, J.C. Internet of Mobile Things: Overview of LoRaWAN, DASH7, and NB-IoT in LPWANs standards and Supported Mobility. *IEEE Commun. Surv. Tutor.* **2018**, *21*, 1561–1581.
52. Ikpehai, A.; Adebisi, B.; Rabie, K.; Anoh, K.; Ande, R.; Hammoudeh, M.; Gacanin, H.; Mbanaso, U. Low-Power Wide Area Network Technologies for Internet-of-Things: A Comparative Review. *IEEE Internet Things J.* **2018**, *6*, 2225–2240.
53. LoRaWAN™ 1.0.3 Specification, LoRa Alliance, Inc. 2018. Available online: https://lora-alliance.org/resource-hub/lorawanr-specification-v103 (accessed on). 18th September 2020
54. Semtech SX1278. Available online: https://www.semtech.com/products/wireless-rf/lora-transceivers/
sx1278 (accessed on). 18th September 2020
55. LoRa Tools. Available online: https://www.loratools.nl/#/airtime (accessed on). 18th September 2020
56. Zypher. Available online: https://www.airbus.com/defence/uav/zephyr.html (accessed on). 18th September 2020

3. LDCA: Lightweight Dynamic Clustering Algorithm for IoT-Connected Wide-area WSN and Mobile Data Sink using LoRa

This chapter presents the proposed networking algorithm to improve network coverage, capacity, and energy efficiency for the WSN with mobile sensor nodes and data sink that utilizes LoRa for wireless connectivity. Wireless Sensor Network (WSN) using LoRa increases network coverage by extending the link. Mobile data sink with the Lightweight Dynamic Auto Reconfigurable Protocol (LDAP), as described in the previous chapter, can further extend this coverage. However, the mobile data sink may require travelling through multiple paths to cover more area for some applications like environmental monitoring and smart farming. An increasing number of data sinks may reduce the travel time for every data sink, extending the network coverage with additional cost and energy. Clustering is performed by grouping multiple sensors so that all can be connected to one or more sensor nodes by direct wireless link to increase the WSN coverage and improve energy efficiency. In a clustered WSN, sensor nodes of the distant clusters send their data through another sensor node (elected as the cluster head using the clustering algorithm) as a repeater. Nowadays, clustering is performed offline for the WSN with static sensor nodes and data sink. The WSN with mobile sensor nodes or data sinks requires real-time clustering during (or just before) the data accumulation process performed by the mobile data sink. Excessive processing and data transmission activities involved in frequent and real-time clustering reduce the energy efficiency and hence network lifetime. Therefore, this research proposes a lightweight and real-time clustering algorithm to reduce clustering time and increase energy efficiency. It also enhances the WSN lifetime, capacity, and coverage area.

The proposed Lightweight Dynamic Clustering Algorithm (LDCA) utilizes LDAP and performs real-time clustering before every data transfer phase to update the sensor node distribution in the WSN, considering the movement of the sensor nodes and data sinks. Due to the single-hop nature of the LDAP, LDCA creates two clusters at a time to reduce data overhead and clustering time. data sink initiates and controls the clustering phase. It elects two Cluster Heads (CHs) from the homogeneous sensor nodes based on their Received Signal Strength Indicator (RSSI), Signal Noise Ratio (SNR) and stored energy level. The possible maximum number of non-overlapped neighbor SNs are assigned to each CHs to maximize their coverage. Unlike other RSSI-based clustering schemes, LDCA avoids distance calculation and complex parameter optimization to reduce the clustering time and energy requirement, which is critical for the long Time on Air (TOA) of LoRa.

This research also proposes new matrices to measure the performance of a real-time clustering algorithm that supports mobility in the WSN. Mathematical models are derived for real-time clustering using LoRa, memory requirement and clustering efficiency of the constrained sensor node and data sink for various mobility scenarios. The proposed LDCA reduces the energy requirement to 33% compared to static clustering by reducing the number of

concurrent clusters and hops. In addition, a hardware-based approach was used to validate the LDCA algorithm and evaluate its performance in terms of energy efficiency, packet delivery rate, and network lifetime.

The development work, analysis and findings of this chapter is reported in the below mentioned published journal manuscript. The student contributed to the main idea, implementing code, writing the original draft, evaluation and revision of the manuscript.

G.M.E. Rahman and K.A. Wahid, "LDCA: Lightweight Dynamic Clustering Algorithm for IoT-Connected Wide-Area WSN and Mobile Data Sink Using LoRa," in *IEEE Internet of Things Journal*, vol. 9, no. 2, pp. 1313-1325, 15 Jan.15, 2022, doi: 10.1109/JIOT.2021.3079096.

Funding: This research is supported by a grant from the Natural Sciences and Engineering Research Council of Canada (NSERC).

LDCA: Lightweight Dynamic Clustering Algorithm for IoT-Connected Wide-area WSN and Mobile Data Sink using LoRa

Gazi M. E. Rahman, Member, IEEE, and Khan A. Wahid, Senior Member, IEEE

Abstract—Wide-area monitoring applications of an Internet of Things (IoT) connected Wireless Sensor Network (WSN) consists of sensor nodes (SNs) with limited hardware and energy sources. The distributed nature of such a network and the difficulty of remote access makes it more demanding to design an energy efficient WSN. Moreover, long-range and low-power wireless connectivity is a challenge in IoT-connected applications. Present WSN topologies deal mainly with fixed SNs, SN distribution, and fixed data sink (DS). The majority of the control layer is implemented in the lower hierarchical layer or in a virtual middle layer, which reduces the network lifetime due to excessive processing and data transmission activities. This paper proposes a real time lightweight dynamic clustering algorithm (LDCA) for a WSN that supports the following two scenarios with limited processing resources: (a) with mobile DSs and static SNs (such as, DS mounted on UAV and autonomous vehicles), and (b) with mobile SNs and static DSs (such as, livestock monitoring or autonomous robots in smart farming, and urban monitoring). The proposed algorithm is based on the Received Signal Strength Indicator and Signal to Noise Ratio of a LoRa (Long Range) interface and its residual energy. Mathematical models were derived for real-time clustering using LoRa. Memory requirement and clustering efficiency of the constrained SN and DS for various mobility scenario were evaluated. The proposed LDCA reduces the energy requirement to 33% compared to static clustering, by reducing the number of concurrent clusters and hops. In addition, a hardware-based approach was used to validate the LDCA algorithm, and evaluate its performance in terms of energy efficiency, packet delivery rate, and network lifetime.

Index Terms— Dynamic clustering, lightweight algorithm, LoRa, Internet of Things, Wireless Sensor Network, mobile sink, and mobile sensor node

3.1 Introduction

Wireless sensor network (WSN) faces challenges with the increased demand for wider coverage area. Existing long-range wireless technologies, like LoRa or ZigBee, are yet to support wide-area coverage in the range of hundreds of km due to the inherent limitations of higher power consumption, reduced LOS (Line of Sight), and complex network topology. The satellite-based long-range wireless monitoring [1] is not cost effective. Therefore, there is an opportunity to use ground-based LoRa wireless link and UAV (unmanned aerial vehicle) [2] to extend the coverage area and remote accessibility. Combining these two technologies to improve the coverage further has technical challenges, like accessibility, low-energy

requirement, and network management. This paper focuses to overcome these challenges by proposing a real-time clustering algorithm for a LoRa based network.

Unlike WSNs with short-range links, in a long-range WSN like urban monitoring or environment monitoring in the mountains, the sensor nodes (SNs) are often not densely populated and distributed along various dimensions. For this type of wide-area monitoring applications, SNs may need to transfer data to the data sink (DS) or base station (BS) over multiple hops, which is not energy efficient, and reduces the WSN lifetime. SNs in a wide-area WSN may lack sufficient sources of energy and have less accessibility. Therefore, a mobile DS mounted on the UAV can be introduced for the wide-area WSN. The advantages of using a UAV are that they can be refueled or recharged at the base-station or charging stations easily and frequently. On the other hand, applications like, smart farming with moving SNs (mounted on livestock) may move without any predefined path, where a fixed multi-hop topology is not possible. Moreover, depending on the applications, all the SNs of a WSN need to be of very low power, especially those run by batteries and at remote locations. Energy-efficient SNs may also have limited processing resources like memory and processing speed.

Hierarchical designs are already proposed that utilize heterogeneous network, clustering, and data compression to improve energy performance, WSN lifetime, and monitoring-area coverage of the WSN. Clustering is achieved by grouping the SNs in a geographical area [3]. Each cluster has a head, called cluster head (CH), which transfers or relays the accumulated data to the BS or DS directly or through other CHs. Clustering is one of the basic techniques used to improve WSN performance. Many algorithms are used for clustering, mainly in equally or uniformly distributed WSNs, where the positions and number of SNs are fixed. When clustering is used in a static WSN, residual energy is a primary consideration. Most algorithms are based on a low-energy adaptive clustering hierarchy (LEACH) [4], its variants [5], or LEACH with minor improvements [6]. Some algorithms use other parameters, like the quality of service (QoS) [7], the distance between the SNs and DS, or the geographical location of the SNs [8]. Clustering is also implemented using a control layer in a WSN or fog computing [9] of the IoT framework. In [10] multiple CHs are used in a single cluster with CH rotation. Multiple hops are also proposed for energy balance in the WSN.

All these static clustering algorithms suffer hot-spot and coverage problems due to an unexpected short life of some SNs near the DS, creating coverage problems for some SNs that use the SN as a hop. To overcome these problems and make the WSN scalable, fault-tolerant, and balanced, and to stabilize the network for different topologies, unequal clustering is proposed. This unequal clustering uses the random selection of CHs [11], the response time of a hello message [13], and GPS (Global Positioning System) [12] to get the location of a SN. The SN needs to change its transmit power to reach the BS [14], after the distance is calculated between the SN and BS using RSSI (Received Signal Strength Indicator) [15]. The main

limitations of these unequal clustering algorithms are: (1) the WSN deployment complexity of multi-layered clustering, (2) additional resource requirements of a fog-based virtual control layer, (3) higher data transmission of a software-based offline optimization for information gathering, and (4) a long transmit-time for WSNs during multi-hop routing or information-gathering phase.

Moreover, the SNs and DS's mobility in a WSN results in topology changes dynamically; as a result, it requires a dynamic and real time clustering algorithm, which involves both the SN and DS. LoRa, used for the wide-area WSN, has a higher time on-air (TOA) than other LPWAN (Low Power Wireless Area Network) technologies. Therefore, the clustering algorithm also needs to be fast enough for the mobile DS and SN while maintaining the wireless link between the DS and the candidate CHs. Considering the dynamic requirements of a WSN in wide-area monitoring applications, this paper focuses on the low-power, resource-constrained, and self-reconfigurable devices of the SNs. It also considers the mobility of the SNs and DS for wider coverage. The contribution of this work is as follows:

1. A novel lightweight dynamic clustering algorithm (LDCA) is proposed for homogeneous WSN with resource-constrained SNs and a LoRa (Long Range) wireless interface, based on RSSI, SNR (Signal to Noise Ratio), and residual energy along with a mobile DS and mobile SNs. The performance of the proposed LDCA is evaluated in terms of network lifetime, clustering time, and hop requirement.

2. A resource-constrained SN is developed for a homogeneous hierarchical wide-area monitoring application. The SN can reconfigure itself dynamically both as an edge node and a repeater node (RN) or a CH.

Recent work on dynamic clustering using mobile DS and BS relocation is described in the next section. Section 3.3 describes the system model with mobile SNs and a mobile DS, and their possible applications in order to illustrate the proposed algorithm. The proposed clustering algorithm is described in section 3.4. The experimental results are presented in Section 3.5. Section 3.6 presents the performance of the LDCA and comparisons with other related work in terms of efficiency and other features. Section 3.7 concludes the paper with the future scope of LDCA applications.

3.2 Related Work

In traditional dynamic clustering, most of the algorithms use a variable threshold and CH rotation. These algorithms do not support a mobile DS or SNs due to changes in network topology in the WSN. The research based on a mobile DS has mainly focused on path planning

[16] of the DS through various optimization approaches. BS relocation also has been proposed using a predefined path for a WSN with a fixed cluster, where the member SNs elect their CHs based on predefined weight [17]. The DS's repositioning in a known clustered WSN may not be suitable for an unclustered wide WSN.

The work in [18] uses a mobile DS for isolated SNs and shows how the lifetime and data throughput can be increased by using multiple mobile DSs. Scheduling for a mobile DS is proposed in [19] to support data transfer for SNs with variable sensing intervals. It focuses mainly on the SN's memory overflow management which can easily be done using larger local storage. It does not provide any CH election algorithm and may increase the DS's mobility rate in a wide WSN. Fuzzy logic is used in [20] for clustering and CH election, and a super CH is selected to communicate with the mobile DS, which may increase hops in a wide WSN and introduce heterogeneity. Ant colony optimization is used in [21] for the shortest path-planning of multiple mobile nodes, where the CHs are located in the center of the cluster, and the mobile DSs travel in a loop. This is suitable to minimize the travel path for a densely populated circular WSN. An optimization solution is proposed in [22] which considers the data transmission delay that a SN can tolerate. However, it does not consider the DS's travel-time from one SN to another SN and not the environment-dependent radio parameters like the RSSI. A multi-hop data transmission protocol to a mobile DS is proposed in [23], using static CHs called i-agents. Because all SNs and the DS need to know their absolute locations, the protocol is not suitable for a WSN with long-range links. Clustering based on dynamic thresholding of random numbers is proposed in [24] using the distance from the sink to transfer data to the BS by a moving agent. All the related calculations are performed by the SNs and may generate overhead. This algorithm is suitable for a densely populated WSN with the BS located in the center.

3.3 System Model

In addition to the mobile SNs and DS used for applications like environmental monitoring, water quality monitoring, and smart farming may have poor or no cellular coverage to connect a WSN with the IoT network, and the SNs may need to be distributed geographically over a wide area. On the contrary, applications like a smart city have better cellular coverage with densely populated sensor nodes. A mobile DS can improve wireless coverage for a widely distributed WSN, and a mobile SN (such as smart farming with moving livestock or a smart city with moving pedestrians) can be used to cover more data sources. However, the mobility of a DS or SNs in a WSN creates topology changes and may cause hot-spots in the WSN. Figure 3-1 shows the application-specific WSN model that is addressed in this research by proposing a dynamic clustering algorithm. It shows four types of WSN applications: (1) urban monitoring in a smart city, (2) environmental monitoring, and (3) smart farming based on LoRa, where any SN can act as a CH to transfer data to the mobile DS (mounted on an UAV or any other vehicle),

and (4) applications where a mobile CH can transfer data to a static base station (BS). LoRa alternates to the cellular network in a WSN for IoT connectivity through the LoRa-IoT gateway. For urban monitoring with partial cellular data coverage, a static BS or a mobile DS (at position 3) can also act as a gateway using the IP (Internet Protocol) link over the cellular data network; or a mobile CH can transfer data to a static BS or LoRa-IoT gateway.

On the other hand, a smart farming application may not have any cellular data coverage. The mobile DS (position 4) collects sensor data from the moving livestock through the CH and uploads it to the IoT server when it comes under cellular coverage (position 5). For applications like environmental monitoring or water quality monitoring that may have both static and mobile SNs, the mobile DS may need to travel a long distance to be under cellular data coverage. Therefore, the mobile DS collects data from the WSN (position 1) and travels close enough to a static LoRa-IoT gateway (position 2) to upload the data to the IoT server.

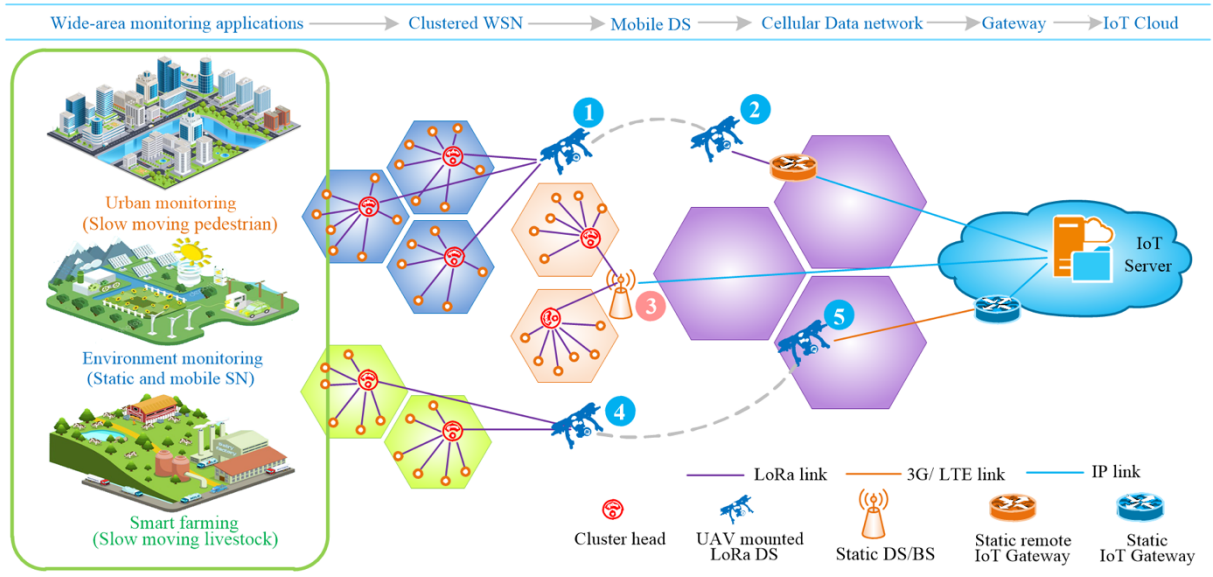

Figure 3-1. Wide-area monitoring applications using IoT-connected WSN with mobile DSs and mobile or static SNs

While designing a WSN for wide-area monitoring applications, we need low-power and long-range wireless technology for the sensor network and a different wireless communication technology for IoT connectivity with higher bandwidth and less dependency on the power requirement. To provide and maintain cellular coverage for a widely distributed WSN, mainly in rural areas, is not feasible either commercially or technologically due to lack of accessibility. Therefore, we need a non-cellular wireless network for a widely distributed WSN in some areas along with the existing cellular network, depending on its availability. Among the LPWAN (Low Power Wide Area Network) technologies, LoRa is chosen for its low-power and long-

range connectivity based on the performance evaluated in [25, 26]. Unlike LoRaWAN (LoRa Wide Area Network) and NB-IoT (Narrow Band IoT), LoRa-PHY (LoRa Physical) can be used to achieve more flexibility for dynamic topology configuration by implementing a custom data-link with network layers on it. LoRaWAN supports three types (A, B, and C) [27] of channel acquisition, whereas custom channel acquisition can be used for the proposed LDCA.

3.4 Proposed Algorithm

Along with the changes in dynamic topology, the proposed LDCA algorithm uses LoRa for its low-power and long-range capabilities. However, since LoRa has longer TOA than other LPWAN technologies due to its narrow band-width and spreading factor [34], the time required for clustering operation plays an important role in the total energy of the LDCA algorithm. Therefore, to keep the time minimum is one key objective of the work. In addition, to maintain the low energy requirement, the LDCA algorithm must have an efficient data transfer scheme (as explained in section 3.6). For the remote SNs with energy scarcity, the LDCA considered the SN as a resource constrained element in terms of energy and hardware resources [28]. The LDCA works in real-time where, the clustering process is performed by both the DS and SNs. To maintain the homogeneity of the WSN, all the SNs must be capable of functioning as a CH; hence, a SN can reconfigure itself either as an edge SN or as a CH during the data transfer phase. The auto re-configurability aspect is described in subsection 3.4.3.

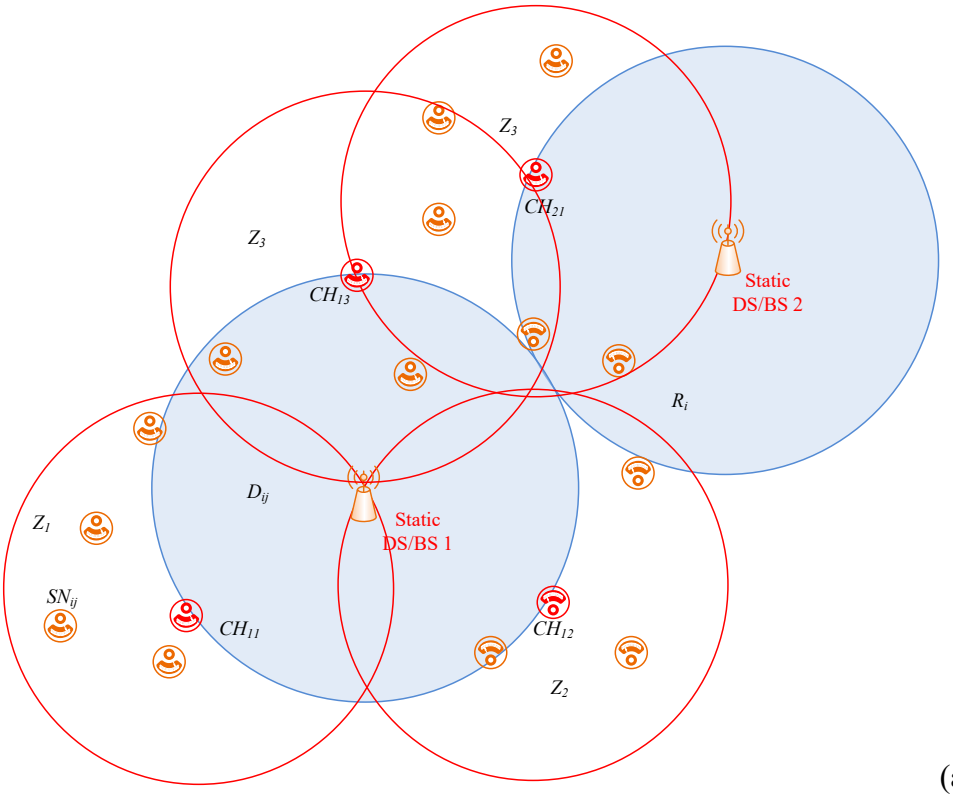

(a)

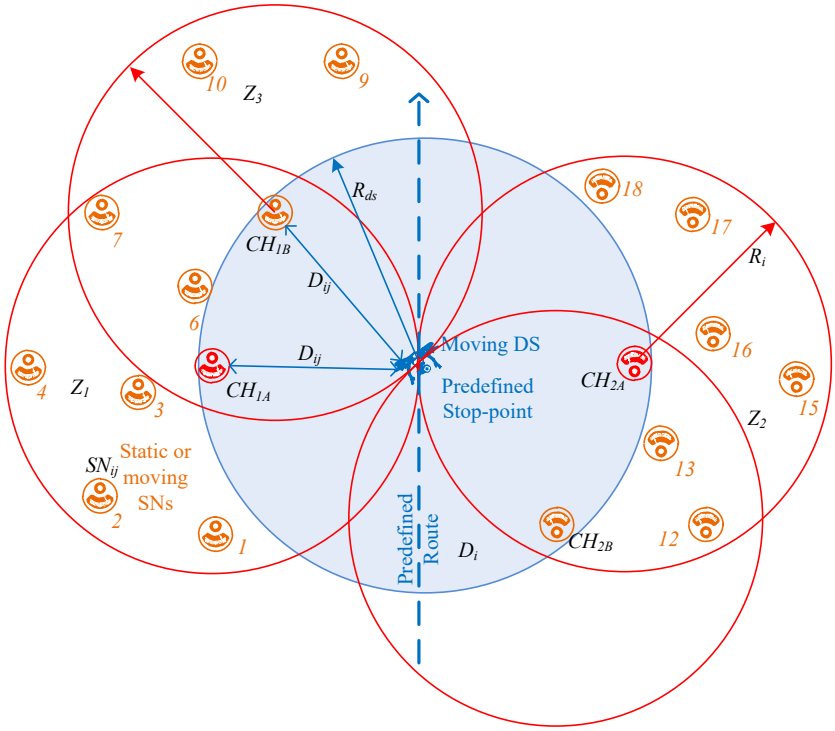

(b)

Figure 3-2. WSN topology in LDCA with (a) moving SNs and static DS/BS, and (b) moving DSs and static (or moving) SNs

Therefore, while developing the algorithm for a wide-area WSN with mobile SNs and/or mobile DS, we establish the following conditions:

1. All the SNs are homogeneous in terms of hardware resources and energy requirement,
2. LoRa transmission power is fixed and the same for all the SNs,
3. The DS is mobile and follows a predefined path and stop-points to keep the routing simple,
4. SNs may have slow mobility in a WSN and will be in the DS (or CH) coverage, maintaining an RSSI threshold for the period of one cycle of operation, and
5. All SNs have a unique physical ID over the WSN.

Figure 3-2(a) shows the WSN with moving SNs and static DS/BS applicable for urban monitoring and start farming applications. Figure 3-2(b) shows the WSN with static SNs and moving DS, which is better matched for environmental monitoring or water quality monitoring applications. It is noticeable that a WSN with the static BS may require more BSs to cover the same area as covered by a WSN with mobile DS. Therefore, WSN with mobile DS is used for a detailed analysis and modeling of the proposed LDCA. It is also applicable for the WSN with

static DS/BS. Figure 3-2(b) indicates the predefined path, direction, and stop-point (using off-line path planning tools or optimization algorithms) for the mobile DS. Thus, all the SNs are distributed around the DS forming two dynamic clusters with the DS's positions. The proposed LDCA uses RSSI and SNR as the QOS (quality of service) parameters, not to calculate the distance or directions of the SNs from the DS or CHs, but to reduce the computational load for the SNs. However, RSSI and SNR have a relationship with the distance between the SN and DS, that is further explained in section 3.5.

For a very short duration, the SNs can be considered static with respect to the DS forming two static clusters on both sides. The two CHs, shown as Z_1, Z_2, with CH_1, CH_2, and D_i are the group of SNs that are in the communication range of the DS. R is the maximum range of LoRa coverage with the predefined threshold for the RSSI and SNR. To cover the maximum possible SNs in a period and to maintain the total time to sink sensor data through the CHs and the overall energy requirement of the CHs at their lowest levels, the following conditions are needed in order to form the clusters and to elect the CH:

1. SNs within the LoRa coverage range of the elected CH will form the cluster,
2. Only one CH will be elected on one side of the DS,
3. A cluster centering the DS will be avoided,
4. No cluster will be considered with SNs on two different sides of the DS, as shown by the shaded area in Figure 3-2, and
5. The DS has an updated local database of the SN's unique ID, whose data are to be acquired for a particular geographical route.

Table 3-1 Symbols used for the algorithm

Symbol	Description	Unit
Z_i	Cluster with the ID i	
CH_i	Cluster head of cluster i	
D_{ij}	Distance between SN and DS	*m*
R_i	LoRa coverage of a CH	*m*
R_{ds}	LoRa coverage of the DS	*m*
$RSSI_{ij}$	RSSI for a SN to DS receive	*dB*
SN_{ij}	Sensor node with the index in cluster i	
E_{ij}	Energy utilization of a SN	*mJ*

3.4.1 Clustering and CH election algorithm

The proposed algorithm has three main phases, which are initialization, clustering, and data transmission. The initialization phase creates the CH-candidate list and elects the CH; it creates the neighbor list for the elected CH with maximum coverage and minimum overlap in the clustering phase. Table 3-1 lists the symbols used for the remaining sections of this paper, where *I* stands for the cluster-index and *j* stands for the node index of a cluster (different from the unique SN-ID that will be used in the communication protocol).

Table 3-2 LoRa Parameters with their default values

Symbol	Description	Value
SF	Spreading Factor	7
BW	Bandwidth (KHz)	250
CR	Code Rate	1
nPR	Preamble Length	8
H	Explicit Header Enable (0: enable)	1
CRC	Cyclic Redundancy Check Enable (1: enable)	0
D	Low Data Rate Enable (0: disable)	0
PL	Pay load (0 to 256 bytes)	

Candidate CH list creation: At the beginning of the clustering and CH election process, the DS will broadcast a CH election request and wait for the response from all the SNs in its coverage R_{ds}. The DS will create a list of the candidate CHs based on their residual energy level, RSSI, and SNR, which will consist of SNs from both sides of the DS. To avoid collision of the SNs transmission, SNs will introduce a time delay as a multiple of the six lower bits of ID (as explained in the protocol sub-section) and the TOA (time on air). The TOA can be calculated using equation (1), derived from the manufacturer datasheet [29] and validated using the online calculator [30] with the LoRa parameters given in Table 3-2.

$$TOA = \left(20.25 + \text{ceil}\left[\left(\frac{2PL-SF+7}{SF}\right)\right]5\right)\left(\frac{2^{SF}}{BW}\right) \quad (1)$$

For a 10-byte CH request message, the TOA will be 18.05ms. Therefore, for the recommended duty cycle of 2s, we can calculate the maximum number of SNs in a cluster as

$$N_{max} = \text{ceil}\left(\frac{Duty\ Cycle}{2\ TOA}\right) = 64 \quad (2)$$

For a densely populated WSN where all SNs are within the coverage of the DS, we can have a total of 64 SNs. For a uniform distribution of SNs, a cluster has 32 SNs on each side of the DS. The possibility of a collision of the SNs' transmitted messages, as shown in Figure 3-2, depends on the relative positions of the SNs within the coverage area R_{ds} of the DS with a Node Degree (number of neighboring nodes) [8] of 6 for a widely distributed WSN. These SNs are considered to be at the same distance from the DS (D_{ij}=radius of R_{ds}/2). Therefore, if all six SNs have the same lower 6-bits of their ID; the possibility of data collision of their transmitted messages will be

$$P_{col} = 6\left(\frac{1}{64}\right) = 0.094 \qquad (3)$$

However, this can further be reduced by reassigning the IDs of the SNs during their deployment.

Neighbor list creation: This can be done using either an offline database stored in the DS or regenerating the database dynamically depending on the application. For an application with static SNs offline database, applications with moving SN regenerating database would be preferable. The choice between these two options can be made based on total memory and energy requirements.

1) Static SN and mobile DS

The offline database is an N-dimension square matrix, where N is equal to the number of SNs of the whole WSN or a geographical part to be covered by the moving DS. For a widely distributed WSN, it may grow up to 256x256 or more. The memory requirement for the neighbor list database can be calculated using equation (4).

$$Memory_{static} = 2k + \left(\frac{k}{8}\right)^2 \qquad (4)$$

Where, k is the number of SNs in the WSN with 16-bit IDs. The first part of the equation (which is $2k$) represents the memory requirement in bytes to hold the IDs of the k number of SNs. The second part (which is $k/8$) is a bitmap for a SN with other SNs having neighborhood relation or not (1 or 0), and the square comes for all the k number of SNs with the remaining (k-1) number of SNs neighborhood relationship bitmap. For self-neighborhood, the specific bit is insignificant; however, it is stored in the memory space for linearity. Therefore, for k=256, memory requirement will be 1536bytes, and for the maximum value of $k = 2^{16}$. The memory requirement will be 68 Mbytes. This memory requirement can be met in a DS as implemented using a RaspberryPi 3B, and no memory is required in the SNs.

2) Mobile SN and static DS

For applications with mobile SNs with static or mobile DS, a dynamic neighbor list is generated by the candidate CH and DS. Therefore, memory constraint SN is considered. In this process, the DS will send a neighbor-list update message to the SNs listed in the candidate CH list created in step-1. Each candidate CH will broadcast a Presence message, receives the response, generate a neighbor list of its own, and send it to the DS. The memory requirement in the candidate CHs for the dynamic neighbor list can be found using equation (5).

$$Memory_{list} = 2i + \sum_{x=1}^{i} 2j_x \qquad (5)$$

Where, i is the number of SNs in the CH candidate list, assuming each of them has its cluster, and this number will be two at the end of the CH election process. The dynamic database will be an $i.j_{max}$ matrix as follows.

$$\begin{bmatrix} SN_{x=1,j=1} & \cdots & \cdots & \cdots & SN_{i=1,j=j_{max}} \\ & \cdots & \cdots & \cdots & \cdots & \cdots \\ & \cdots & \cdots & \cdots & \cdots & \cdots \\ & \cdots & \cdots & \cdots & \cdots & \cdots \\ SN_{x=i,j=1} & \cdots & \cdots & \cdots & SN_{x=i,j=j_{max}} \end{bmatrix}$$

The memory requirement for this matrix can be calculated using equation (6).

$$Memory_{dynamic} = 2i + 2j_{max} + \left(\frac{i}{8}\right)\left(\frac{j_{max}}{8}\right) \qquad (6)$$

Where, i = number of SNs in the specific CH candidate, $i = 2$ at the end of the CH election process which examines only two CHs in two clusters.

CH election and clustering: This step's main objective is to elect only two CHs and their clusters with minimum overlap. After prioritizing candidate CHs based on energy, the RSSI, and SNR, the candidate with the maximum number of neighbors will be elected as CH1. A single-bit flag is used to count the neighbors in the neighbor list, and then a bitwise AND operation is performed to elect CH1 and CH2. Similarly, an exclusion list is generated which is not in the neighbor list of the CH1 and CH2. This process can be done iteratively by choosing

different candidate CHs to minimize the overlap. The clustering phase needs to be done once before the data accumulation by the DS, and the same clustering phase will be performed for the next geographical location or for rotation of the CH. CH rotation can be performed using threshold values for one or any combination of residual energy, RSSI, and SNR of the present CH. Table 3-3 summarizes the CH election from 4 candidate-CHs based on their neighbor list, as shown in Figure 3-2(b). Here, numeric IDs are used for the SNs other than the candidate CHs for simplicity. In cluster 1, CH1A and CH1B are chosen as CH candidates with 7 and 5 neighbors SNs, respectively. As CH1A has more non-overlapping SNs than CH1B, it is elected as the CH for cluster 1. Similarly, CH2A is chosen for cluster 2.

Table 3-3 CH election and clustering: Candidate CHs with their neighbor list

Cluster ID	Candidate CH	Neighbor List (Overlapped)	Total SN	Total non-overlapped SN
1	CH1A (5)	1,2,3,4, (6, 7, CH1B)	7	4
1	CH1B (8)	9, 10, (CH1A, 6, 7)	5	2
2	CH2A (14)	15,16,17, 18 (CH2B, 12, 13)	7	4
2	CH2B (11)	(12, 13, CH2A)	3	0

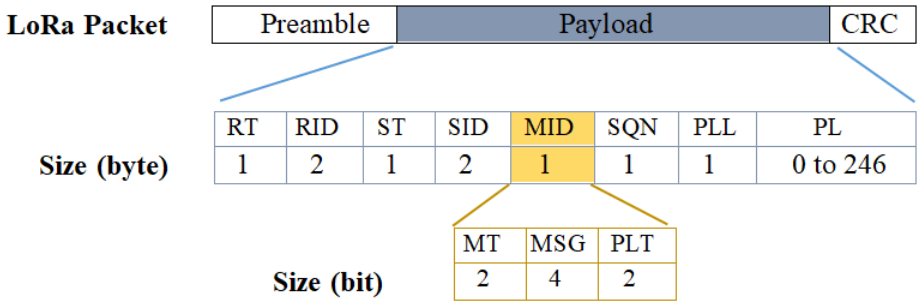

Figure 3-3. Implemented message format for LDCA to be used with LoRa-PHY

3.4.2 Data transfer protocol

To implement the proposed algorithm, a lightweight communication protocol over the LoRa-PHY is also proposed. Unlike LoRaWAN, a data sink controlled channel access scheme is implemented using the SN-ID. A master initiated communication protocol keeps the SN's energy requirement low, avoids collision of SN transmission, and provides better synchronization in the WSN. Figure 3-3 shows the message format with the LoRa preamble and CRC (Cyclic Redundancy Check), where implicit header mode is used to reduce LoRa TOA. One single packet can be 12 to 256 bytes depending on the regional channel utilization limit

defined by the LoRa alliance. The packet transmitter and receiver types (ST, RT) can be any of the data sink, cluster heads, and end nodes.

Table 3-4 IoT-WQM communication packet description

Tag	Full name	Description and values
RT	Receiver Type	1: sink, 2: CH, 3: node
RID	Receiver ID	0-65535
ST	Sender Type	1: sink, 2: CH, 3: node
SID	Sender ID	0-65535
MID	Message ID	Message and payload type
MT	Message Type	0x0 - 0x3 0x0: Data transfer, 0x1: Command
MSG	Message	0x0 - 0xF 0x1: Req., 0x2: Ack., 0x3: Data, 4
PLT	Payload Type	0x0 - 0x3
SQN	Msg. seq. number	0-255
PLL	Payload Length	Not used (set1), For future use

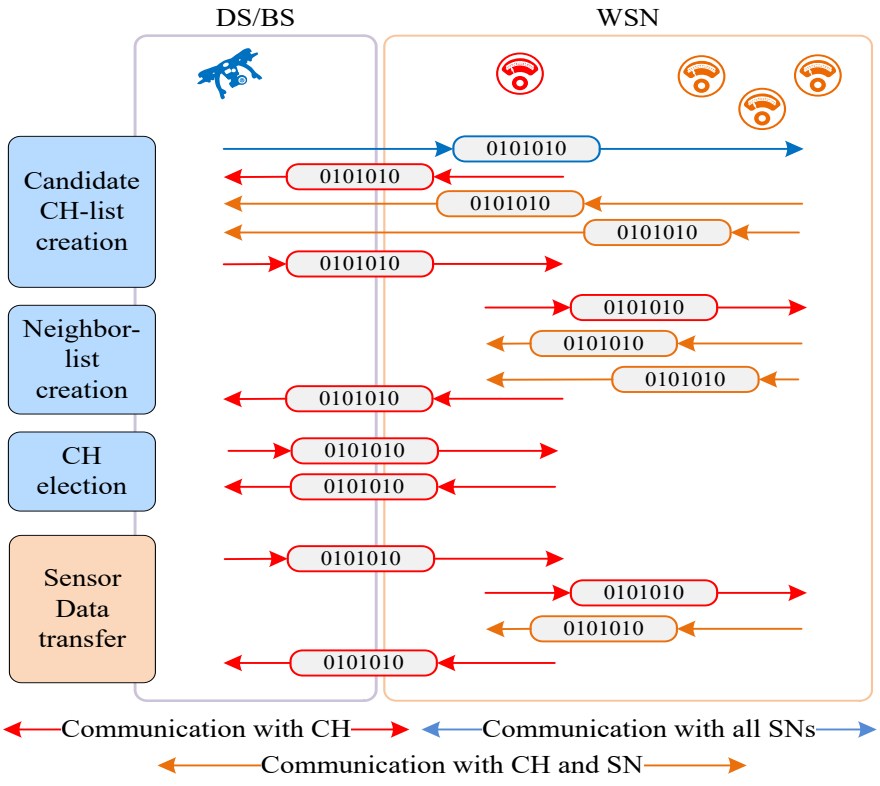

Figure 3-4. LDCA message flow during the clustering and sensor data transfer phases.

Table 3-4 describes all the fields of the LoRa-Packet. Receiver, Sender types facilitate the SNs and data sink to configure the WSN as star, tree, or cluster dynamically according to the WSN application requirement. SQN keeps track of the link between data requests in order to cope with the multi-node transmission, mainly in a mesh network. PLT facilitates data transfer for a LoRa packet of a payload larger than 247 bytes. The payload consists of the sensor data, measured parameter unit, and timestamp. It also includes the SN-ID which implements the message transfer by the CH. Figure 3-4 shows the simplified message flow for LDCA clustering, CH election, and sensor data transfer phases. The WSN shows two different types of SNs; the red SN is the probable CH, and the rest, with lower RSSIs (far from the DS), have a lower probability of being elected as the CH.

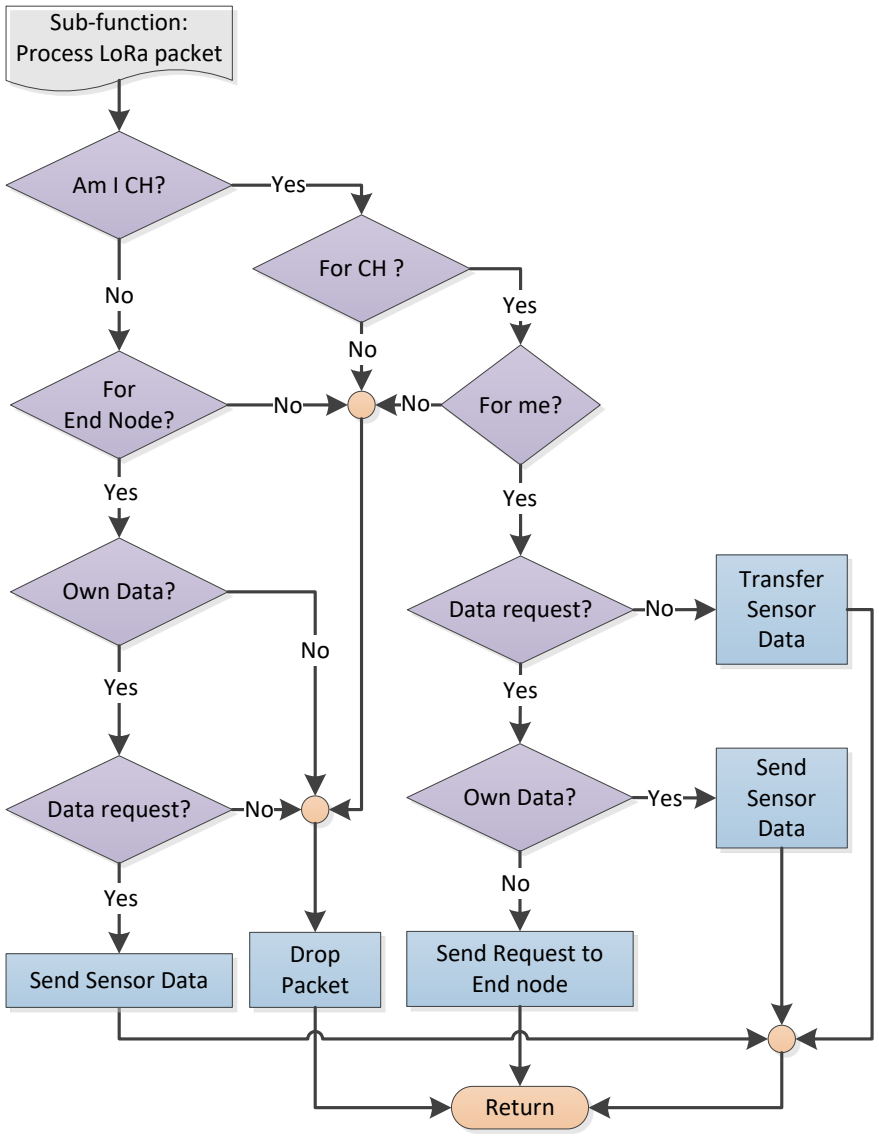

Figure 3-5. Dynamic auto reconfiguration algorithm for SN/CH operation in data transmission phase.

3.4.3 SN auto reconfiguration

During dynamic clustering after CH election, all SNs communicate only with the CH; however, the DS can request direct information from the SNs for validation if required. Both the SNs and CH perform their tasks depending on the DS request, and the DS can change the CH if required. Therefore, all the SNs must have the capability to function like a CH which requires a dynamic reconfiguration algorithm of the SN. Figure 3-5 shows the algorithm of SNs required for this dynamic activity. It does not include LoRa packet processing and transmission functions.

3.4.4 Timing model

This proposed algorithm is time sensitive due to its dynamic nature and CSS (Chirp Sprayed Spectrum) modulation used for LoRa communication. The required time for clustering and data acquisition by a moving DS and moving SNs is governed by the area and number of SNs to be covered, and the frequency of the data collection, which can be written as

$$T_{cl} = (1 + j)T_1 + (1 + j)kT_2 + k(T_3) + 2T_4 \quad (7)$$

where T_1 is for the presence message between the DS and SNs,
T_2 is for neighbor list request messages,
T_3 is for neighbor list update messages,
T_4 is for the CH election confirmation message, and
k is the number of shortlisted SNs for the CH election

As T_1, T_2, and T_4 are the TOA of 8-byte messages, they can be replaced by TOA_8. T_3 depends on the number of SNs in the coverage area of the candidate CHs. Its maximum value depends on the total SNs in the coverage of that DS at a particular position, which is 64 according to N_{max} as calculated in (2). Therefore, the maximum time can be calculated using (9), which is 3273.5ms, using only one shortlisted CH, as shown in Figure3-2. Equation (7) shows that the total time required for the LDCA with a set of given LoRa parameters is linearly dependent on the number of SNs present in the DS coverage area.

$$T_{cl} = (3 + j + k + jk)TOA_8 + k.TOA_{64} \quad (8)$$

$$\begin{aligned} T_{cl\_max} &= 15.5(j + jk) + 125.5k + 46.5 \quad (9) \\ &= 1117.5k + 1038.5 \quad [j=N_{max}=64] \\ &= 3273.5 \text{ ms} \quad [k=2] \end{aligned}$$

Figure3-6 shows the required time for the LDCA at a given position of the DS for different values of k (number of candidate CHs). It also shows the lowest value of k for a different density of the WSN (represented by the number of SNs, here *j*) that should be used to populate the list of possible CHs, which is *j*/2, in order to consider at least one CH for two SNs. Therefore, forming less number of clusters using small values of *k* gives less time. For LDCA with only two clusters at a time can use *k* = 4, which is two times the number of clusters, considering the tradeoff between the lowest clustering time and highest number of candidate CHs at the same time. The goal is to achieve lower clustering time that will increase the mobility of the DS (by reducing flight time), and minimize the clustering energy.

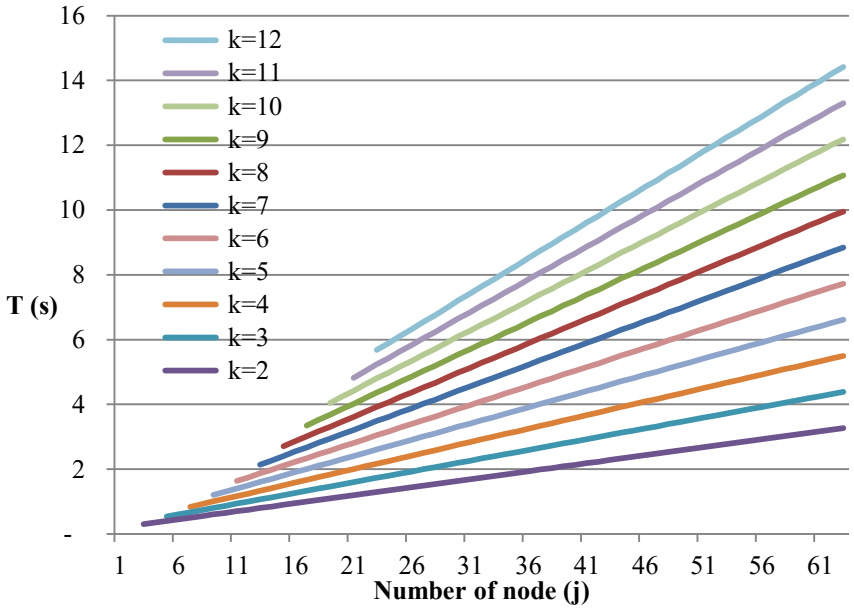

Figure 3-6. LDCA clustering time required for different densities (in terms of number of SNs) of the WSN and number of candidate CHs (*k*)

3.4.5 Energy model

The total energy required for the proposed algorithm depends mainly on the energy required for wireless message transmission during the clustering phase and CH election process, which depends clearly on the LoRa TOA directly of those operations. The total energy of the WSN can be expressed as

$$E_{WSN} = E_j + E_k = f(j, TOA_8) + f\left(k, TOA_8, TOA_j\right) \quad (10)$$

where,

E_j is the energy required for all the SNs = $P_{TX}.T_J$,

E_k is the energy required for shortlisted SNs = $P_{TX}.T_k$,

P_{TX} is the power requirement for LoRa transmission,

$T_j = j.T_1 + \left(\sum_{x=1}^{k} j_x\right).T_2$

$T_k = k.T_1 + k.T_3$

$T_1 = T_2 =$ TOA$_8$ and T_3 are as explained in subsection 3.4.3. Therefore, from (10), the total energy of the network can be written as (11), where j_x is the number of neighboring SNs with every shortlisted CH that depends on their coverage. For simplicity, the possible maximum neighboring SNs of every shortlisted CH is considered equal to the total number of the SNs under the DS coverage. At a particular position given by j, this will give the possible maximum energy requirement (E_{max}) as (12) of a WSN for the LDCA. The maximum clustering energy (E_{max}) is linearly related to the total number of SNs in the DS's coverage and the number of SNs in the shortlisted CHs as shown in (7). P_{TX} is highly dependent on the hardware type used for the SNs; we measured it in the lab for the SNs used for this research.

$$E_{SN} = \{(j + k + \sum_{x=1}^{k} j_x).TOA_8 + k.T_3\}.P_{TX} = f\{(j + k + \sum_{x=1}^{k} j_x).TOA_8 + k.T_3\} \quad (11)$$

$$E_{max} = \{(j + k + j.k).TOA_8 + k.T_3\}.P_{TX} = (T_{cl} - 3.TOA_8).P_{TX} = (T_{cl} - 46.5).P_{TX} \quad (12)$$

3.5 Experimental results

We conducted both simulation-based and experimental validation of the timing and energy model of the proposed LDCA and evaluated its performance. The experiment consisted of several sensor nodes and a mobile data sink. The resource-constrained SN consisted of an 8-bit microcontroller (ATMega328) with 32KB of ROM, and 2KB of RAM, which ran at 16 MHz. Each had a LoRa-Phy module to communicate with the DS. The DS consisted of a 32-bit system (Raspberry pi 3) that can support a lightweight operating system like Linux to run routing and media conversion operations as a LoRa-IoT gateway [31]. The DS had three wireless interface types: LoRa to communicate with SNs, 3G (or NB-IoT), and WiFi to communicate with the IoT network.

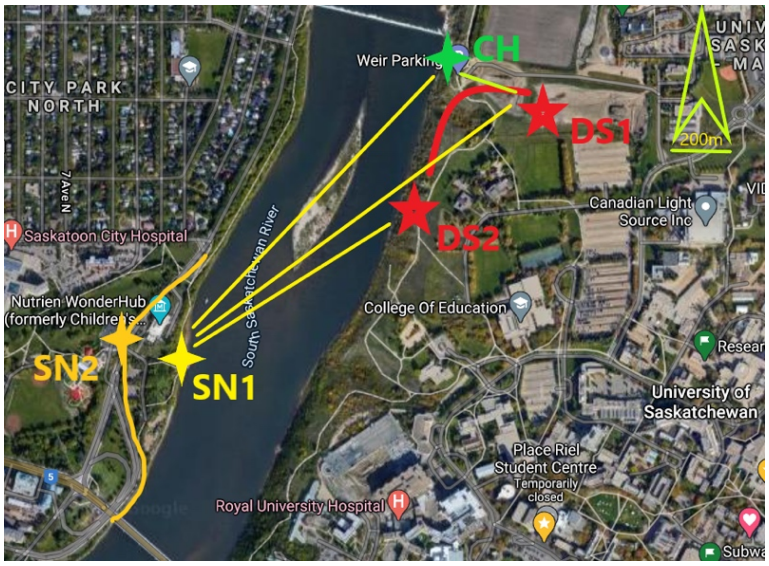

Figure 3-7. LoRa QoS measurement using moving SN and moving DS to validate the use of RSSI and SNR for LDCA

3.5.1 Validation of hypothesis

The first phase of the experiment was to measure the RSSI and SNR of LoRa for a variable distance between the SNs and DS to validate the hypothesis used in this work to develop the LDCA. Figure 3-7 shows the simplified experimental setup, where the yellow "star" indicates a SN and the green "star" is a CH; the red "star" is the DS moving between the positions DS1 and DS2 along the path as shown by a red line. The distance between the DS and SN varies from 800m to 1200m, as shown by yellow lines. After clustering, the DS received data from the SN through the CH. While receiving data from the SN, there was no LOS (line of sight) at some DS's positions due to the geographical terrain of the test site.

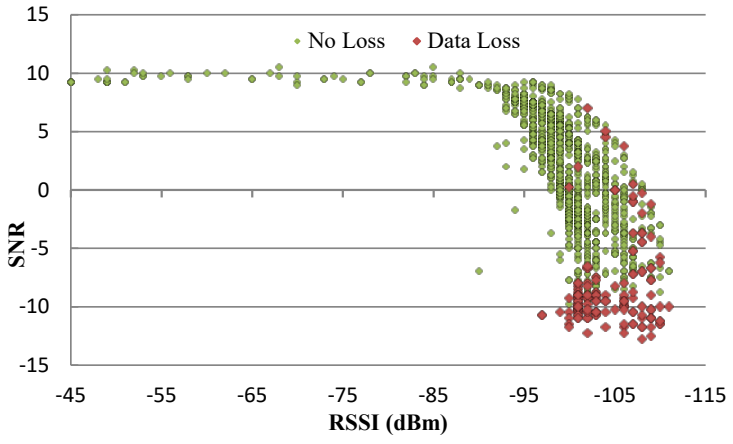

(a)

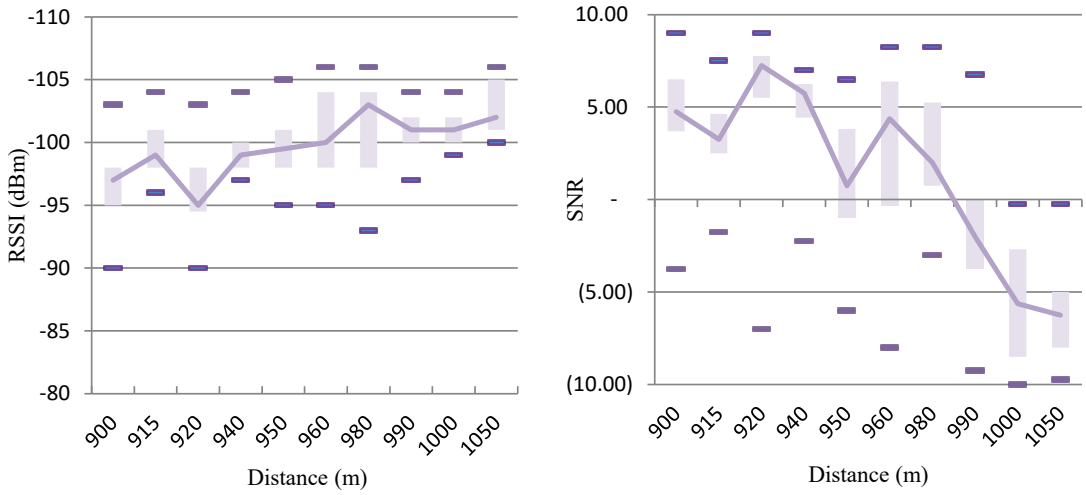

Figure 3-8. (a) Partial Packet loss at different RSSI and SNR, (b) RSSI, and (c) SNR changes at different distances between the SN and DS

The LoRa module was configured for 20dBm transmit power, -144dB receiving sensitivity; other parameters are shown in Table 3-3. More than 800 packets were collected successfully in two different experiments. Besides monitoring the RSSI and SNR, partial (a few bytes) packet loss was also measured. Packet loss was found mainly above 1050m distance with an SN without LOS (Line of Sight), and it was reflected in the RSSI-SNR plot using red dots, where SNR goes below -10 and the RSSI below -96dB as shown in Figure 3-8(a). Figure 3-8(b) and (c) show the RSSI and SNR values for different distances between a SN and the mobile DS, respectively. Although it does not give an accurate measure of the distances due to environmental conditions, we can still use the relations of RSSI-SNR-Distance to generate the candidate CH list. Multiple SNs with the same RSSI can be shortlisted based on their SNR and then using the neighbor list as described in section 3.6 while electing the CHs. A similar experiment was performed for a moving SN (shown by an orange star and an orange line in Figure 3-7) mounted on a ground vehicle keeping the DS static (DS2 position). Here we experienced some packet loss mainly at no LOS condition at a higher distance than 1200m.

3.5.2 Energy requirement

Energy requirement of the SN was measured to calculate the lifetime of the SN and to validate the clustering efficiency in terms of energy requirement. The SN has three main components measuring the energy consumption: the microcontroller (MCU), the LoRa module, and the sensors. Power consumption varies at different events, depending mainly on the algorithm and the SN or CH operation modes. The events used to measure the SN's energy were

sensor reading, LoRa receives, LoRa transmits, and data processing modes. A DC (direct current) energy logging system is connected with the SN to monitor its input voltage, current, and power. The data logger measured voltage and current at a resolution of 1mV and 1mA, respectively. Figure 3-9(a) shows the laboratory setup for this measurement.

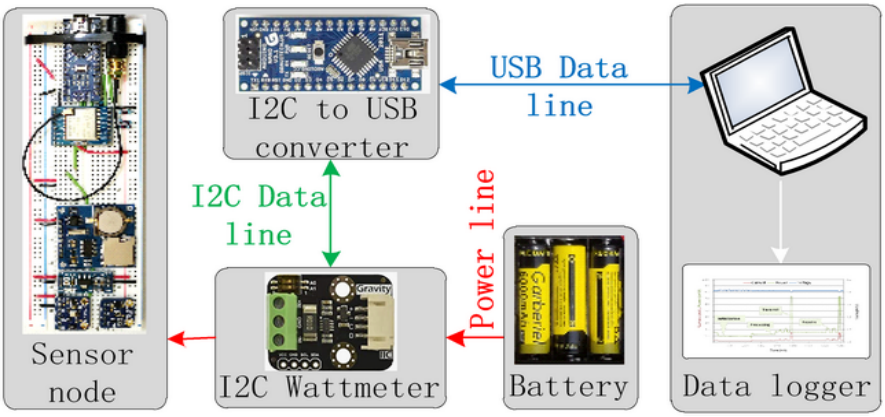

(a)

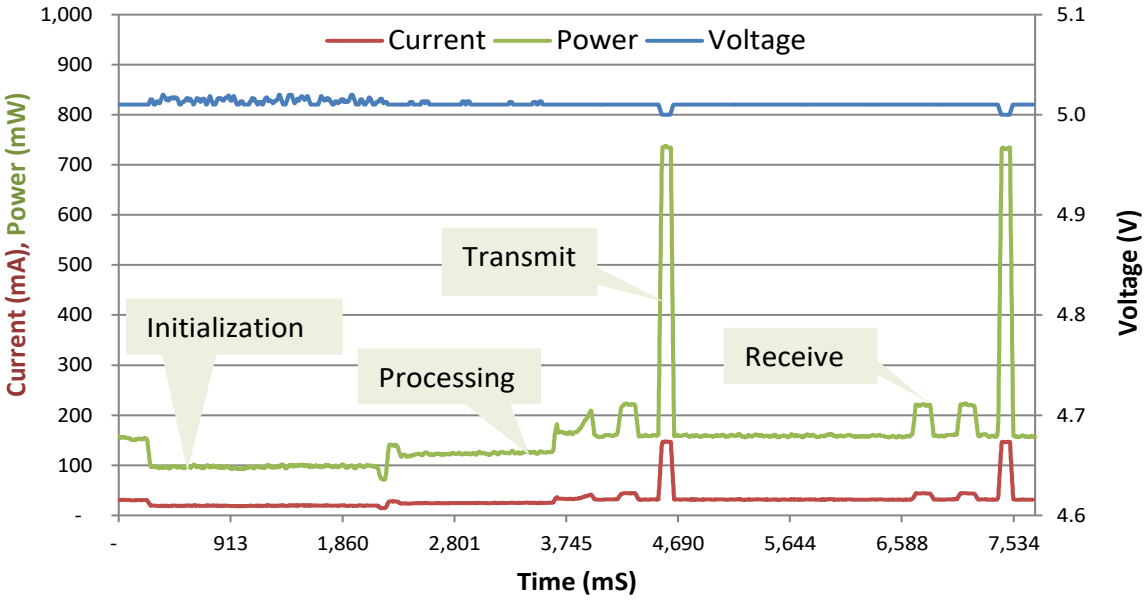

(b)

Figure 3-9. (a) Energy measurement; (b) data logger's output showing voltage, current and power at different events

Table 3-5 Event-wise Power calculation of the SN for sensor data transfer

Event	Duration (mS)	Voltage (V)	Current (mA)	Power (mW)
Active (Sensor read)	2,407	5.01	31	155.31
LoRa receive	336	5.01	44	220.44
LoRa transmission	135	5.00	148	740.00
MCU Sleep mode		5.00	4	20.00

For the measurement, the SN performed normal sensor data transfers at three-second intervals. Figure 3-9(b) shows continuous measurement of the parameters (voltage, current and power), from which event specific values were extracted. Table 3-5 summarizes the event duration, voltage, current, and power consumption of those events for a complete data transfer cycle.

3.6 Performance analysis

Unlike other static or offline clustering algorithms, the proposed LDCA algorithm performs clustering before every data transfer phase. Therefore, the same performance matrices cannot be used to compare their performance. Some newly defined performance matrices are used to measure the performnace of the LDCA scheme, which are described below:

3.6.1 Clustering time

For a real-time algorithm like the proposed LDCA, clustering is formed before every data transmission phase. Therefore, clustering time needs to be considered for real-time clustering. However, most of the static clustering algorithm performs the clustering (or re-clustering) phase off-line one time for multiple data transfer phases. Lower clustering time will ensure higher mobility in the WSN. It will increase the coverage area by increasing the available time for traveling (for the scenarios of Figure 3-1, it is UAV flight time). For the proposed LDCA, the clustering time depends on the number of candidate CHs and their neighbor SN (j and k in (7)). Therefore, clustering time can be minimized by optimizing the value of k, which is only possible by keeping the number of cluster as low as possible. As explained in subsection 3.4.3, the dynamic cluster number is kept only two (so that $k = 4$ can be used) for the proposed LDCA. Clustering time depends mainly on message transfer time between DS-SN and CH-SN using the LoRa interface. As the required processing time is very low (less than 1% of the total time) compared to the LoRa TOA, it contributes most to the clustering time. Figure 3-6 shows the clustering time for different values of k as found from the simulation. TOA increases with the decrease of the bandwidth of the link; LoRa (with 250 KHz BW) has very high TOA compared

to the TOA of Zigbee (with 2MHz bandwidth) [34]. Therefore, short-range links like Zigbee will require less time for LDCA implementation than the LoRa links. For the same reason, the LDCA may also be suitable for a densely populated wide WSN with a Zigbee wireless link. Besides, LDCA can create more than two clusters for static BS with moving SNs, increasing the clustering time. It is shown in figure 3-6 that the clustering time will be around 8s to form three clusters using k=6.

3.6.2 Clustering efficiency

In a real-time algorithm, every data transfer phase has a clustering phase to achieve the maximum mobility. Since, all the SNs take an active part in this phase, the energy consumption should be as low as possible compared to that of the data transfer phase. The clustering phase in LDCA requires extra energy comparing the static clustering algorithm causing an energy overhead. The clustering efficiency of the LDCA depends on how little energy is required for the clustering phase compared to the data transfer phase. Therefore, it can be evaluated as the ratio of the energy required for data transfer to the total (both data transfer and clustering) energy consumption of the SNs, which can be calculated using (13), where ϵ_{CL} is clustering energy efficiency. E_T is the total energy required for a complete data transfer cycle and the clustering phase, and E_{CL} is the energy required for the clustering phase. The maximum energy required for clustering (E_{max}) can be calculated using (14), derived from (12) using P_{TX}= 0.74 Watt (= 740mW from Table 3-5). It shows that, it is linearly dependent on the total clustering time (T_{cl}).

$$\epsilon_{CL} = \frac{E_T - E_{CL}}{E_T} \tag{13}$$

$$E_{max} = 0.74T_{cl} - 34.41 \text{ mJoule} \tag{14}$$

Table 3-6 Energy efficiency, Maximum energy consumption of a candidate CH, and WSN lifetime for the proposed LDCA for different values of k

K	**2**	**4**	**6**	**8**	**10**	**12**
Energy efficiency, ϵ_{CL}(%)	99.59	99.31	99.02	98.74	98.46	98.17
Maximum Energy, E_{max} (Joule)	4.77	8.08	11.39	14.69	18.00	21.31
WSN lifetime (Cycle*)	1278	1274	1270	1266	1262	1258

* Cycle = one clustering phase and data transfer phase

3.6.3 Network lifetime

One way to measure the network lifetime is to count the data transfer round before the first SN goes out of coverage due to lack of energy. For a static or off-line algorithm, only the data transfer phase is considered for counting the round, as the clustering phase (being off-line) does not consume any energy. On the contrary, real-time clustering is performed for every data transferring phase that consumes energy. Therefore, a real-time clustering algorithm like the LDCA with high energy overhead or low clustering efficiency will reduce the network lifetime significantly.

The lifetime of the LDCA network depends on a CH's lifetime. The lifetime of the WSN can be found based on the energy model, time model, and the experimental lab data, which is summarized in Table 3-6 along with the clustering efficiency for different lengths of the candidate CH (k) list.

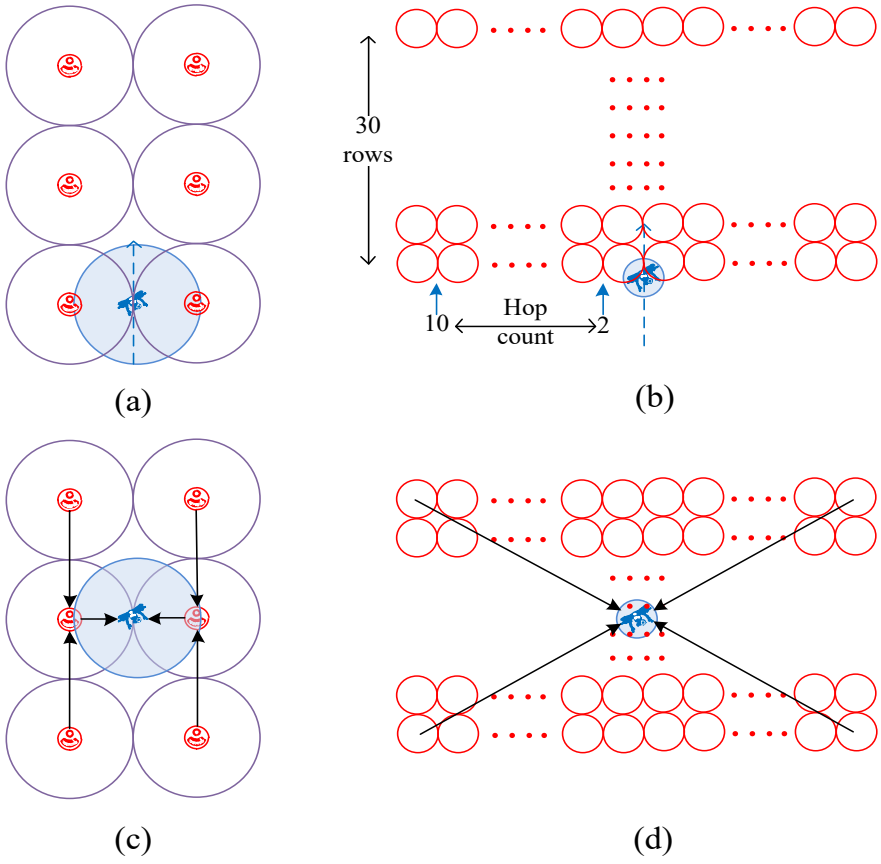

Figure 3-10. (a) WSN with long-range link, mobile DS, and LDCA (b) WSN with short-range link, mobile DS, without LDCA, (c) WSN with long-range link and static DS, and (d) WSN with short-range link, and static DS.

3.6.4 Network topology and coverage

It is the logical network connectivity used for data transfer. For static clustering, it is predefined (path and hops) during the clustering phase and becomes static after the clustering phase until re-clustering. All the data transfer phases use this static network topology; it can be star or tree to utilize multiple hops. However, it cannot be static for a long duration for a network with moving elements (here SN or DS). Therefore, every data transfer phase needs to have a clustering phase to define the topology. Among different topology types, star topology is used between the SNs and DS through only one CH for the proposed LDCA. It avoids multiple hops to achieve maximum mobility or to perform the clustering in the shortest possible time.

Unlike most of the offline clustering, LDCA works in real time and requires only single hop to support any changes in the network topology. Due to the functional differences with other static and traditional dynamic clustering algorithms (where the DS is static), the performance of the proposed LDCA cannot be compared to them. However, the network topology can be considered in terms of the number of SNs and DSs while keeping the monitoring area coverage fixed. Based on DS mobility and the range of wireless link used, the following types of WSNs (clustered and non-clustered) are compared with the WSN (with the mobile DS) using the LDCA.

1. WSN with long-range link, mobile DS, and LDCA,
2. WSN with short-range link, and mobile DS, and without LDCA,
3. WSN with long-range link and static DS,
4. WSN with short-range link and static DS, and
5. WSN with long-range link and mobile DS without clustering.

WSNs with short-range wireless links mostly use Zigbee of 50m to 200m range. LoRa of 1km to 5km range is used as the long-range wireless link. For this comparison, all these WSNs are considered homogenous. All the SNs can be elected as CHs to retransfer sensor data to the DS or BS. Therefore, the maximum number of hops (from the farthest SNs to the DS) can be used for energy calculation. Although these values are highly dependent on the SN distribution and the DS's relative position, a uniform distribution of SNs is assumed to keep the static DS at the middle of the coverage area. For the mobile DS, only a single trip is considered. Figure 3-10 shows the network topology for different types of WSN covering the same area of 2km by 3km. Figure 3-10(a) shows a clustered WSN with LoRa SNs that has 6 clusters (2 clusters at a time) and a mobile DS with the implementation of the LDCA. Figure 3-10(b) shows the WSN with short-range SNs and a mobile DS, as used in [15]. Figure 3-10(c) shows the LoRa WSN with a static DS in the middle of the coverage area, as implemented in [32]. Figure 3-10(d) shows a WSN similar to Figure 3-10(b) with a static DS. Solid arrows show the data

connectivity path, and the dotted arrows show the direction of the mobile DS travel path. The WSN, as implemented in [33], is not shown in this figure as there is no clustering performed.

Network configuration, quantity of elements and hop used for these WSNs are summarized in Table 3-7. WSNs with a short-range wireless link (here Zigbee) need more SNs to achieve higher granularity of data and maintain the link continuity with fixed and constant transmission power over the network. On the other hand, the WSNs with LoRa need more SNs mainly to increase the granularity of the sensor data. Therefore, the LoRa-based WSNs that are mentioned here may not require as many SNs as in WSNs with short-range links.

Table 3-7 Comparison of WSNs: mobile vs. Static DS, and using LoRa and short-range wireless link for the SNs

	Static DS		**Mobile DS**		
Clustering type	Static		Not used	Other	LDCA
Link-type	Short-range [21]	Long Range [32]	Long-range [33]	Short-range [17]	Long-range
Number of SNs	600	300	300	600	300
Maximum Hops (c)	10	2	1	10	1
Rotations/clustering phase	Multiple	Multiple	NA	Multiple	1
Number of clusters (b)	60	6	NA	60	2
Average cluster size	10	50	NA	10	50
Clustering time	NA	NA	NA	Offline	T_{CL} = f(TOA)
Mobility	Static	Static	Static	Mobile DS	Mobile SN and DS
Clustering efficiency (ϵ_{CL})	NA	NA	NA	NA	Above 98%
Network lifetime[1] (Rotations)	600-1250	700-1470	1283	600-1250	1278
Network topology	Static (Star/tree)	Static (Star/tree)	NA	Dynamic (P2P)	Dynamic (Star)
Network coverage	Less than km (all directions)	Few km (all directions)	Above 100km (one direction)	Less than km (all directions)	Above 100km (all directions)
Max energy per transmission[2]	3.3	0.9	0.3*	3.3	0.3**

[1]Cannot be compared with LDCA as, it use one rotation per clustering phase to achieve mobility (detailed in table 3-6), static clustering uses multiple hops, values are calculated/projected.

[2]one mJoule per transmission per SN using the CH (hop).

* May need multiple travel paths to cover the SN distributed laterally.

** For more number of SNs (up to 600, same as the WSN with the short-range link) it will be 0.6Joule which is still less than the energy required for the traditional clustering with a static multi-hop WSN.

3.6.5 Data transfer energy

Energy requirement in the data transfer phase can be compared between different types of WSNs and the WSN using the LDCA. The energy used for the data transmission for a multi-

hop link can be calculated as $a.b(1+c)/2$, where a is the number of SNs in a cluster, b is the number of clusters constructed at the same time, and c is the number of hops required to transfer the data from the cluster to the DS. Energy consumption for different WSN topologies is shown in Table 3-7. However, using the same number of SNs with LoRa will require less than 20% of the energy required for the WSNs with short-range links due to more hops. The WSN with the LDCA requires only 33% of energy required in a LoRa-based WSN with static DS. The energy required for the clustering procedure is not shown here as it is very low compared to the sensor data transmission energy.

3.6.6 Other features and comparison

In addition to the improvement of monitoring area coverage and energy performance, the LDCA has the following additional advantages over other clustered WSNs with or without mobile DS.

1. In static clustering, CH rotation is a must after some data transfer phases in order to maintain homogeneity of the WSN, which can easily be achieved by changing the mobile DS's route and the stop-points for the LDCA.

2. Most of the RSSI-based clustering algorithms calculate the distance between the SN and DS, which increases processing costs and may give erroneous values of the distance. On the contrary, the LDCA uses both RSSI and SNR values to elect the CH without calculating the distances. This reduces the processing load and provides protection from environmental effects on the wireless link, which is very important for wide-area applications.

3. Static clustering algorithms use various offline optimization algorithms to avoid overlapping of a specific SN, which is done dynamically in the LDCA by updating the neighbor list online in the clustering phase.

4. Traditional clustering algorithms may require various synchronization schemes to avoid a collision while receiving the message from the SNs. However, the DS-controlled LDCA is inherently synchronized due to ID-specific TDMA (time divided multiple access) communication during the clustering phase.

5. Both static and traditional dynamic (with a static DS) clustering need to be static in terms of the network topology. This is not required for the LDCA due to the simplicity of implementing only two clusters at a time and re-clustering along with the mobility of the DS after every data transfer phase.

Table 3-8 comparison of features with clustering algorithms using mobile DS or BS

Features	**Proposed LDCA**	**[17]**	**[18]**	**[19]**	**[20]**	**[21]**	**[22]**	**[23]**	**[24]**
WSN geometry	No need for any specific geometry	Circular	Circular, BS at the center	Not specified	Not specified	Circular	Not specified	Not specified	Circular, BS at the center
DS/BS mobility	Mobile DS	Mobile DS	Mobile DS	Mobile DS	Static BS relocation	Some mobile SNs work as DS	Mobile DS	Mobile DS	Static BS with Mobile agent
SN mobility	Mobile and Static	Static only	Static only	Static only	Static only	Static only	Static only	Static only	Static only
DS path planning	Offline with/without fixed stop-point (SP)	Fixed circular	Offline with fixed SP	Fixed SP	NA	Not specified	Not specified	Not specified	NA
Clustering process	Dynamic, real time for every rotation	Static, one time for multiple rotation	Static, one time for multiple rotation	Static, one time for multiple rotation	Dynamic, offline for multiple rotation	Dynamic, offline for multiple rotation	No clustering	No clustering	Static, offline for multiple rotation
Processing load to the SN/CH	Very low load for SN and CH	High, use CH broadcast	High, use CH broadcast	High for DS, SN buffering and scheduling	DS/SN not involved	DS/SN not involved	NA	NA	DS/SN not involved
Immune to environment	Yes, use RSSI and SNR	No, use static location	No	No	No	No, Use distance and path length	No	No, use static location	No, Use distance
Data Routing	Single hop through the CH	Multiple hops through DS	Single hop through CH	Single hop	Multiple hops	Single hop through CH	Direct to DS, SN wait for DS	Multiple hop through agent node	Inter-cluster routing with multiple hops
Other limitations	Clustering time depends on LoRa configuration	SN and DS relative position is static	CH requires high energy	May increase DS mobility	Need super CH deployed manually	CH needs to be at virtual center	DS traveling time is not considered.	May cause data retransmission due to use of multiple agent nodes	Complex routing algorithm

Besides the above advantages, other features of the proposed LDCA are compared with algorithms that use mobile DSs and are summarized in Table 3-8. Most of the algorithms with mobile DSs are for WSNs with a short-range wireless links and static SNs, and are distributed in a circular pattern keeping the BS or CHs in the center. Therefore, most of them are not suitable for widespread WSNs with irregular distributions of SNs, features which, the proposed LDCA is designed to handle. Other than [22], all the WSNs use star or mesh [23] topology in contrast to both point-to-point and star topology used by the LDCA, which permits the SNs to be mobile for some WSN applications like smart farming. There is no clustering used in [22] and [23]. The WSNs of [17-19, 24] keep the cluster static. The clustering performed in [21] remains fixed (hence static) during the mobility of the DS. On the other hand, the proposed LDCA performs clustering all through the mobility of the DS and also facilitates mobility of the SNs. Unlike the proposed LDCA, most of the algorithms that perform clustering use the SNs' physical locations or calculated distances from the DS/BS. The average path length of the DS and the tolerable delay in transferring the data are considered in [21] and [22], respectively. Therefore, all these algorithms do not consider the ambient environmental influences on the radio signal as is done in the proposed LDCA using the RSSI and SNR for the clustering process. These algorithms perform the complicated optimization offline [19-21] or require a considerable amount of processing resources somewhere in the WSN involving the CHs or the

SNs. By contrast, the proposed LDCA requires a minimal number of SNs, as the DS performs most of the process during its mobility. Most of the algorithms perform ether single-hop or multi-hop data transfer to the mobile DS. Direct communication between the SNs and the DS is performed only in [19] and [21], and the proposed LDCA. As shown in Table 3-8, the algorithms using a mobile DS were not evaluated using the same parameters, such as the energy efficiency or the number of rotations vs. the WSN lifetime. However, their performances in terms of various features like WSN coverage, the processing load of the algorithm, dynamic nature, and resource requirement of the SNs are sufficient for comparison with the proposed LDCA, where it can be seen that the LDCA performs better than the rest.

3.7 Conclusion

This paper addresses the challenge to increase the coverage for a widely distributed WSN without using multiple hops among clusters that need to be connected with the IoT network, by proposing a lightweight dynamic clustering algorithm (LDCA). It overcomes the limitations of static clustering and can be implemented using resource constraint sensor nodes. The proposed LDCA uses residual energy, RSSI, and SNR to include the wireless quality depending on environmental parameters. It also use the distance between the sensor node and the DS without any distance calculations in the WSN. The LDCA uses single-hop data transfer from the SNs to the mobile DS through the CHs. The cluster size is variable up to 64 SNs with the LoRa interface for wide-area WSN applications. It constructs only two clusters each round, which reduces the load of the SN. It avoids the CH rotation which would be difficult for a wide WSN with mobile SNs. Unlike most of the clustering algorithms, this paper presents the memory requirement calculations during the clustering phase showing the feasibility of the proposed LDCA for a resource-constrained SN. As WSN is data-centric, simplified data transfer is a must to reduce the total energy consumption to increase its lifetime. The proposed LDCA can facilitate dynamic path planning for the DS, along with a preplanned fixed path. As a future improvement, the average SN memory requirement for sensor data buffering could be included for mobility calculations to reduce DS mobility where real-time data transmission is not required. Some regional separation could be included based on the data acquisition interval to improve the WSN lifetime by reducing the DS mobility requirement.

3.8 References

1. J. Morón-López et al., "Implementation of Smart Buoys and Satellite-Based Systems for the Remote Monitoring of Harmful Algae Bloom in Inland Waters," in *IEEE Sensors J*, vol. 21, no. 5, pp. 6990-6997, 2021, doi: 10.1109/JSEN.2020.3040139.
2. R. A. Nazib and S. Moh, "Energy-Efficient and Fast Data Collection in UAV-Aided Wireless Sensor Networks for Hilly Terrains," in *IEEE Access*, vol. 9, pp. 23168-23190, 2021, doi: 10.1109/ACCESS.2021.3056701.

3. H. Ferng and J. Chuang, "Area-partitioned clustering and cluster head rotation for wireless sensor networks," in *2017 Int. Conf. on Mach. Learn. and Cybern. (ICMLC)*, Ningbo, China, 2017, pp. 593-598, doi: 10.1109/ICMLC.2017.8108977.
4. W. B. Heinzelman, A. P. Chandrakasan, and H. Balakrishnan, "An application-specific protocol architecture for wireless microsensor networks," *IEEE Trans. on Wireless Commun.*, vol. 1, no. 4, pp. 660-670, Oct. 2002, doi: 10.1109/TWC.2002.804190.
5. S. K. Singh, P. Kumar, and J. P. Singh, "A Survey on Successors of LEACH Protocol," *IEEE Access*, vol. 5, pp. 4298-4328, 2017, doi: 10.1109/ACCESS.2017.2666082.
6. S. Arjunan and S. Pothula "A survey on unequal clustering protocols in Wireless Sensor Networks," *J. of KSU- Comput. Info. Sci.,* vol. 31, no. 3, pp. 304-317, 2019, doi: 31. 10.1016/j.jksuci.2017.03.006.
7. K. Xu, Z. Zhao, Y. Luo, G. Hui, and L. Hu, "An Energy-Efficient Clustering Routing Protocol Based on a High-QoS Node Deployment with an Inter-Cluster Routing Mechanism in WSNs," *Sensors*, vol. 19, no. 12, pp. 2752-2774, Jun. 2019, doi: 10.3390/s19122752.
8. A. Jorio, S. E. Fkihi, B. Elbhiri, and D. Aboutajdine, "An Energy-Efficient Clustering Routing Algorithm Based on Geographic Position and Residual Energy for Wireless Sensor Network", *J. of Comput. Netw. and Commun.*, vol. 2015, 2015. https://doi.org/10.1155/2015/170138
9. Z. Sun, L. Wei, C. Xu, T. Wang, Y. Nie, X. Xing, and J. Lu, "An Energy-Efficient Cross-Layer-Sensing Clustering Method Based on Intelligent Fog Computing in WSNs," *IEEE Access,* vol. 7, pp. 144165-144177, 2019, doi: 10.1109/ACCESS.2019.2944858.
10. Asaduzzaman and H. Y. Kong, "Energy efficient cooperative LEACH protocol for wireless sensor networks," *J. of Commun. and Netw.*, vol. 12, no. 4, pp. 358-365, Aug. 2010, doi: 10.1109/JCN.2010.6388472.
11. J. Yu, Y. Qi, and G. Wang, "An energy-driven unequal clustering protocol for heterogeneous wireless sensor networks," *J. Control Theory Appl.* Vol. 9, pp. 133–139, Mar. 2011, doi: 10.1007/s11768-011-0232-y.
12. S. Lee, H. Choe, B. Park, Y. Song, and C.K. Kim, "LUCA: an energy-efficient unequal clustering algorithm using location information for wireless sensor networks", *Wirel. Pers. Commun*, vol. 56, pp. 715–731, Feb. 2011, doi: 10.1007/s11277-009-9842-9.
13. J. Yu, Y. Qi, G. Wang, Q. Guo, and X. Gu, "An energy-aware distributed unequal clustering protocol for wireless sensor networks", *Int. J. Distrib. Sens. Networks*, vol. 7, no. 1, Jul. 2011, doi: 10.1155/2011/202145.
14. G. Chen, C. Li, M. Ye, and J. Wu, "An unequal cluster-based routing protocol in wireless sensor networks", *Wirel. Networks*, vol. 15, pp. 193–207, Feb. 2009, doi: 10.1007/s11276-007-0035-8.
15. E. Ever, R. Luchmun, L. Mostarda, A. Navarra, and P. Shah, "UHEED – an unequal clustering algorithm for wireless sensor networks", in *Proceedings of the 1st International Conference on Sensor Networks, Sensornets 2012*, Rome, Italy, Feb. 2012, [Online], Available: https://eprints.mdx.ac.uk/id/eprint/8481
16. H. K. Srivastava and R. K. Dwivedi, "Energy Efficiency in Sensor Based IoT using Mobile Agents: A Review," in *2020 Int. Conf. Power Electron. IoT Appl. Renewable Energy and its Control (PARC)*, India, Feb. 2020, pp. 314-319, doi: 10.1109/PARC49193.2020.236617.
17. J. Wang, Y. Gao, W. Liu, A. Kumar, and H. Kim, "Energy Efficient Routing Algorithm with Mobile Sink Support for Wireless Sensor Networks", *MDPI Sensors*, vol. 19, no. 7, p. 1494, Mar. 2019, doi: 10.3390/s19071494.
18. H. A. H. Al-Behadili, S. K. A. AlWane, Y. I. A. Al-Yasir, N. O. Parchin, P. Olley, and R. A. Abd-Alhameed, "Use of multiple mobile sinks in wireless sensor networks for large-scale areas," *IET Wireless Sensor Systems*, vol. 10, no. 4, pp. 175-180, Aug. 2020, doi: 10.1049/iet-wss.2019.0208.
19. S. Redhu and R. M. Hegde, "Cooperative Network Model for Joint Mobile Sink Scheduling and Dynamic Buffer Management Using Q-Learning," *IEEE Transactions on Network and Service Management*, vol. 17, no. 3, pp. 1853-1864, Sept. 2020, doi: 10.1109/TNSM.2020.3002828.

20. A. Verma, S. Kumar, P. R. Gautam, T. Rashid and A. Kumar, "Fuzzy Logic Based Effective Clustering of Homogeneous Wireless Sensor Networks for Mobile Sink," *IEEE Sensors Journal*, vol. 20, no. 10, pp. 5615-5623, 15 May15, 2020, doi: 10.1109/JSEN.2020.2969697.
21. A. Pang, F. Chao, H. Zhou and J. Zhang, "The Method of Data Collection Based on Multiple Mobile Nodes for Wireless Sensor Network," *IEEE Access*, vol. 8, pp. 14704-14713, 2020, doi: 10.1109/ACCESS.2020.2966652.
22. Y. Yun and Y. Xia, "Maximizing the Lifetime of Wireless Sensor Networks with Mobile Sink in Delay-Tolerant Applications," *IEEE Transactions on Mobile Computing*, vol. 9, no. 9, pp. 1308-1318, Sept. 2010, doi: 10.1109/TMC.2010.76.
23. J. Kim, J. In, K. Hur, J. Kim and D. Eom, "An intelligent agent-based routing structure for mobile sinks in WSNs," *IEEE Transactions on Consumer Electronics*, vol. 56, no. 4, pp. 2310-2316, Nov. 2010, doi: 10.1109/TCE.2010.5681105.
24. J. Wang, X. Gu, W. Liu, A. Kumar, H. Kim, and Hye-Jin. "An empower hamilton loop based data collection algorithm with mobile agent for WSNs", *Hum. Cent. Comput. Inf. Sci.*, vol. 9, no. 18, May 2019, doi: 10.1186/s13673-019-0179-4.
25. H. C. Lee and K.H. Ke, "Monitoring of Large-Area IoT Sensors Using a LoRa Wireless Mesh Network System-Design and Evaluation," *IEEE Trans. On Instrumentation and Measurement*, vol. 67, no. 9, pp.2177-2187, Sep. 2018, doi: 10.1109/TIM.2018.2814082.
26. W. Ayoub, A. E. Samhat, F. Nouvel, M. Mroue, and J. Prévotet, "Internet of Mobile Things: Overview of LoRaWAN, DASH7, and NB-IoT in LPWANs Standards and Supported Mobility," *IEEE Communications Surveys & Tutorials,* vol. 21, no. 2, pp. 1561-1581, Apr. 2019, doi: 10.1109/COMST.2018.2877382
27. *LoRaWAN™ 1.0.3 Specification, LoRa Alliance, Inc, 2018*, Accessed: Sep. 30, 2020. [Online]. Available: https://lora-alliance.org/resource-hub/lorawanr-specification-v103
28. M. N. Khan, A. Rao and S. Camtepe, "Lightweight Cryptographic Protocols for IoT Constrained Devices: A Survey," in IEEE Internet of Things J, early access, Sep. 24, 2020. doi: 10.1109/JIOT.2020.3026493.
29. *Semtech SX1278*, Accessed: Sep. 30, 2020. [Online]. Available: https://www.semtech.com/products/wireless-rf/lora-transceivers/sx1278
30. *LoRa air time calculator*, Accessed: Sep. 30, 2020. [Online]. Available: https://www.loratools.nl/#/airtime
31. G.M.E. Rahman, K.A. Wahid, and A. Dinh, "IoT enabled Low power and Wide range WSN platform for environment monitoring application", *2020 IEEE Region 10 Symposium (TENSYMP),* Dhaka, Bangladesh, 2020, pp. 908-911, doi: 10.1109/TENSYMP50017.2020.9230959.
32. J. M. Marais, R. Malekian, and A. M. A. Mahfouz, "Evaluating the LoRaWAN Protocol Using a Permanent Outdoor Testbed," *IEEE Sensors*, vol. 19, no. 12, pp.4726-4733, Jun. 2019, doi: 10.1109/JSEN.2019.2900735.
33. G. M. E. Rahman and K. A. Wahid, "LDAP: Lightweight Dynamic Auto-Reconfigurable Protocol in an IoT-Enabled WSN for Wide-Area Remote Monitoring." *Remote Sens.*, vol. 12, no. 19, pp. 3131-3151, Sep. 2020, doi: 10.3390/rs12193131.
34. J. Cheon, H. Hwang, D. Kim, and Y. Jung, "IEEE 802.15.4 ZigBee-Based Time-of-Arrival Estimation for Wireless Sensor Networks." *Sensors*, vol. 16, no. 2, pp-203-213, Feb. 2016, doi: 10.3390/s16020203.

4. LSAQ-LoRa: Lightweight Synchronization Algorithm for Quasi-orthogonal LoRa Channels in Wide-area Wireless Sensor Network:

This chapter describes the proposed channel synchronization algorithm to increase the data rate of a LoRa Link. Wireless Sensor Network (WSN) uses clusters as a group of sensor nodes to increase network coverage, capacity, and controllability. All the sensor nodes in a cluster communicate with the cluster head to transfer the sensor data. The CHs closer to the gateway carry the data from other cluster heads, which cannot reach the gateway directly. Wide-area WSN can utilize LoRa in a cluster for wider coverage. However, a single LoRa link may not provide a sufficient data rate for the cluster heads carrying high data volume. High-speed wireless technologies such as cellular networks, which may require more energy and cost, can solve this problem. This research proposes a Lightweight Synchronization Algorithm for Quasi-orthogonal LoRa channels (LSAQ) to increase the data rate of the LoRa link. LSAQ facilitates synchronous transmission using multiple LoRa physical channels for a single link between two nodes utilizing the quasi-orthogonality nature of LoRa.

At first, the quasi-orthogonality nature of LoRa is investigated for the same radio channel using different bandwidths, spreading factors (SF) and radio frequencies at the same transmit power and distance using multiple communication modules in parallel. The air interface is observed using a Software Defined Radio (SDR) enabled receiver. This experiment found that multiple channels with different radio frequencies are unsuitable for co-channel interference. Interference is also observed for the radio channels of the same frequencies with different bandwidths. Different SFs for different radio channels with the same radio frequency and bandwidth show better performance. They are worth investigating further for parallel transmission to increase the combined data rate of a logical channel (combination of multiple physical channels).

According to the performance, a specific combination of SFs is assigned to multiple radio channels (called a physical channel). Time On Air (TOA) of the physical channels differs at different SFs. Therefore, a channel synchronization scheme is required. This research developed a synchronization algorithm called LSAQ for the LoRa physical channels. LSAQ can adapt the synchronization using different packet sizes or a different number of data packets of the same size for different physical channels of different SFs depending on the application requirement. This packet synchronization ensures maximum channel utilization achieving the maximum data rate improvement for the logical channel. Thus, the receiver receives the simultaneous LoRa packets, performs the data sequencing, error checking, and acknowledges the sender accordingly.

This research also derived mathematical models to evaluate network size and data rate improvement for various combinations of the SF and bandwidth used for parallel data transmission using LoRa physical layers. It classifies the combination of SFs for different WSN applications in network density and coverage area. It shows that parallel transmission using two physical channels with two consecutive SFs gives optimum data rate improvement. Maximum data rate improvement is measured as 58% using SF = 7 and 8. Maximum network capacity improvement is found at 46% for the SF = 8 and 9.

The development work, analysis and findings of this chapter is under review in the IEEE Transactions on Industrial Informatics. The student contributed to the main idea, implementing code, writing the original draft, and evaluating and revising the manuscript.

LSAQ-LoRa: Lightweight Synchronization Algorithm for Quasi-orthogonal LoRa Channels in Wide-area Wireless Sensor Network

Gazi M. E. Rahman, M*ember, IEEE*, and Khan A. Wahid, *Member, IEEE*

Abstract: This paper proposes a parallel data transfer scheme utilizing the quasi-orthogonality feature of LoRa. The proposed Lightweight Synchronization Algorithm for Quasi-orthogonal channels (LSAQ) uses multiple Spreading Factors (SF) in the same radio channel to form a logical channel with a higher data rate. It achieves up to a 46% improvement in network capacity and a data rate improvement of 58% when compared with a Wireless Sensor Network (WSN) using LoRa Medium Access Control (MAC) layer protocols. This research validates the performance of LoRa orthogonality in terms of multiple Bandwidths (BW), multiple radio channels and multiple SFs. It presents the data packet sequencing and channel synchronization algorithms for the logical channel required for the LASQ scheme. It also derives a mathematical model to evaluate the data rate and energy performance of the proposed LSAQ.

Keywords: LoRa, Synchronous transmission, Image transfer, Wide-area WSN, IoT, Orthogonality, Data rate.

4.1 Introduction

LoRa can be used instead of wireless technologies such as Zigbee, Sigfox, and cellular data communication when wider coverage [1] is required in a Wireless Sensor Network (WSN). In a WSN with multiple clusters and multi-hop links, the cluster head (CH) closest to the Data Sink (DS) or Gateway (GW) is required to transfer a large amount of data received from clusters far from the DS or GW. Multi-hop data transfer may be used for wide-area coverage instead of increasing transmission power (requires more power) for better WSN efficiency, as it increases the coverage area in the WSN. Internet of Things (IoT) applications involving inter Unmanned Aerial Vehicle (UAV) data communication [2] is not feasible using the current LPWAN due to its low data rate compared to Wi-Fi and 4G cellular networks. Literature shows that a higher Spreading Factor (SF) of LoRa may not suit applications requiring higher data rates and greater coverage [3]. A LoRa-based WSN may have a limited network capacity due to its high Time On Air (TOA) and low data rate compared to other wireless technologies. WSN applications such as wide-area environmental monitoring and smart farming may also require mobile nodes [4]. Therefore, this research is focused on the requirement of data transmission at a higher data rate over a LoRa link between two nodes in a WSN. Inspired by the quasi-orthogonality of LoRa, this paper proposes a Lightweight Synchronization Algorithm for Quasi-orthogonal channels (LSAQ) of LoRa in a WSN. This paper therefore:

1. Proposes a synchronization algorithm for multi-SF parallel transmission (called LSAQ).
2. Practically evaluates the quasi orthogonality in SF and Radio Frequency (RF) channels and explores possible SF combinations for parallel transmission.
3. Implements the identified SF combinations and evaluates the data rate improvement.
4. Derives a mathematical model for the proposed LSAQ regarding SF allocation for parallel transmission, timing, data-rate, and energy performance.

LoRa data transmission uses a series of symbols, much like M-ary Frequency Shift Keying (FSK), which is done using multiple chirps. LoRa is quasi-orthogonal in the time domain in terms of SF [5] for high values of M. Therefore, only some specific combinations of SF and Bandwidth (BW) showing different slopes in the frequency-time plane are orthogonal [6] and can be used for concurrent transmission. This orthogonality is limited due to inter-SF collision and can be overcome by proper SF selection [7]. A network with data transmission where multiple nodes use the same SF is limited by the Co-SF interference, which requires the Signal to Interfering Noise Ratio (SINR) to be higher than 6 [8]. Such a high SINR is not achievable for co-located LoRa modems in the parallel data transmission scheme and is avoided for parallel data transmission between two nodes, which is further explained in section 4.4. Besides, parallel transmission facilitates a higher data rate while keeping the LoRa's Chirp Spread Spectrum (CSS) modulation unchanged.

The following section highlights the recent research works for LoRa data rate improvement and its implementation for burst data transmission, followed by the proposed LSAQ in detail. The validation procedure performed to determine the use of LoRa quasi-orthogonality is described in section 4.4. Section 4.5 analyzes LSAQ's performance and highlights its features compared with other similar schemes. The conclusion highlights the limitations and future scope of research to improve LoRa capacity and further data-rate improvements.

4.2 Related work

Different SF-based clustering [9] is used to increase network capacity. Asynchronous transmission using LoRa physical channels in a multi-hop network [10] increases network coverage. Inter-SF collision becomes severe with increased numbers of nodes and their distance from the receiver or GW [11], which can be improved with equal SF loading by allocating an equal number of nodes per SF. However, equal SF loading may present limitations in applications with higher channel utilization due to the varying Time On Air (TOA) at different SFs. The Pyramid [12] algorithm can detect collisions of the same SF in real-time and thus improve throughput of the LoRa link between two nodes. Depending on the link quality, dynamic selection of the SF and BW [13] can improve the packet delivery rate (PDR), where the connections of different PDR are divided into three modes (low, medium, and high), and

the nodes decide the modes. Switching between any two modes first requires switching to the low data rate. This mode-switching requires increased control messages, which may in turn increase network traffic and reduce the goodput (effective data rate) of the network.

In addition to LoRa network capacity, previous literatures improve LoRa channel capacity by enhancing the modulation technique. The use of Interleaved Chirp Spreading (ICS) in parallel with basic Chirp Spreading [14] increases the capacity by 42%. One extra bit was added in the LoRa symbol for ICS, which increases the capacity by 14% and 8% for SF = 7 and SF = 12 respectively. Slope Shift Keying (SSK) with ICS [15] used up, down and interleaved up and down chirp modulation, which also increases data rate. It achieved a 28.6% data rate improvement compared with the same SF and BW of CSS LoRa. Time-domain multiplexing was used for LoRa modulation [16] to distribute the bits of a symbol among different SFs, that doubles the data rate with minor degradation of Bit Error Rate (BER), mainly at the lower SF (SF = 7). Any improvement in the modulation technique results in changes in the LoRa physical layer which may not be compatible with the basic LoRa-based network.

Some research works proposes an enhancement of the network access techniques for the LoRa communication protocol. An enhancement of the network access techniques for the LoRa communication protocol has been propose in [17], achieving the highest data rate possible. To achieve this higher data rate, the SF must be higher for nodes that require less hops to reach the DS. This algorithm focuses on capacity-based allocation and an iterative process. Distance-based SF allocation using Exponential Windowing Scheme (EWS) [18] reduces co-SF interference and improves network capacity. It uses an offline optimization algorithm for static nodes and achieves 18.2% to 55.25% Packet Delivery Rate (PDR) compared to similar SF allocation algorithms. However, data throughput decreases exponentially with the increase of nodes from 1k nodes to 8k nodes. It also requires Global Positioning System (GPS) based location data or Received Signal Strength Indicator (RSSI) based distance calculation and manual distance measurement. The proposed LSAQ does not require offline calculation to support mobility in the WSN.

Superimposed signals in different SFs used in the LoRa GW are decoded by the demodulator [19] using two groups (odd and even) of SFs. All the nodes need to maintain strict synchronization to utilize the MAC layer that considers all the packets of different SF as a single transmission packet. The use of high SF also has a higher probability of collision; therefore, all the SFs still may not be practical. It may need node classification to maintain the SF-based packet distribution.

LoRa Wireless Area Network (LoRaWAN) is an ALOHA-based media access protocol and suffers from a higher collision rate as the network grows, which reduces the throughput [20]. Hint messages used in multiple ad-hoc slot allocation [21], in addition to the LoRaWAN slots, helps burst data transfer and increases throughput by reducing control overhead. The use of

Listen Before Talk (LBT) in WSN using LoRa requires higher energy and synchronization. Out-of-band synchronization using Frequency Modulation Radio Data System (FM-RDS) [22] frees some LoRaWAN channels; however, it requires extra hardware and alternate wireless links. Cantor [23] is used in a LoRaWAN GW to collect network parameters from the nodes, calculate the optimized Packet Reception Rate (PRR), and then estimate the actual downlink PRR using an optimization algorithm. It uses a regression model (WW: Wane and Wax, alternate increase, and decrease) for a realistic PRR determination. This algorithm improves goodput by up to 70%. Cantor uses windowing for the Acknowledge (ACK) which performs better for higher SF, however it may not be optimized in a clustered WSN with mixed SFs.

Multiple-Input Multiple-Output (MIMO)-LoRa [24] uses multiple SFs for parallel transmission to improve BER at higher SF such as 10, 11, and 12. It uses a precoding matrix to optimize the total SNR and peak transmit power to select the SFs. However, the precoding may cause a continuous processing load for resource constrained nodes, which can be minimized by synchronous multi-SF transmission in the proposed LSAQ scheme.

4.3 Proposed Lightweight Synchronization algorithm for quasi-orthogonal LoRa channels (LSAQ)

4.3.1 LoRa LSAQ Channel

Network capacity and coverage can be improved by improving the data rate of the links used in the network. The proposed LSAQ focuses on the data rate of a LoRa link of the network by reducing the total data transmission time (T_{tx}) between nodes and GW (or DS) regardless of the application type. LSAQ utilizes LoRa's SF-based quasi-orthogonality for parallel data transmission by efficiently selecting multiple SFs for the LoRa Physical (LoRa-PHY) channels. A LoRa physical layer frame is shown in Figure 4-1 (a) named as the LoRa physical channel. The LoRa-PHY channel supports a programmable Coding Rate (CR) between 1 and 4 bits for forward error correction to provide better interference tolerance. Therefore, the actual Bit Rate (BR) depends on the SF, CR and the BW. The BR is calculated using equation (1), which gives a maximum BR of 37.5 kbps (for BW = 500 KHz, CR = 1 and SF = 6).

$$BR = SF.\frac{4}{4+CR}.\frac{BW}{2^{SF}} \quad (1)$$

In Figure 4-1(b), two or more LoRa physical channels are grouped to transfer data in parallel. These channels have the same configuration of BW, RF and CR, but have different SFs and are synchronized to transfer the data stream. Due to the similarity of configuration and operation, the rest of this manuscript has named these channels as Logical Channel (LC) to facilitate describing the proposed LSAQ. All the pay load sizes are variable according to the

transceiver configuration. The payload size ranges from 1 to 255 bytes. The total number of bits (n_{PL}) in the frame can be calculated using equation 2.

$$n_{PL} = 8 + max\left(0, \left\lceil \frac{8PL - 4SF + 8 + CRC + H}{4(SF - DE)} \right\rceil (CR + 4)\right) \qquad (2)$$

Where PL is payload length in bytes, CRC is 16 bits if enabled and 0 otherwise, $H = 20$ when the header is enabled and 0 otherwise. DE is 2 when the low data rate optimization is used, otherwise it is 0.

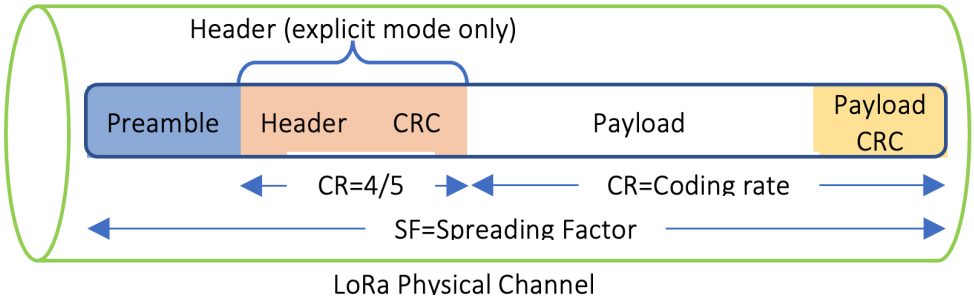

(a)

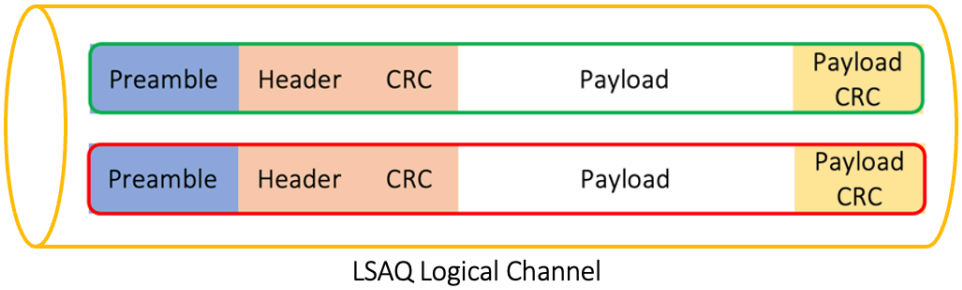

(b)

Figure 4-1. LoRa frame structure (a) Physical channel, and (b) logical channel used in LSAQ

4.3.2 LoRa WSN Capacity

This research considered a LoRa WSN to cover a wide area supporting mobile nodes, as shown in Figure 4-2. These networks consist of multiple clusters. Nodes are connected with the CHs using star topology, and the CHs are connected with the DS (or gateway) using star or tree topologies. The CHs are elected among the nodes dynamically by the DS (or upper control layer of the network). While maintaining homogeneity in the network, CHs do not have gateway

functionality. Network capacity can be evaluated considering multiple clusters with a single DS or GW. Data from the clusters can be transferred to the static GW through the CHs using multiple hops, as shown in Figure 4-2 (a) or using a mobile DS directly from each CHs, thus avoiding multiple hops [4] as shown in Figure 4-2 (b). For both network topologies, CHs acquire data from the nodes and transfer it to the GW or DS. The data transfer volume between the CHs and GW (or DS) depends on the network size or the number of nodes in a cluster. For a WSN with a static GW, considering equal clustering and only one wing of the network (i.e. all the clusters are aligned in one single communication line), the maximum nodes per cluster can be calculated using the following equation

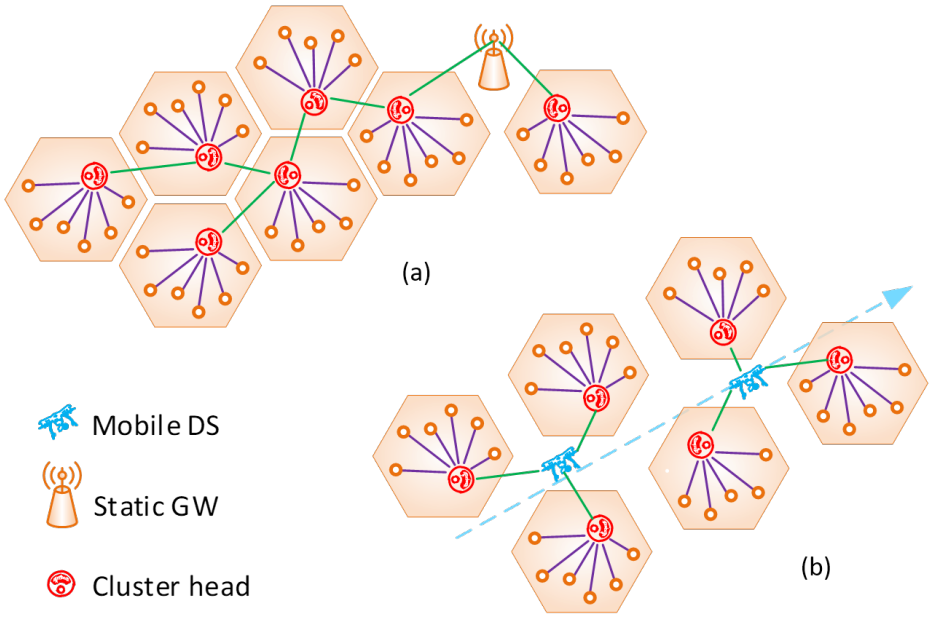

Figure 4-2. Data transfer from the nodes in a WSN using LoRa
(a) through multiple CHs to the GW, and (b) using single CH to the mobile DS

$$N_{max} = \left\lfloor \frac{2IL^2}{T_{tx}(r-L)r} \right\rfloor \quad (4)$$

where T_{tx} (in seconds) is the total TOA for a single packet data transfer considering the TOAs for both the data itself and other control messages such as Request (REQ) and ACK, which are considered to have 8 bytes; I is the required data transfer interval; L is the link length in km; and r is the coverage radius in km in one direction. The total number of nodes in the WSN can be calculated using equation (5).

$$N_{WSN} = \left\lfloor \frac{2IL^2}{T_{tx}(r-L)r} \right\rfloor \left(\frac{r}{L}\right) \approx \frac{2IL}{T_{tx}(r-L)} \quad (5)$$

In a WSN with mobile DS, the DS acquires data in mobility at U (km/h) speed, while maintaining the link with the CHs, as shown in the Figure 4-2 (b). The maximum number of nodes in those clusters can be calculated using equation (6).

$$N_{max} = \frac{3600.L}{U.T_{max}} \quad (6)$$

The equation shows that network capacity in terms of the number of nodes is inversely proportional to the network coverage radius and T_{tx}, hence on LoRa's TOA. Therefore, in both WSN topologies, the only way to increase the number of nodes in the WSN is to reduce the T_{tx} (or T_{max}) by reducing the LoRa TOA. However, low TOA values can be achieved at lower SFs by sacrificing the LoRa range. LoRa-LSAQ can increase the data rate in a LoRa network at higher SFs while maintaining the WSN coverage and capacity.

Table 4-1: LoRa WSN size in terms of nodes depending on SF, BW, and the data size to be transmitted.

Transferred Data size (Byte)				**220**				**51**				**22**			
SF	**BW (KHz)**	**Link length (km)**	**Hop count**	**T_{tx} (ms)**	**Cluster size (Static GW)**	**WSN size (Static GW)**	**Cluster size (Mobile DS)**	**T_{tx} (ms)**	**Cluster size (Static GW)**	**WSN size (Static GW)**	**Cluster size (Mobile DS)**	**T_{tx} (ms)**	**Cluster size (Static GW)**	**WSN size (Static GW)**	**Cluster size (Mobile DS)**
7	500	2	49	121	6	300	297	58.3	12	600	617	48.1	15	750	748
7	250	2	49	242	3	150	148	116.6	6	300	308	96.2	7	350	374
7	125	2	49	484	1	50	74	233.2	3	150	154	192.4	3	150	187
8	500	5	19	212.8	22	440	422	105.3	44	880	854	87.4	54	1080	1029
8	250	5	19	425.6	11	220	211	210.6	22	440	427	174.8	27	540	514
8	125	5	19	851.2	5	100	105	421.2	11	220	213	349.6	13	260	257
9	500	10	9	379.6	52	520	474	190.1	105	1050	946	154.3	129	1290	1166
9	250	10	9	759.2	26	260	237	380.2	52	520	473	308.6	64	640	583
9	125	10	9	1518.4	13	130	118	760.4	26	260	236	617.2	32	320	291

Table 4-1 shows the maximum possible WSN size in terms of the number of nodes (calculated using equation 4, 5, and 6), which depends on the SF, BW and payload size, while transferring data at 15 min intervals. For a static GW configuration, link length is defined based

on our experimental result with Line Of Sight (LOS). The mobile DS is mounted on a Zypher [25] UAV and moved at an average speed of 100 kmph. In both scenarios, it does not show the higher SFs' (SF = 10 to 12) and lower BW's analysis due to very high TOA, which is not suitable for a payload size of 240 bytes. LoRaWAN uses a typical payload of 51 Bytes and 22 Bytes is the minimum payload size to give the minimum TOA for the specific SF and BW. Figure 4-3 shows the effect of varying the WSN size (in terms of nodes or on the total transmission time) using 240 bytes and 51 bytes payload sizes. The lowest data transmission time can be achieved when the SF is at its lowest value (SF = 7), however it limits the WSN size due to the reduction of the link length. Therefore, lowering the SFs may not increase the data rate in a WSN with higher nodes or wider coverage using multiple hops giving higher total transmission time. WSN size for parallel transmission using multiple SFs using the proposed LSAQ is further explained in section 4.5.

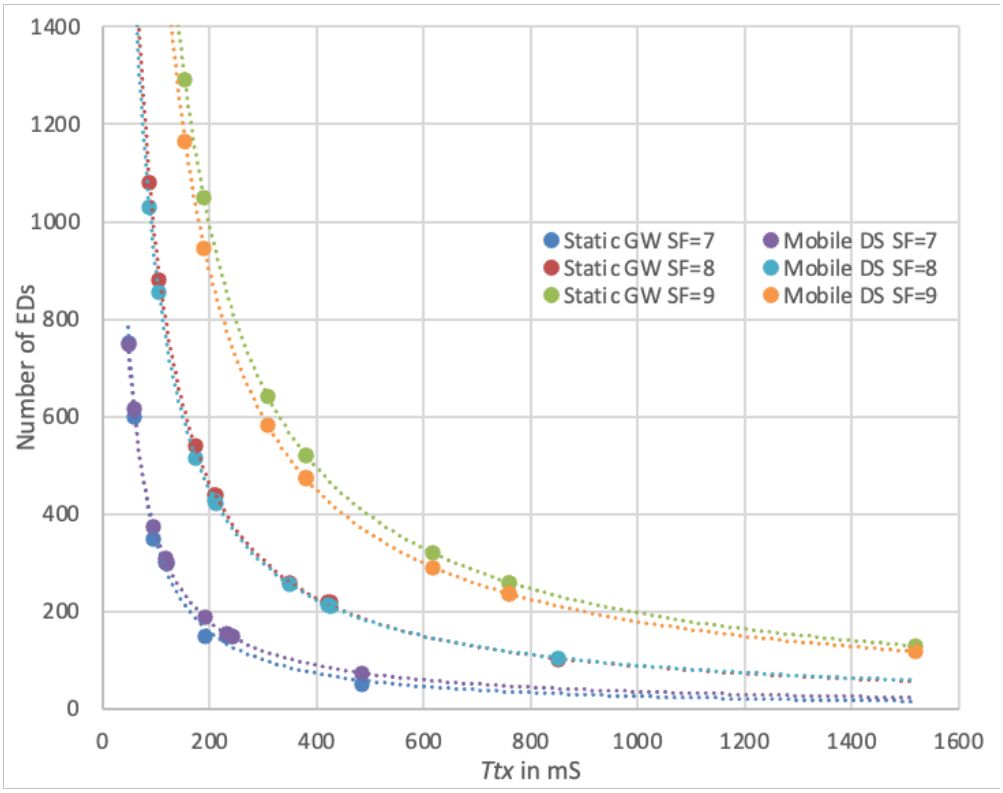

Figure 4-3. Cluster size dependence on the total data transmission time (T_{tx}) using different values of LoRa SF, BW and data size.

4.3.3 LSAQ functions:

LSAQ includes the application-specific SF selection, packet distribution (or accumulation in the receiver end) and synchronization among the physical channels in the LC. The following subsections describe the SF selection, data packetization and synchronization function.

Table 4-2: TOA values for different BW and SF for PL = 240 bytes

SF	BW = 500 KHz		BW = 250 KHz		TOA Ratio	% RDRI
	TOA (ms)	DR (kbps)	TOA (ms)	DR (kbps)		
6	52.1	37.5	104.2	18.75		71
7	92.2	21.870	184.4	10.935	0.583	75
8	164.0	12.500	327.9	6.250	0.572	78
9	292.1	7.030	584.2	3.515	0.562	80
10	533.0	3.906	1,066.0	1.953	0.556	82
11	963.6	2.148	1,927.2	1.074	0.550	83
12	1804.3	1.172	3,608.6	0.586	0.546	

A) SF Selection:

Maximum data rate of LoRa depends on the TOA, which directly depends on the BW and SF, as shown in equation (7) which is derived from equation (3) using CR = 1, H = 1 and DE = 0.

$$TOA = \left(20.25 + \left\lceil \frac{2PL - SF + 7}{SF} \right\rceil 5\right)\left(\frac{2^{SF}}{BW}\right) \tag{7}$$

TOA will be the lowest for all the SFs where BW is 500 KHz. Table 4-2 shows the TOAs for 250 KHz and 500 KHz BW when SF is varied. It indicates that the TOA with BW 250 KHz and SF 7 is only 20.4 ms (184.4 – 164) higher than the TOA with 500 KHz and SF 8. That gives a 12% improvement (reduction) of TOA between these two LoRa settings. However, this differs from 55% to 57% for the same BW with different SF. Data rate differences between two LoRa physical channels of the same BW and different SFs are compared and presented here as the relative data rate improvement (RDRI = 1-DR_i / DR_{i+1}). Therefore, parallel transmission using 250 KHz and 500 KHz BW can be used for two consecutive SF values in two different logical channels. Parallel transmission can be achieved using multiple RF channels of the same BW with different SFs. Therefore, SF 7, 8, 9, and 10 can be used for channel-1 and channel-2, which gives eight LoRa physical channels for parallel transmission. However, it is not feasible to use more than two physical channels to improve the data rate and energy consumption at the same time. Different BW with different SFs is not used in the proposed LSAQ to avoid data loss due to inter LoRa channel interference (characteristic of quasi-orthogonality).

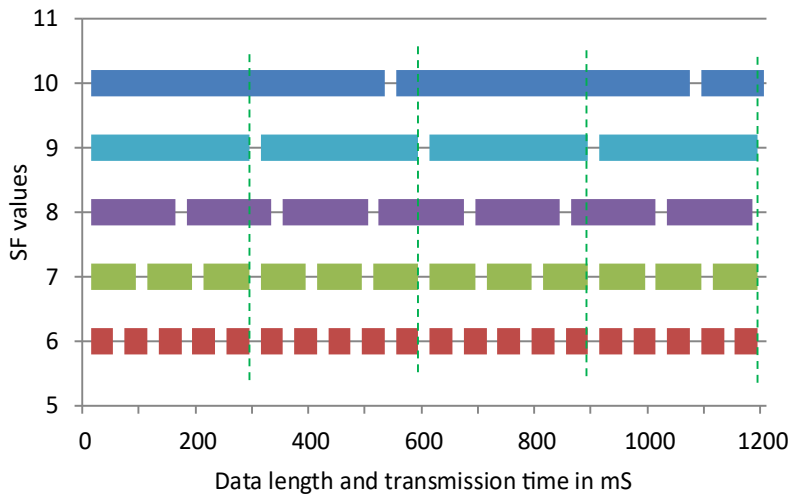

Figure 4-4. LoRa packet stream for synchronized burst transmission using LSAQ with different SFs in the same RF channel with same BW.

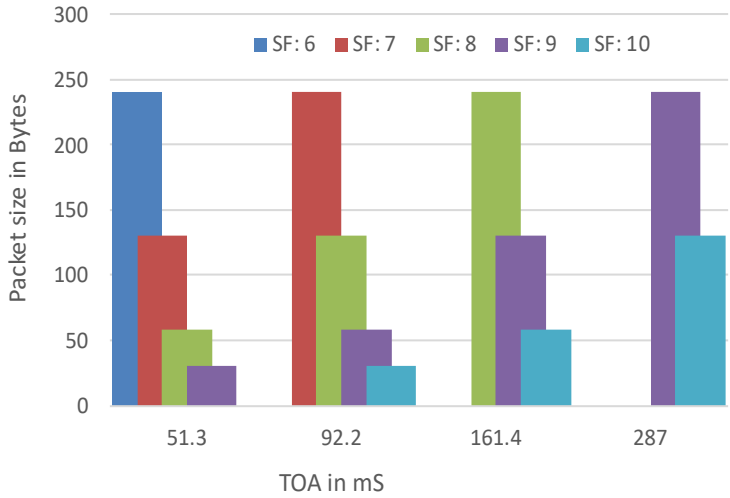

Figure 4-5. LoRa packet size for synchronized parallel data transmission using different SF in the same RF channel with same BW.

B) Data packetization

LSAQ uses Quasi-orthogonal multiple access of LoRa using multiple SFs within a single LC. Synchronization within a LC is highly dependent on the TOAs of the specific SF and time delay due to the data processing performed by the packetization function. Figure 4-4 shows data packet streams with 240-byte payloads transferred over 500 KHz BW at different SF values. Different physical channels can transfer packets simultaneously for varying TOAs. It is noted

that the processing time is considered the same for all the physical channels. It is observed, denoted by the green dotted lines, that the packets transferred in the LoRa physical channels using SF 7 have better synchronization with packets transferred parallelly using SF 9 than with SF 8 or SF 10 while maintaining the same packet size for all the SFs. As shown in Figure 4-4, for a LC with two LoRa physical channels using SF 7 and SF 9, the number of synchronized data packets are 1 and 3 when using an equal packet size with 240-byte payloads and the LoRa configuration used in equation (7). Parallel transmission of unequal packet size can be done by keeping the TOA the same for different SFs, as shown in Figure 4-5.

C) Synchronization

Synchronous access in an LC can be maintained in two ways. First, by distributing the data packets equally in the channels. Second, by using data packets of different sizes over the LoRa physical channels to maintain equal channel utilization based on the parameters provided by the data packetization function. The synchronization function assigns specific sequence numbers for the segmented data packets sent over the LoRa physical channels to facilitate packet loss detection and data block construction at the receiver end. Figure 4-6 shows the synchronization functions for an LC consisting of only two LoRa physical channels with SF1 and SF2 and the same BW. The calling function provides the LoRa BW and SF index as m and n respectively, where m varies from 1 to 3 for different BW used among 125 KHz, 250 KHz and 500 KHz, and n varies from 0 to 6 for different SF values from 6 to 12. For the transmission of equal packet size ($q_1 = q_2$), the synchronization function calculates the number of packets, r, to be sent using the physical channel having lower TOA, at the same time one packet of the same size is sent using the other physical channel (that has higher TOA). As an example, for a LC with two physical channels with SF1 = 7 (m_1=1) and SF2 = 9 (m_2 = 3) and the same BW ($n_1 = n_2$), r will be 3. For unequal packet size ($q_1 \neq q_2$), which is provided by the data packetization function, r will be 1.

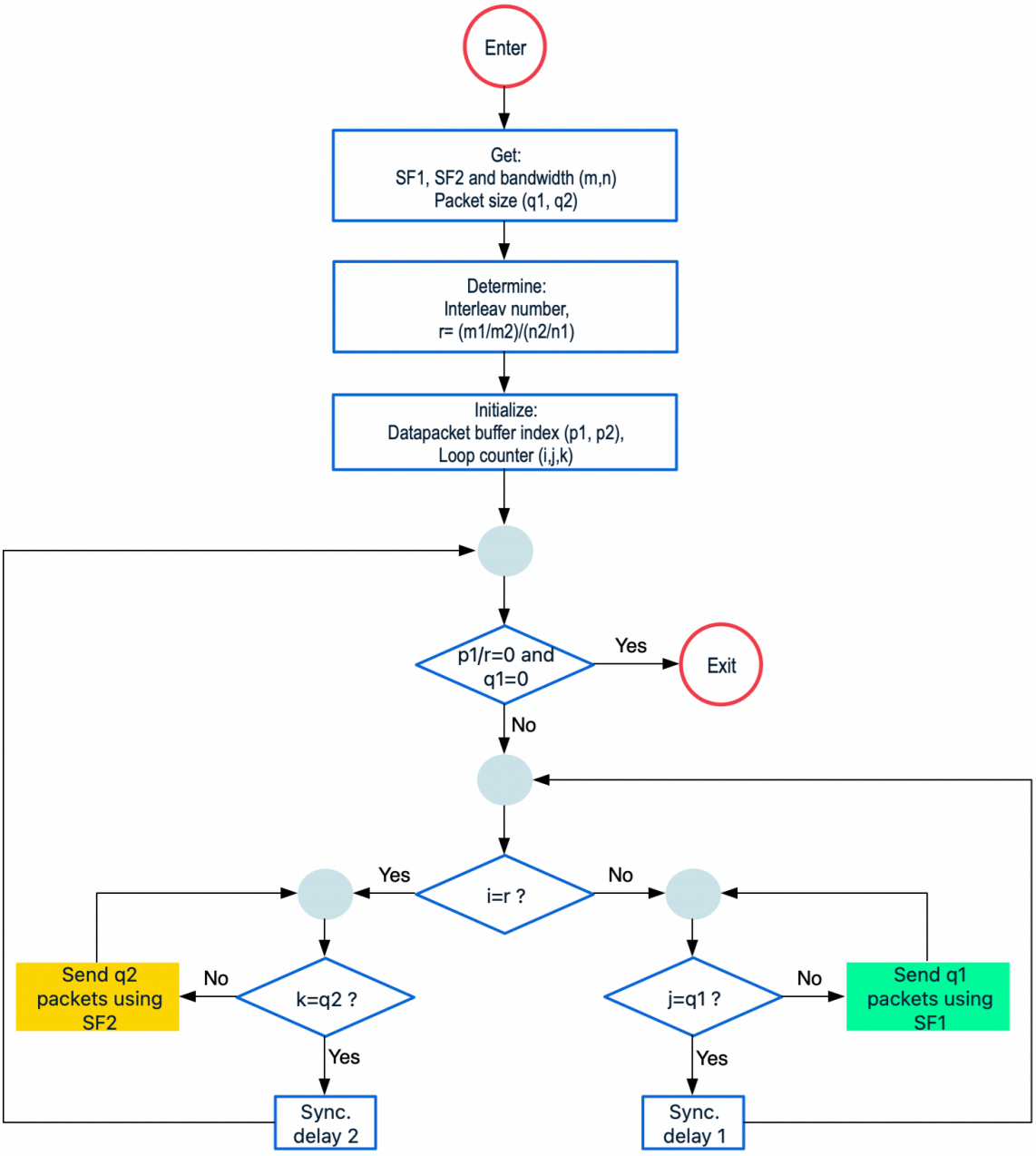

Figure 4-6. LSAQ packet synchronization algorithm for different SFs

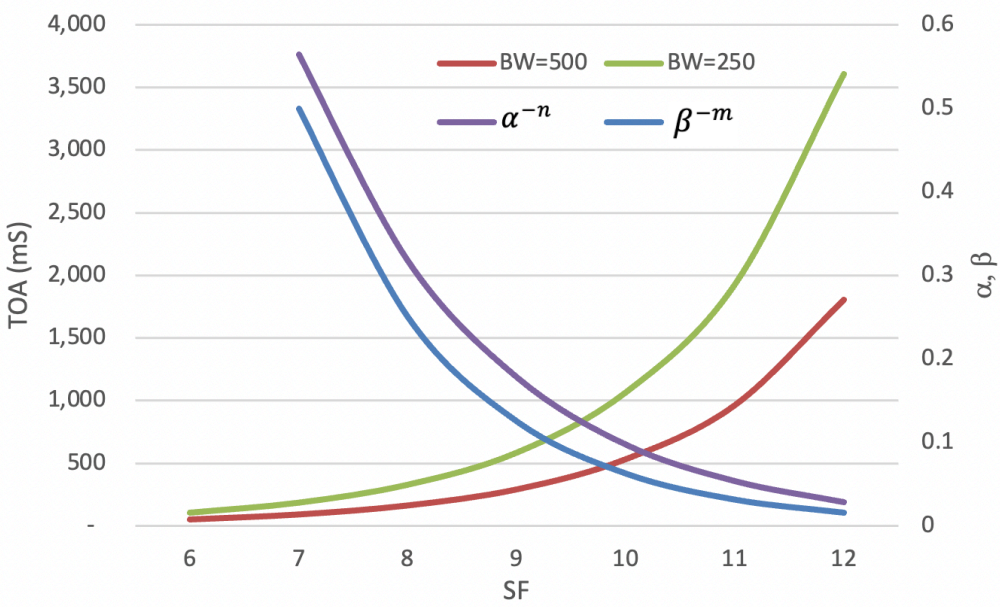

Figure 4-7. TOA variation with the change of BW and SF values to determine the value of α and β

4.3.4 Mathematical Model:

A) LSAQ Data Rate

The actual data rate for LSAQ depends on the equivalent or total TOA for the parallel LoRa physical channels, which can be represented by the following equation

$$TOA_{total} = \sum_{m=1}^{3}\sum_{n=0}^{5} TOA_{m,n}$$
$$= \sum_{m=1}^{3}\sum_{n=0}^{5} TOA_0(\alpha^{-n}\beta^{-m}) \quad (8)$$

TOA_0 is the TOA at SF 6 for a specific BW. Table 4-2 shows that the TOA is lowest at SF 6 for a specific BW. The increment of the TOA for other SF is represented by α. The TOA increment for the same SF at different BW is represented by β. For multiple LoRa physical channels with the same BW and SF, equation (8) can be written as equation (9), where k represents the number of duplicities of the LoRa physical channels.

$$TOA_{total} = k \sum_{m=1}^{3} \sum_{n=0}^{5} TOA_0(\alpha^{-n}\beta^{-m}) \quad (9)$$

Figure 4-6 shows the variation of TOA for different SF and BW, from which we can determine the value of α and β, which vary for different SF and BW. However, it varies only by 10%. Therefore, an approximation is used where $\alpha = 0.56$ ($\alpha = f(TOA_i, TOA_{i-1})$ and $\beta = 0.5$ ($\beta = 0.5^{(SF-6)}$).

Burst data transmission using the LSAQ requires multiple LoRa packets to be transmitted sequentially, as shown in Figure 4-4. This packet sequence can transmit a data stream in multiple time slots, as done in TDMA, due to the TOAs at different SFs. The number of packets for a burst transmission may also induce further underutilization. This utilization can be maximized using odd or even SF values for the stream of data packets, which corresponds to either SF 7 and SF 9 and SF 8 and SF 10 being paired together. However, it depends on the data processing and the bus communication time which is found similar for all SFs. Therefore, odd or even paired SFs may not be the best choice for maximum resource utilization.

$$T_{tx} = TOA_{tx} + T_u \quad (10)$$

$$TOA_{tx} = \sum_{m=1}^{3} \sum_{n=0}^{6} F_{m,n}\, TOA_0(\alpha^{-n}\beta^{-m}) \quad (11)$$

$$T_u = u \sum_{m=1}^{3} \sum_{n=0}^{6} F_{m,n} \quad (12)$$

$$\varphi = 1 - \frac{TOA_n - u}{T_{tx}} \approx 1 - \frac{TOA_1 - u}{T_{tx}} \quad (13)$$

$$DR_{LSAQ} = (1 - \varphi)\frac{PL}{T_{tx}} \quad (14)$$

For the burst transmission of multiple LoRa packets, the total burst transmission time (T_{tx}) includes the total TOA and the processing time (T_u), as shown in equation (10). However, the number of packets (F) that need to be transferred will differ for different SF. Considering the same processing time for all the SFs, TOA_{tx} and T_u can be rewritten as equations (11) and (12). From Figure 4-4, it can be shown that the synchronization loss will be lowest when the TOA is

the minimum time required for a packet, which is TOA_n - u, and that the transmission time utilization can be expressed by equation (13). The lowest TOA occurs for the lowest SF used, which is 7 for $n = 1$. Therefore, the synchronization loss can be minimized by using the smallest SF possible and then transmitting the largest packet possible using the same SF. The effective data rate of LSAQ can be calculated using equation (14), using PL as the payload size in bits and T_{tx} as time in seconds.

B) Energy Model

The total energy requirement can be determined by calculating the total energy required for a logical channel from the energy required for the associated LoRa physical channels (specific SF and BW) and the energy required for the processing of burst data. Equation (15) shows the total energy requirement for burst data transmission where P_{tx} is the LoRa transmission power and P_u is the processing power. The power required for the LoRa transceiver is same for all BW and SF with the same transmission power. Therefore, P_{tx} is replaced with the power required (P_0) at SF 7 and BW 500 KHz. Energy efficiency for the burst transmission can be calculated using equation (16).

$$E = P_{tx}(TOA_{tx}) + P_u T_u$$

$$E = P_0 \sum_{m=1}^{3} \sum_{n=0}^{6} F_{m,n}\, TOA_0(\alpha^{-n}\beta^{-m}) + P_u \sum_{m=1}^{3} \sum_{n=0}^{6} F_{m,n} \quad (15)$$

$$\eta = \frac{P_{tx} TOA_{tx}}{P_{tx} TOA_{tx} + P_u T_u} \quad (16)$$

4.4 Experimental setup and validation

The implementation of LSAQ assumes that multiple SFs are used in the same RF channel with the same BW, which is not assigned for any other link at the same time in the network to avoid co-channel interference. Unlike the GW LoRa modems, available LoRa transceivers at the time of writing this paper do not support multiple simultaneous transmissions or receptions. Therefore, the node has multiple LoRa transceivers connected and controlled by a single processor to avoid process-sharing complexity. Here, in a clustered WSN, the nodes can be the CHs that accumulate data from the sensor nodes (SN) of a cluster at a lower data rate using the

LoRa physical channel and transfer data to the DS or GW using a LC. Figure 4-8 shows the functional (hardware and software) blocks of the of the LSAQ nodes with multiple LoRa transceiver modules used for the LSAQ implementation. All the transceivers are connected using the same type of digital bus and are configured to have the same digital bus speed and LoRa parameters (BW, CR, DE, and H), except for SF as mentioned in equation (3). The transferred data volume is measured in bytes. Three experiments were performed to validate this research.

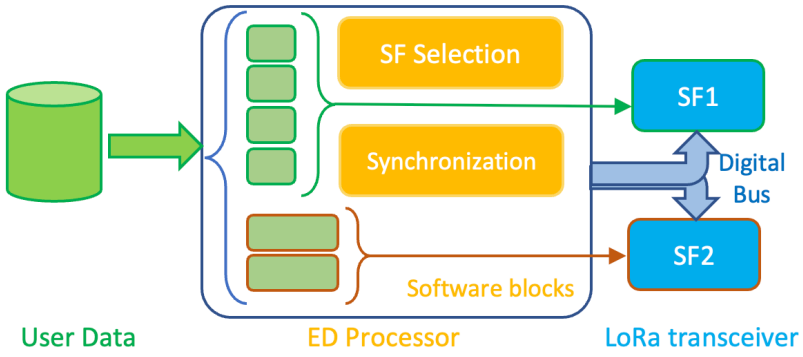

Figure 4-8. Functional blocks of a LSAQ node.

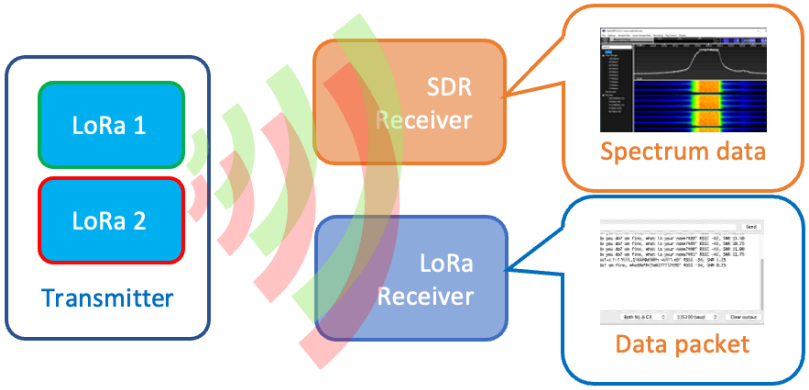

Figure 4-9. LoRa parallel data transfer experimental setup.

1) Parallel transmission using multiple radio channels with the same BW and same SF,
2) Parallel transmission using the same radio channel with different BWs and the same SF, and
3) Parallel transmission using the same radio channel with the same BW and different SFs.

While varying the experimental parameters as required during the experiment, the remaining LoRa parameters were kept constant throughout the experiment. We used two LoRa transmitters simultaneously and monitored the radio spectrum using a Software Defined Radio (SDR) based spectrum analyzer. The data quality, RSSI and SNR of the transmitted signal were monitored using a LoRa receiver configured for specific SF, BW, and radio channels. The experimental setup is shown in Figure 4-9.

Table 4-3: LoRa packet processing time and loss measured for the parallel transmission scheme

Tx_SF	TX_SW delay (ms)	Packet loss (%)	Average Tx time (ms)	Data processing time (ms)
7	<5	50	113	10
7	>5	0	113	10
7	10	0	117	10
8	5	0	188	10
9	5	0	312	10
10	5	0	577	20
11	5	0	1038	10
12	5	2	1935	44

4.4.1 Data processing time

Before performing the parallel transmission, the minimum data processing time was measured at BW 500 KHz for different SFs. Table 4-3 shows the experimental SF values used, processing time, packet transmission time and packet loss. It was seen that a software delay of less than 5 ms caused intra-channel packet loss as high as 50%. Data packet processing required 10 ms to 44 ms depending on the SF used. This processing time was highest for SF 12. It also notably had a 2% packet loss with a 5 ms software delay.

4.4.2 Transmission of multiple parallel radio channels

Inter radio channel interference was monitored to determine the best radio channels for parallel data transmission. In this experiment, the receiver was configured with SF 7, BW 250 KHz and the radio channel frequency equal to 916 MHz. The transmitter was configured with different radio channel frequencies ranging from 900 MHz to 940 MHz; BWs of 125 KHz, 250 KHz and 500 KHz; and SF values from 7 to 12. The radio channel was monitored using a spectrum analyzer, which showed more than one reflected channel other than the transmitted channel. This caused interference for the configured radio channel. Figure 4-10 shows a reflected radio channel at 915.4 MHz for the transmitted signal using a 916 MHz radio channel

with BW 250 KHz and SF 7. Although the reflected channel's signal level was poor compared to the actual channel, the receiver configured for the reflected channel received 5% to 10% of the packets with 20% data loss. Therefore, it was determined that multiple physical channels with different radio frequencies could not be used for parallel transmission.

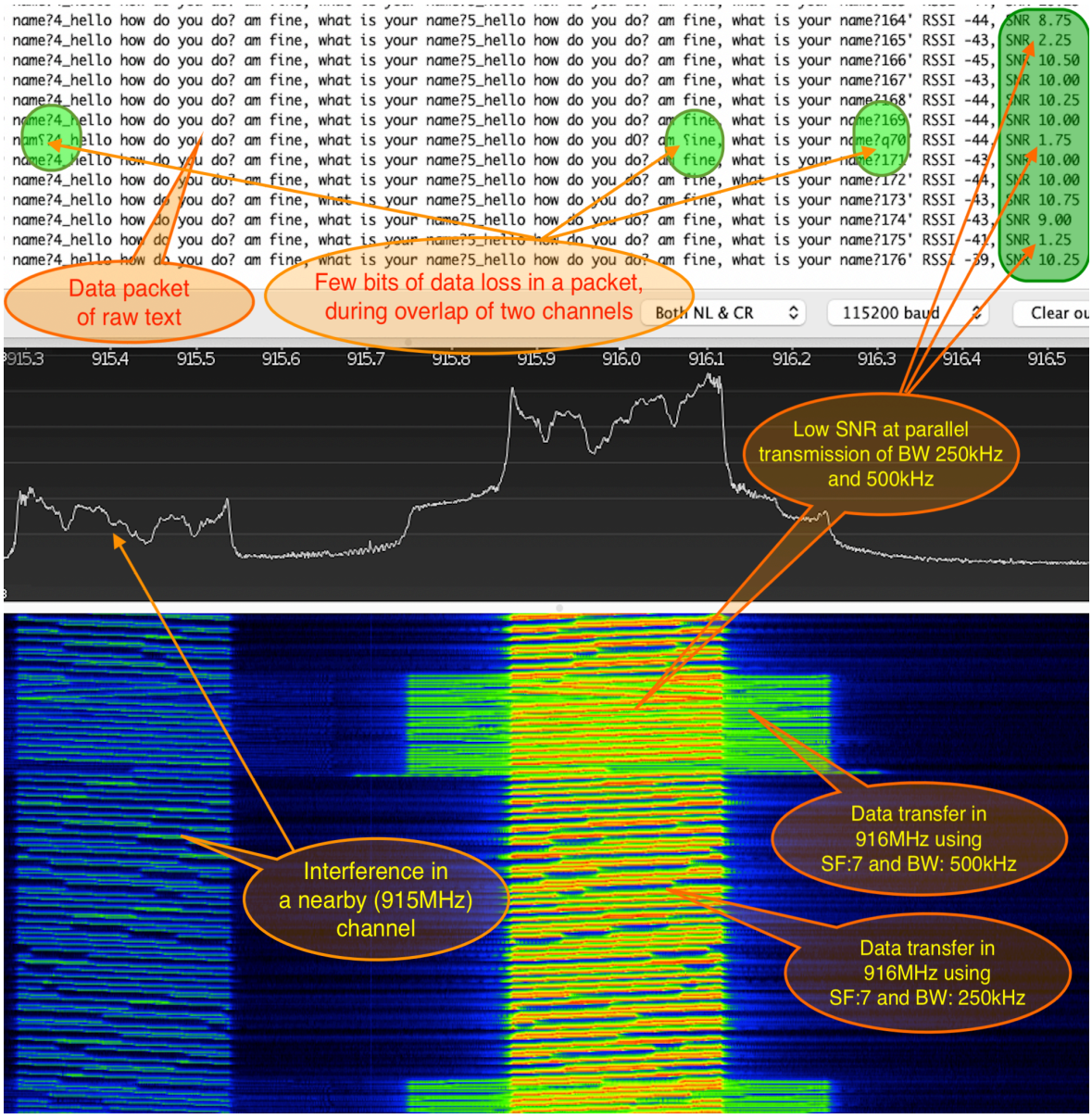

Figure 4-10. Different LoRa bandwidth and channel interference: The reflected radio channel (915.4 MHz) monitored for inter channel interference. Data loss for LoRa parallel data transmission using two different BWs (BW 250 KHz and 500 KHz) with same SF (7) and radio channel frequency (916 Mhz).

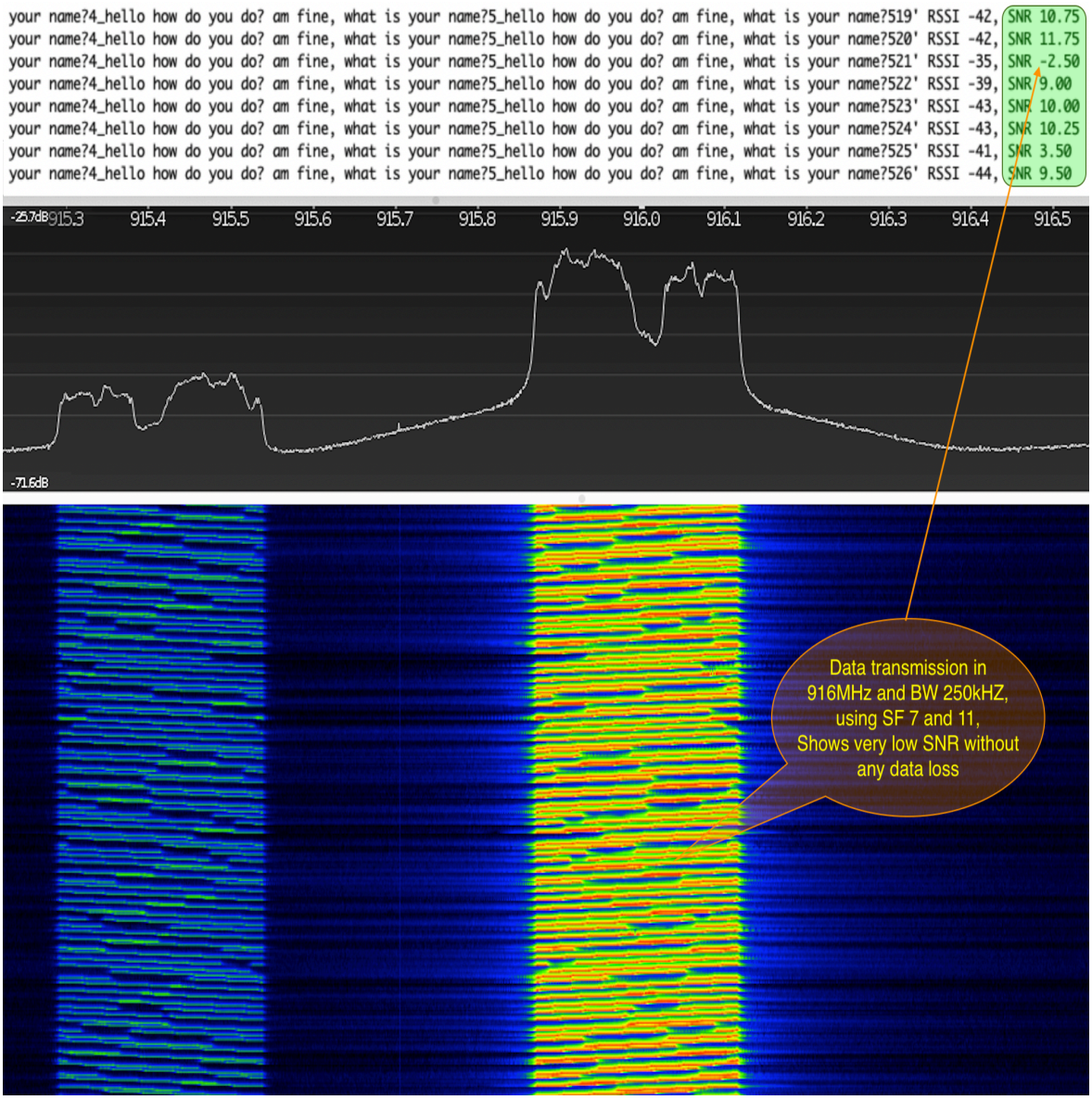

Figure 4-11. Parallel SF transmission without loss: LoRa parallel data transmission using different SF (SF 7 and SF 8) with the same BW 250 kHz and radio channel frequency (916 MHz), showing no significant data loss.

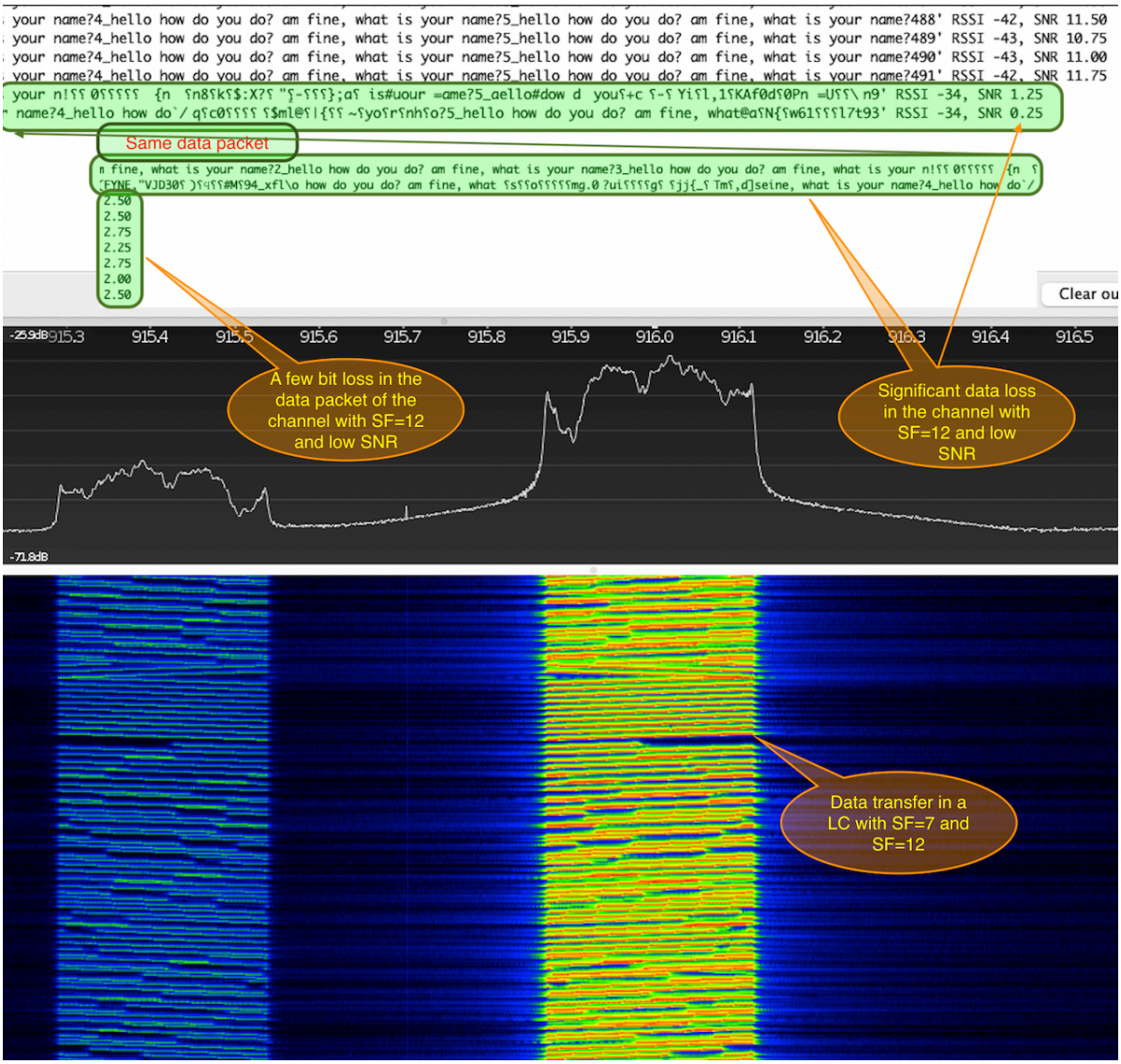

Figure 4-12. Parallel SF transmission with data loss: LoRa parallel data transfer using different SF (SF 7 and SF 12) with the same BW 250 KHz and radio channel frequency (916 MHz), showing some data loss due to inter SF interference in the physical channel with SF 7.

4.4.3 Transmission of multiple parallel bandwidths

In this experiment, one transmitter was configured to transmit 240 bytes of data using the 916 MHz radio channel with BW 250 KHz and SF 7. Another transmitter was configured to transfer a 10-byte LoRa packet using the 916 MHz radio channel with SF 7 and the BWs 125 KHz, 250 KHz, and 500 KHz. The receiver was configured using the 916 MHz radio channel with BW 250 KHz and SF 7. Figure 4-10 shows the parallel transmission of different BWs with the same SF and radio channel. The receiver received the data from the transmitter of a similar configuration (916 MHz, BW 250 KHz, and SF 7). However, the transmitted data with a BW

of 500 KHz causes noise that affects the LoRa physical channel with a 250 KHz BW, resulting in a SINR decrease from 10 to 1.25. We also observed a few bits of data loss in 20% of the overlapped data packets, denoted by green circles in Figure 4-10. Therefore, physical channels of different BW could not be used for parallel transmission (due to the quasi-orthogonality property of LoRa).

4.4.4 Transmission of multiple parallel SFs

In this experiment, two transmitters were configured with different SFs. One was configured with SF 7 and BW 250 KHz to send 240 bytes using the 916 MHz radio channel. Another module was configured for different SFs from 8 to 12, fixing the BW at 250 KHz, and transmitting only 10 bytes of data using the same radio channel. No data loss was observed for the parallel transmission using SF 7 and SFs from 8 to 11. The noise level was increased during the parallel transmission; hence the SINR went down to -2.5 from 10 for SF 7 and 8, as shown in Figure 4-11. However, no data loss was found for the SF combination. Data loss was found with the combination of SF 7 and SF 12 where the SINR was below 1.25 for SF 7 and 2.5 for SF 12 as shown in the Figure 4-12. This may result from inter-SF interference due to the longer overlapping duration of the two transmission channels with their TOAs of 198 ms and 660 ms respectively. Therefore, long-duration overlapping should be avoided during parallel transmission by choosing the SFs as close as possible or reducing the packet size for the LoRa physical channels with higher SF in the logical channel of different SFs.

4.5 Performance analysis

The proposed LSAQ overcame the bottleneck problem that limited the network capacity, coverage, and data rate. Figure 4-13 shows that parallel transmission using SF 7 and SF 8 can increase network capacity compared to WSNs using multiple SFs asynchronously as done in SF-based clustering [7]. LSAQ increases WSN capacity by 10% for densely populated urban applications and by 44% for urban WSNs with wider coverage. Similarly, LSAQ can increase network capacity by 46% for the WSNs that transfer large packets (up to 240-byte packets). Table 4-4 summarizes the application specific LSAQ performance in terms of network capacity, considering a data transfer interval of 15 min using a BW of 500 KHz. It shows a decrease in network capacity for densely populated WSN with SF 7 and 9 due to their longer TOA difference than SF 7 and 8 or SF 8 and 9. On the other hand, a decrease in network capacity is shown for using the SF 7 in the combination due to reduced coverage compared to SF 8 and 9.

Table 4-4: LSAQ network capacity for application specific WSN

WSN application	Data packet size	LSAQ implementation	Network size	% Improvement
Densely populated urban WSN	51 Bytes	SF=7 & 8	1150	10%
		SF=8 & 9	1660	44%
		SF=7 & 9	810	Decrease
Wide-area WSN	240 Bytes	SF=7 & 8	500	Decrease
		SF=8 & 9	760	46%
		SF=7 & 9	400	Decrease

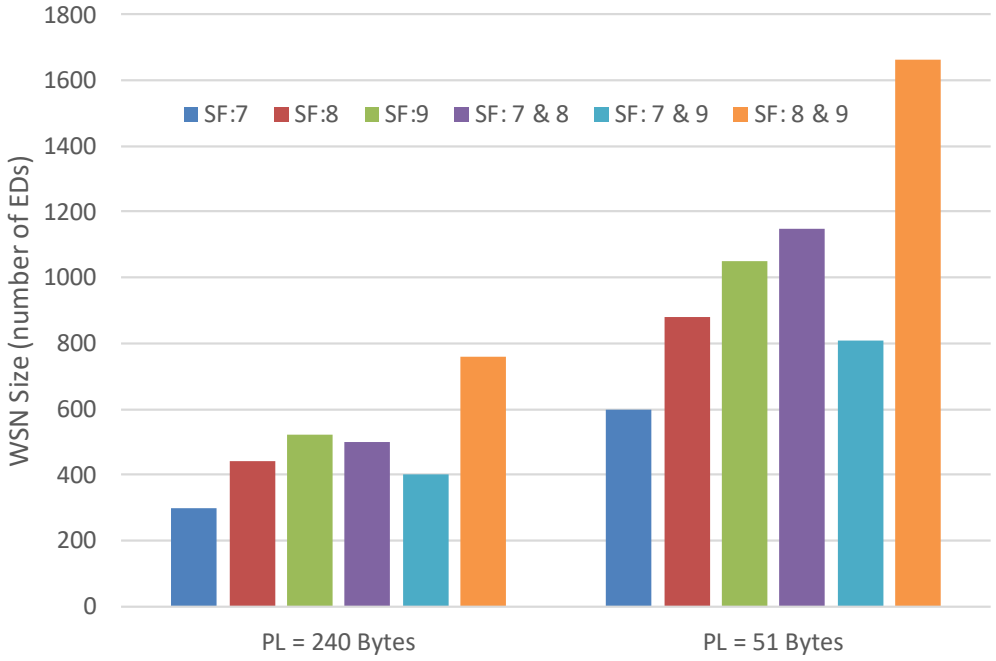

Figure 4-13. WSN size (with Static GW) dependence on different SF used for BW = 500 KHz and with 240B and 51B payload.

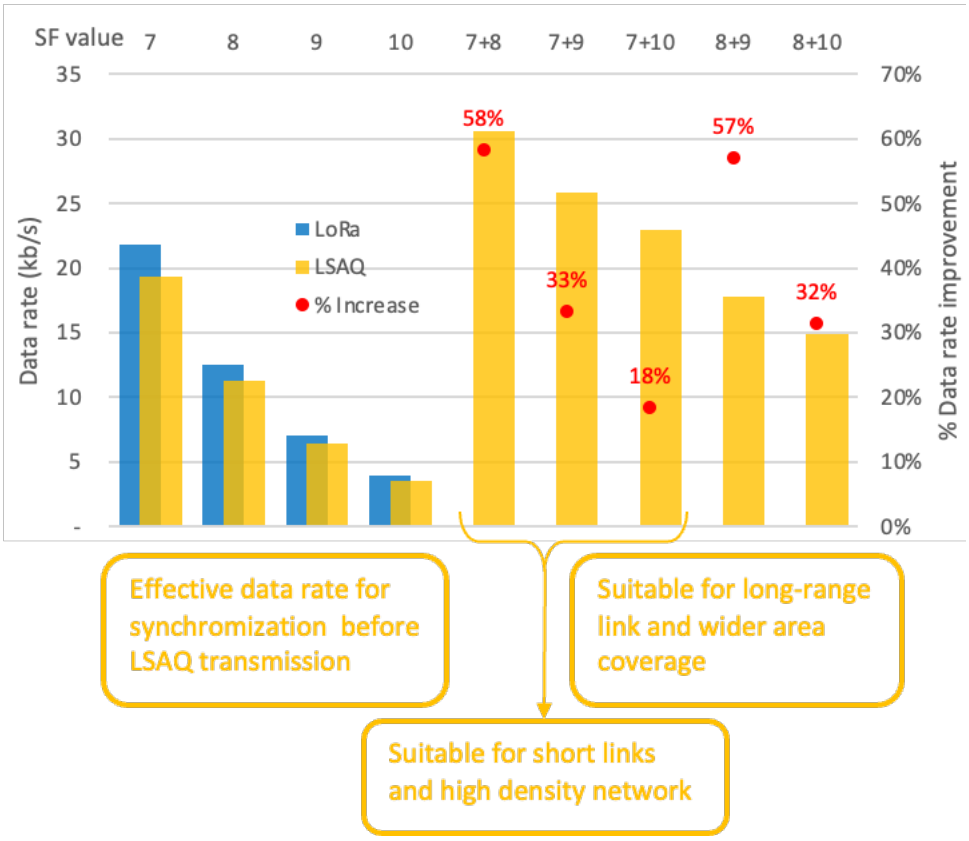

Figure 4-14. Data-rate improvement using LSAQ based parallel data transfer using various SF combination.

Figure 4-14 shows the LSAQ data-rate improvement efficiency compared with the LoRa physical channels based on a BW of 500 KHz and payload size of 240 bytes. It shows a reduced data rate using certain channels due to the synchronization loss of LSAQ. Combining two lower SFs (such as SF 7 and 8) gives a higher data rate than combining two higher SFs (such as SF 8 and 9). As described earlier, the selection of SF combinations also depends on the application. A combination of more than two SFs such as 7, 8 and 9 may give a data rate of 37.11 kb/s, which is 21% higher than that of using only SF 7 and 8. Similarly, combining one more SF (SF 10) with the three SFs may give a 10% increase in the data rate. This gain in data rate by combining more than two LoRa modems may not be feasible for lightweight nodes that require synchronization.

Besides improving network capacity and data rate, LSAQ has the following advantages over the LoRa capacity improvement schemes available during performing this research:

1) LSAQ utilizes the current LoRa CSS modulation technique to facilitate easy hardware implementation before any single-chip solution is available. It will also help facilitate the

LoRa network's adoption of the proposed scheme by adding one extra LoRa modem on each node. Using multiple LoRa modules may increase the node cost until the implementation of a multi-SF transmitter in a single chip solution is commercialized.

2) LSAQ is backward compatible. The network capacity of LoRa WSNs can easily be increased by adding one extra LoRa modem and implementing LSAQ in the CHs or in the repeater nodes.
3) Since the increased data rate of LSAQ decreases the TOA of a LoRa network, it can be used in WSNs with both static and moving DSs or GWs. Therefore, it will further increase the coverage area of the WSN.
4) The software stack of the proposed LSAQ is designed to be lightweight, targeting resource constrained nodes. Therefore, it can be easily implemented in low-end nodes with only a few kilobytes of program memory and less than a kilobyte of data memory.

Table 4-5 compares the proposed LSAQ with the other LoRa capacity improvement schemes, that utilizes improvement in modulation and in LoRa physical channels. ICS-CSS and SSK-ICS improved LoRa capacity by changing the basic CSS modulation. Therefore, it will not be readily applicable until chip-level implementations are available. Due to the change in modulation, these schemes may not be compatible with basic LoRa-based applications. Moreover, these changes in the modulation technique may increase the network capacity by up to 42% compared to the 46% improvement achieved by the proposed LSAQ. TDM-LoRa modulation doubled the data rate increasing the BER at lower SF (SF 7), whereas LSAQ improves up to 58% data rate using the SF 7 and 8.

The network access protocol proposed by [17] used multiple SFs in different clusters to equalize the transmission time. The CH closest to the GW may suffer from the bottleneck problem if it is assigned high SF values. As it is an application layer improvement on top of LoRaWAN MAC layer, its implementation will be simpler than LSAQ as it uses its own MAC layer while needing extra LoRa modules for parallel transmission.

Cantor [23] and EWS [18] aided the LoRaWAN MAC by improving the Packet Reception Rate (PRR) or PDR. Cantor proposed a parametric optimization algorithm that may cause higher control traffic in the network. Although it increases the goodput by up to 70%, the EWS may suffer from a higher collision rate due to miscalculation of the distance at poor RSSI. Unlike CSMA, used in LoRaWAN, LSAQ avoids the collision by using LBT and multiple SFs, instead of RF channels, for parallel transmission. However, the Cantor and Negative ACK implementation may not require any hardware changes depending on the processing and energy requirements.

The MIMO-LoRa [24] can receive multiple signals with different SFs parallelly transmitted by the same nodes based on SINR and transmission power optimization without any synchronization. This is unlike LSAQ, which requires synchronization within the same node, thus requiring a complex algorithm. Moreover, it is not suitable for low SFs like the proposed LSAQ. However, LSAQ may not be suitable for higher SFs due to higher inter-SF interference. As a non-LoRaWAN protocol, it may not support the WSNs built on LoRaWAN.

Table 4-5: Comparison of the proposed LSAQ with other LoRa capacity improvement schemes.

	ICS-CSS [14]	**SSK-ICS [15]**	**TDM-Lora [16]**	**[17]**	**EWS [18]**	**Cantor [23]**	**MIMO-LoRa [24]**	**LSAQ**
Technique	Modulation	Modulation	Modulation	Dynamic SF Allocation	Optimization algorithm	Optimization algorithm	Application layer protocol	Selection and Synchronization algorithm
LoRa orthogonality	Similar to basic CSS	Similar to basic CSS	Quasi-orthogonal in radio channel	Similar to basic CSS	SF orthogonality	Similar to basic CSS	SF orthogonality	SF orthogonality
Performance improvement	42% DR gain with 3.39% increase of bit error rate (BER)	28.6% DR improvement for the same SF and BW	Doubled the DR, increased BER at lower SF (SF=7)	62.8% DR improvement at SF = 7, for multi-hop WSN	18.2% to 55.25% DR improvement comparing other SF allocation algorithm	70% DR improvement in terms of good put.	Improved 10% to 50% DR at SNR less than 10	58% (SF = 7, 8), 33% (SF = 7, 9) DR improvement 10% (SF = 7, 8), 44% to 46% (SF = 8, 9) Network capacity improvement
Compatibility	Not compatible to LoRa-Phy			Compatible with LoRaWAN-MAC			Not compatible with LoRaWAN	Hardware (HW) compatible to LoR-Phy module, not to LoRaWAN MAC
Implementation	Need HW redesign			No HW redesign requires, need SW implementation			May need HW redesign	No HW redesign, and simple SW implementation required.
Limitations	Not compatible with the basic LoRa network due to change in modulation technique			Bottleneck issue for the node closer to the GW for multi hop network, due to use of high SFs	Require location date from GPS or calculated from RSSI.	Calculation and control message overhead for the optimization algorithm	Performs better at higher SFs (10, 11, 12)	Not suitable for combination of high SF (12) with low SF (7).
Advantages	May not impact the implementation of available LoRaWAN.			Support for LoRaWAN	Increased network size.	Compatible with LoRaWAN	Increased network coverage area	Lightweight, wide area WSN, and support for WSN with mobility

4.6 Conclusion

This paper addressed the challenges of the low data rate and high TOA of LoRa, which limits the WSN capacity in terms of the number of nodes and coverage area where multi-hop data transmission is required. LoRa GWs support the parallel reception of multiple SFs, and

some media access protocols utilize this capability to increase the WSN capacity. This can further be enhanced through parallel transmission from a node or CH using multiple SFs, as proposed by LSAQ. In this research, we investigated the possible means of parallel transmission in a LoRa network while focusing only on the SF in order to overcome the RF channel related interferences utilizing the quasi-orthogonality of LoRa. The analysis presented in this paper may help the future researcher to overcome LoRa's limitations with regards to parallel transmission and to potentially achieve further improvements using LoRa channels in parallel. The use of more than two SFs in parallel by one node, using the same RF-channel and BW, can be further investigated by introducing an optimization algorithm for the synchronization process. The proposed LSAQ was implemented using multiple LoRa modules due to the unavailability of multi-channel LoRa transmitter ICs, which can be replaced using a single IC solution as used in the LoRa GWs. LoRa WSN capacity can be improved by extending the LSAQ scheme to implement inter-node synchronization for alternate SF-group allocation among the nodes. Therefore, LSAQ may further increase LoRa's capacity to use in different WSN applications without changing the CSS modulation techniques.

4.7 References

[1] G.M.E.Rahman and K.A.Wahid,"LDAP: Lightweight dynamic auto- reconfigurable protocol in an IoT-enabled WSN for wide-area remote monitoring," in *Remote Sens.*, vol. 12, no. 19, pp. 3131–3151, Sep. 2020, doi: 10.3390/rs12193131.

[2] O. S. Oubbati, M. Atiquzzaman, P. Lorenz, M. H. Tareque and M. S. Hossain, "Routing in Flying Ad Hoc Networks: Survey, Constraints, and Future Challenge Perspectives," in *IEEE Access,* vol. 7, pp. 81057-81105, 2019, doi: 10.1109/ACCESS.2019.2923840.

[3] D. Zorbas and X. Fafoutis, "Time-Slotted LoRa Networks: Design Considerations, Implementations, and Perspectives," in *IEEE Internet of Things Magazine*, vol. 4, no. 1, pp. 84-89, March 2021, doi: 10.1109/IOTM.0001.2000072.

[4] G. M. E. Rahman and K. A. Wahid, "LDCA: Lightweight Dynamic Clustering Algorithm for IoT-Connected Wide-Area WSN and Mobile Data Sink Using LoRa," in *IEEE Internet of Things Journal*, vol. 9, no. 2, pp. 1313-1325, 15 Jan.15, 2022, doi: 10.1109/JIOT.2021.3079096.

[5] M. Chiani and A. Elzanaty, "On the LoRa Modulation for IoT: Waveform Properties and Spectral Analysis," in *IEEE Internet of Things Journal*, vol. 6, no. 5, pp. 8463-8470, Oct. 2019, doi: 10.1109/JIOT.2019.2919151.

[6] F. Benkhelifa, Y. Bouazizi and J. A. McCann, "How Orthogonal is LoRa Modulation?," in *IEEE Internet of Things Journal*, doi: 10.1109/JIOT.2022.3173060.

[7] A. Waret, M. Kaneko, A. Guitton and N. El Rachkidy, "LoRa Throughput Analysis With Imperfect Spreading Factor Orthogonality," in *IEEE Wireless Communications Letters*, vol. 8, no. 2, pp. 408-411, April 2019, doi: 10.1109/LWC.2018.2873705.

[8] O. Georgiou and U. Raza, "Low Power Wide Area Network Analysis: Can LoRa Scale?," in *IEEE Wireless Communications Letters*, vol. 6, no. 2, pp. 162-165, April 2017, doi: 10.1109/LWC.2016.2647247.

[9] G. Zhu, C. -H. Liao, T. Sakdejayont, I. -W. Lai, Y. Narusue and H. Morikawa, "Improving the Capacity of a Mesh LoRa Network by Spreading-Factor-Based Network Clustering," in *IEEE Access*, vol. 7, pp. 21584-21596, 2019, doi: 10.1109/ACCESS.2019.2898239.

[10] C. Liao, G. Zhu, D. Kuwabara, M. Suzuki and H. Morikawa, "Multi-Hop LoRa Networks Enabled by Concurrent Transmission," in *IEEE Access*, vol. 5, pp. 21430-21446, 2017, doi: 10.1109/ACCESS.2017.2755858.
[11] D. Croce, M. Gucciardo, S. Mangione, G. Santaromita and I. Tinnirello, "LoRa Technology Demystified: From Link Behavior to Cell-Level Performance," in *IEEE Transactions on Wireless Communications*, vol. 19, no. 2, pp. 822-834, Feb. 2020, doi: 10.1109/TWC.2019.2948872.
[12] Z. Xu, P. Xie and J. Wang, "Pyramid: Real-Time LoRa Collision Decoding with Peak Tracking," IEEE INFOCOM 2021 - IEEE Conference on Computer Communications, 2021, pp. 1-9, doi: 10.1109/INFOCOM42981.2021.9488695.
[13] R. Fernandes, M. Luís and S. Sargento, "Large-Scale LoRa Networks: A Mode Adaptive Protocol," in *IEEE Internet of Things Journal*, vol. 8, no. 17, pp. 13487-13502, 1 Sept.1, 2021, doi: 10.1109/JIOT.2021.3064932.
[14] P. Edward, M. El-Aasser, M. Ashour and T. Elshabrawy, "Interleaved Chirp Spreading LoRa as a Parallel Network to Enhance LoRa Capacity," in *IEEE Internet of Things Journal*, vol. 8, no. 5, pp. 3864-3874, 1 March1, 2021, doi: 10.1109/JIOT.2020.3027100.
[15] A. Mondal, M. Hanif and H. H. Nguyen, "SSK-ICS LoRa: A LoRa-Based Modulation Scheme with Constant Envelope and Enhanced Data Rate," in *IEEE Communications Letters*, doi: 10.1109/LCOMM.2022.3150666.
[16] S. An, H. Wang, Y. Sun, Z. Lu and Q. Yu, "Time Domain Multiplexed LoRa Modulation Waveform Design for IoT Communication," in *IEEE Communications Letters*, vol. 26, no. 4, pp. 838-842, April 2022, doi: 10.1109/LCOMM.2022.3146511.
[17] G. Zhu, C. -H. Liao, T. Sakdejayont, I. -W. Lai, Y. Narusue and H. Morikawa, "Improving the Capacity of a Mesh LoRa Network by Spreading-Factor-Based Network Clustering," in *IEEE Access*, vol. 7, pp. 21584-21596, 2019, doi: 10.1109/ACCESS.2019.2898239.
[18] D. Saluja, R. Singh, S. Gautam and S. Kumar, "EWS: Exponential Windowing Scheme to Improve LoRa Scalability," in *IEEE Transactions on Industrial Informatics*, vol. 18, no. 1, pp. 252-265, Jan. 2022, doi: 10.1109/TII.2021.3074377.
[19] Y. Hou, Z. Liu and D. Sun, "A novel MAC protocol exploiting concurrent transmissions for massive LoRa connectivity," in *Journal of Communications and Networks*, vol. 22, no. 2, pp. 108-117, April 2020, doi: 10.1109/JCN.2020.000005.
[20] A. Rahmadhani and F. Kuipers, "When LoRaWAN Frames Collide," in ACM WiNTECH, 2018, pp. 89-97, DOI: 10.1145/3267204.3267212
[21] T. Chan, Y. Ren, Y. Tseng and J. Chen, "Multi-Slot Allocation Protocols for Massive IoT Devices With Small-Size Uploading Data," in *IEEE Wireless Communications Letters*, vol. 8, no. 2, pp. 448-451, April 2019, doi: 10.1109/LWC.2018.2875455.
[22] L. Beltramelli, A. Mahmood, P. Ferrari, P. Österberg, M. Gidlund and E. Sisinni, "Synchronous LoRa Communication by Exploiting Large-Area Out-of-Band Synchronization," in *IEEE Internet of Things Journal*, vol. 8, no. 10, pp. 7912-7924, 15 May15, 2021, doi: 10.1109/JIOT.2020.3041818.
[23] D. Xu, X. Chen, N. Zhang, N. Ding, J. Zhang, D. Fang, and T. Gu, "Cantor: Improving Goodput in LoRa Concurrent Transmission," in *IEEE Internet of Things Journal*, vol. 8, no. 3, pp. 1519-1532, 1 Feb.1, 2021, doi: 10.1109/JIOT.2020.3013315.
[24] J. -M. Kang, "MIMO-LoRa for High-Data-Rate IoT: Concept and Precoding Design," in *IEEE Internet of Things Journal*, vol. 9, no. 12, pp. 10368-10369, 15 June15, 2022, doi: 10.1109/JIOT.2022.3143516.
[25] Zypher, Accessed on: Jan 10, 2022, [Online], Available: https://www.airbus.com/defence/uav/zephyr.html

5. DACK-LoRa: Dynamic Acknowledgement Protocol for Sequential and Image Data Transfer using LoRa in Wide-Area Wireless Sensor Network

This chapter presents the proposed data transmission protocol to improve the effective data rate (goodput) while transferring image and sequential data using the LoRa link. Long-distance image and sequential data transmission may not be possible using high-speed wireless technologies such as cellular networks for their coverage limitation and cost. Wide-area Wireless Sensor Network (WSN) applications also have energy and resource constraints to use energy-hungry wireless technologies to serve the purpose. Low-power wireless technologies such as LoRa can meet the distance requirement with a low data rate. Acknowledgement (ACK) message overhead of the protocols used for image and sequential data transmission worsens the effective data rate. This research proposes a lightweight data transmission protocol named Dynamic Acknowledgement (DACK) for the LoRa physical links to increase the data goodput by reducing the ACK message overhead.

Data transmission protocols use Stop-Wait or End-of-Block ACK messages to ensure lossless data transmission. Image and sequential data transmission requiring multiple packets suffer packet overhead. Various image segmentation and packetization schemes are used to reduce image data size and packet overhead. We investigated both these schemes to measure their performance in terms of goodput. The proposed DACK protocol generates an ACK message dynamically when it receives one or more lossy packets. The receiver sends the DACK message with the indexes of the packets containing missing data, and the transmitter retransmits only those missing packets accordingly. Therefore, DACK protocol reduces the total ACK message over the complete image and sequential data transmission period improving goodput compared with other protocols. A mathematical model is derived for DACK and other protocols to measure and compare their performance by measuring the total time of ACK messages used for transmitting the same image data. We found DACK-LoRa protocol reduces the total ACK message duration 10 to 30 times than the Stop-Wait and End-of-block ACK schemes.

The development work, analysis and findings of this chapter will be submitted to an international conference for possible publication. The student contributed to the main idea, implementing code, writing the original draft, and evaluating and revising the manuscript.

DACK-LoRa: Dynamic Acknowledgement Protocol for Sequential and Image Data Transfer using LoRa in Wide-Area Wireless Sensor Network

Gazi M. E. Rahman, Member, IEEE, and Khan A. Wahid, Senior Member, IEEE

Abstract: Wide-area Wireless Sensor Networks with multiple hops and massive Internet of Things applications may require transferring high-volume data or image at a regular and longer interval. Cellular network and satellite-based data communication may not be feasible due to higher energy requirements and low radio resource utilization or high cost. On the other hand, Low Power Wide Area Network technologies including LoRa are not capable of high-volume sequential data or image transfer due to their low data rate. Therefore, modified LoRa modulation techniques and multiple sinks or gateways with parallel operation are proposed to improve LoRa channel capacity. This research proposes a dynamic acknowledgement (DACK) protocol to improve LoRa channel's goodput for sequential data or image transmission by reducing the packet overhead. DACK-LoRa demonstrated a 10 to 30 times reduction of acknowledgement overhead comparing the End of Block Acknowledgement protocols.

Keywords: LoRa, image transfer, Long-range, wide-area monitoring, WSN, communication protocol

5.1 Introduction

Application-specific long-distance images and accumulated sensor data in a wide-area Wireless Sensor Network (WSN) with Internet of Things (IoT) connectivity can be transferred using cellular networks [1]. Satellite-based imaging [2] is used for wide-area remote sensing applications. However, both these technologies may not be feasible technically due to high energy requirements and underutilization of the resources (radio links) or high cost of operation. Low Power Wide Area Network (LPWAN) technologies such as Zigbee [3] and high-speed technologies such as Wi-Fi may not be suitable for their short range [4]. Among the low power and long-range technologies, LoRa provides a better data rate (up to 37.5kbps) than SigFox. Therefore, LoRa can be used to transfer image or sequential data at a range from 1km to 15km with Line of Sight (LOS) [5]. This speed and range may not be sufficient for real-time image or sequential data transmission. However, applications like root architecture imaging [6] may transfer the offline image over the LoRa link.

Previous research achieved 100% packet delivery rate up to 4km sending 13.5kB data [7] in 67s for a long-distance image transmission. Online voice and offline image data [8] of 20.3 KB were transferred in 169ms. Cluster head close to the Base Station (BS) in a wide-area WSN with multiple clusters accumulates data from the remote clusters. This accumulated data may

be sent sequentially [9] to the Base Station (BS) utilizing the LoRa link. Offline firmware update of the remote sensor node [10] is done over the LoRa physical link using multiple processors.

Beside the low data rate, LoRa has high Time on Air (TOA) comparing other LPWAN communication technologies, which increases the total transmission time. Longer range requires higher Spreading Factor (SF) with the cost of higher TOA. Alternatively, multiple hops using lower SF, may reduce the TOA of one hop, however, will increase the total end to end TOA as a multiple of the number of hops. Use of LoRa Wide Area Network (LoRaWAN) protocol further increases this time due to the limit of 1 % duty cycle to accommodate more nodes in the network.

Addressing these challenges, improvement of the data transmission protocol over the LoRa physical layer is focused on in this research. LoRa physical layer transfers data using a 256-byte packet, including all required access control and application layer overhead. Effective data rate or application-specific goodput depends on the LoRa physical layer payload or application layer's data size. This overhead may not impact the throughput for the single packet data transfer. However, for sequential transmission of high-volume data or image data, reduction of packet overhead may increase the goodput. Reduction of acknowledgement (ACK) messages while transferring data packets can improve goodput. This research proposes an application layer protocol that generates Dynamic Acknowledgement (DACK) messages for the missing or lossy data packets to improve the goodput for sequential data and image transmission over the LoRa physical layer. Major contributions of this research are-

- Development of an application layer protocol to send the uncompressed image or sequential data over the LoRa link,
- Development of algorithms for image data segmentation, construction, error checking and ACK message generation, and
- Development of the mathematical model to measure the improvement by determining the total ACK transmission time.

The following section describes the technical background of LoRa followed by the highlights of the recent research works on image transmission algorithms and protocol improvement. Section 5.4 describes the proposed DACK-LoRa in detail, followed by the field trial result and performance analysis for the in-situ root imaging as a use case. The conclusion highlights the limitations and future scope of research to improve the LoRa capacity for image transmission applications in the WSN.

5.2 Technical background

5.2.1 LoRa Modulation

LoRa uses Chirp Spread Spectrum (CSS) modulation at various Industrial, Scientific, and Medical (ISM) bands such as 169 MHz, 433 MHz (Asia), 868 MHz (Europe) and 915 MHz (North America). Most of the LoRa transceivers support a programmable SF from 7 to 12. LoRa supports a programmable Coding Rate (CR) between 1 and 4 bits for forward error correction to provide better interference tolerance. Therefore, the actual Bit Rate (BR) depends on the SF, CR and the channel Band Width (BW), which is calculated using (1). The maximum BR of 21.87 kbps can be achieved for BW= 500KHZ, CR = 1 and SF = 7.

$$BR = SF.\frac{4}{4+CR}.\frac{BW}{2^{SF}} \qquad (1)$$

5.2.2 Range of LoRa link

LoRa supports an adjustable transmission power from -4 dBm to +20 dBm. The receiver sensitivity varies from -120 dB to -136 dB, and it performs better [11] at higher SF and lower BW (-136 dB at SF = 12 and BW = 125 KHz). The range of LoRa link depends on the LOS and the antenna height. Antenna height (h in m), and distance (d in km) between the transmitter and receiver can be calculated using the Fresnel Zone equation shown in (2), considering a 60% Fresnel clearance. Where H_e is earth curvature, and f (in GHz) is the LoRa carrier frequency. It gives an antenna height of 7m for a 1 km link range ignoring the earth curvature.

$$h = H_e + 8.657\sqrt{\frac{0.6d}{f}} \qquad (2)$$

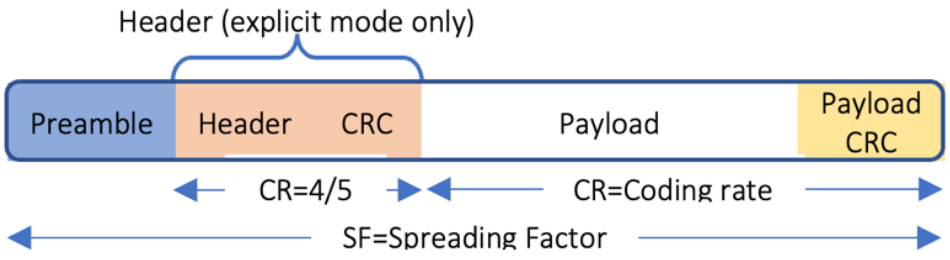

Figure 5-1. LoRa physical channel

5.2.3 Data frame of a LoRa physical channel

A LoRa data frame consists of two mandatory blocks called the Preamble and Payload, along with two optional blocks for the Header and Cyclic Redundancy Check (CRC) of payload, as shown in figure 5-1. All the block sizes are variable according to the transceiver configuration. The payload size ranges from 1 to 255 bytes. The total number of bits (n_{PL}) in the frame can be calculated using (3).

$$n_{PL} = 8 + max\left(0, \left\lceil \frac{8PL - 4SF + 8 + CRC + H}{4(SF - DE)} \right\rceil (CR + 4)\right) \qquad (3)$$

Where PL is payload length in bytes, CRC is 16 bits if enabled and 0 otherwise, H = 20 when the header is enabled and 0 otherwise. DE is 2 when the low data rate optimization is used, otherwise it is 0.

5.2.4 LoRa versus other LPWAN technologies

Other LPWAN technologies such as Narrow Band IoT (NBIoT), IEEE 802.15.4 and Sigfox can be compared with LoRa for remote monitoring and image transfer applications. NBIoT is deployed in the Long-Term Evolution (LTE) cellular network and provide two different data rates for NB-1 (26 kbps) and NB-2 (127 Kbps). NBIoT does not have coverage in the rural area due to high establishment cost and requires more power than LoRa. IEEE 802.15.4 provides the physical and Media Access Control (MAC) layer support for Zigbee, WirelessHART, MiWi, 6LoWPAN, Thread and SNAP. It can provide up to 256 Kbps data rate and up to 1km range with full LOS. IEEE 802.15.4 require comparatively higher power than LoRa for the same coverage range. Sigfox is a proprietary technology that uses the ISM band. It provides a 100-bps data rate with a range from 10 km (urban coverage) to 50km (rural coverage) and permits only 140 messages per day for each node. Comparing with these LPWAN technologies, LoRa requires very low energy for a data rate of up to 37kbps. It has better immunity to interference and higher receiver sensitivity which is required for long range coverage.

5.2.5 LoRa network protocol

LoRa networking protocols such as LoRaWAN assigns the channels in time and frequency domains to accommodate more nodes in the network. Other than resource allocation, it also maintains and controls the connectivity between the SNs and the Gate Way (GW). We can increase goodput by reducing the control overhead of the protocol. Various modified LoRAWAN protocols utilize Slotted ALOHA, Non-Persistence Carrier-Sense Multiple Access

(NP-CSMA), and scheduled Media Access Control (MAC) to expand the network size [12]. Protocols with out-of-band synchronization also bring similar improvements. However, data-rate can be further improved to accommodate high-volume data transfer through a LoRa link.

5.3 Related work:

Wireless Image transmission over the LPWAN technologies utilizes various image preprocessing to reduce the bandwidth requirement. Webp+Base64 compresses JPG image [13] of 20.03 kB to 5.51 kB, which reduces the number of LoRa packets from 81 to 23. However, the reduction of transmission time from 47.7 s to 25.7 s is not according to the reduction of the total packet count. Resource (dynamic memory) limitation may require extra time while processing the image during transmission. Besides, a high processing load and time require high energy. Channel Activity Detection (CAD) mechanism with CSMA [14] is used to assign a LoRa physical channel for lossy grayscale image transmission. CAD sends image when a free channel is detected. Otherwise, the processor must wait for a minimum one-tenth of the maximum TOA (calculated for the LoRa channel used), which was found around 1 s. This wait time may further increase the image transmission time and may not be suitable for lossless image transmission. Compression and Image Recovery Algorithm (CIRA) [15] first compresses YUV420 image of 320x240 size and replaces the 680-byte JPG header by a single byte index to reduce the total image file size. Unlike z-scanning method used in JPG, it divides the image into 12 sections before compression to limit the data losses in a smaller data packet. The segmented image data is sent to the CIRA server over the LoRaWAN where the header-less decompression method is used to reconstruct the image. If the CIRA detects any packet loss, the server sends request to the node for retransmission. The image is segmented to send only the differential block [16] over LoRa to reduce the data volume. The captured 160x160x8-bit grayscale image is divided into 256 segments of 10x10x8-bit images. In the beginning all the segments are sent with their index number adding the Cyclic Redundancy Check (CRC) at the end of the segments. Next time only the differential segment is sent to reduce the data volume. This process is highly application-specific and may not be energy efficient for a resource constrained node to run the dissimilarity detection process.

Protocol specific improvements are done to avoid the image preprocessing load at the node. Multiple SFs [17] are used to send an image parallelly. The transmitting node with the lowest SF distributes the image to the other nodes in different data block size according to their SFs. Then all the transmitters resend the image parallelly for the receivers of same SFs using pear to pear topology. All the receivers resend the received packet to the receiver with the lowest SF to reconstruct the image. Total image transmission time was reduced from 48s to 26s for a JPG image of 200x150 pixels. Therefore, it could not reduce the transmission time (54% using three LoRa channels) as expected due to the re transmissions of the same image. It also shows low

Packet Receive Success Rate (PSR) for the higher SFs, which may further be reduced for bigger image size. Different SFs are used in different time slots [18] to send the segmented images. Multi-Packet LoRa (MPLR) and channel reservation [19] are used to speed up image transfer over LoRaWAN instead of Stop-Wait and ALOHA. The receiver sends ACK and the index of the missing packets after receiving a fixed number of packets instead of sending ACK after every packet. It reduces the collision rate and transmission time by 26% over the ALOHA protocol. This research focuses on the protocol improvement to facilitate both image and sequential data transmission without changing the WSN configuration, LoRa modulation technique, and changing the image file format.

5.4 The proposed DACK-LoRa protocol

ACK messages can be used to reduce data loss for wireless data transmission. As shown in Figure 5-1, LoRa physical packet consists of 255 bytes payload, including the application-specific overhead. The actual useable application-specific data is measured in terms of goodput. However, an ACK message sent for the same type of data (such as an image) transmitted over multiple LoRa packets, may reduce the goodput.

The proposed DACK-LoRa protocol focuses on the reduction of the ACK message while transferring image or sequential data using the LoRa physical channel to improve the channel goodput. Figure 5-2(a) shows the DACK-LoRa packet structure, figure 5-2(b) shows the different types of ACK packets and figure 5-2(c) shows all possible values for every fields in the packet.

Tag	RID	SID	MID	SQN	PL	CRC
Size (byte)	2	2	1	1	0-248	2

(a)

Message	Packet Length (byte)	Hex value
ACK (Stop wait)	10	XXXX-YYYY-02-HH-F00F-ZZZZ
ACK (ETA)	40	XXXX-YYYY-02-HH (32-byte segment bitmap)-ZZZZ
ACK (Dynamic)	10	XXXX-YYYY-02-HH- (F segment bitmap F)-ZZZZ
Image data segment 1	256	YYYY-XXXX-03-01- (Image raw data) -ZZZZ

(b)

Tag	Full name	Value (Hex)
RID	Receiver ID	0001-FFFF
SID	Transmitter ID	0001-FFFF
MID	Message ID	00-FF
SQN	Sequence number	00-FF
PL	Pay load	Any hex
CRC	Cyclic redundancy check	16-bit CRC

(c)

Figure 5-2. LoRa physical packet (a) structure, (b) message and (c) tag detail.

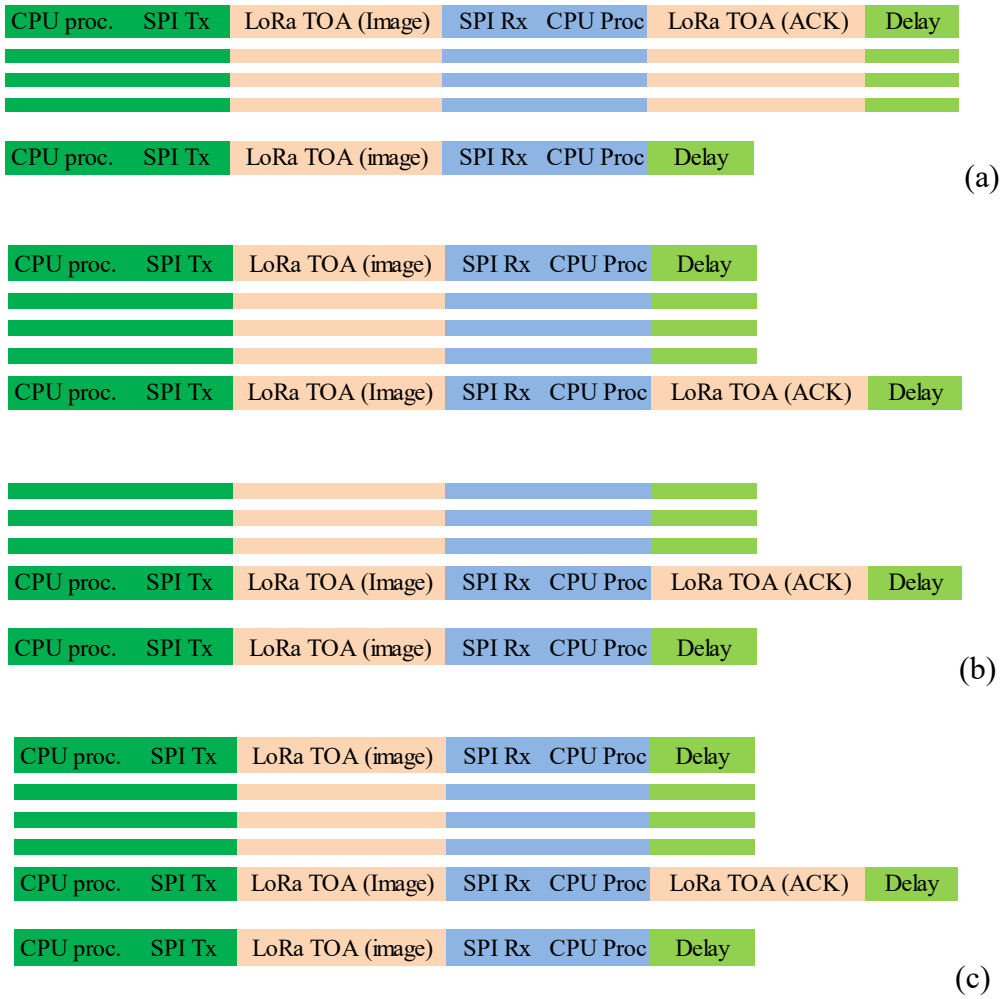

Figure 5-3. Sequential data transfer for multiple LoRa packets using a) Stop-Weight, b) multi-packet acknowledgement and c) dynamic acknowledgement protocols.

The Stop-Wait transmitter waits until receiving an ACK from the receiver. The End-of-Transmission protocol sends an ACK message at the end of receiving the last packet. This type of ACK may include a list of missing packet's sequence numbers. The MPLR sends ACK after a fixed number of packets called block of image data. ACK messages for the blocks that do not have any missing packet may cause message overhead reducing goodput. Dynamic ACK is sent after receiving the last packet or after receiving any lossy packet. This type of ACK message contains the sequence number of the lossy packets. This research proposes a modified version of MPLR protocol by sending the ACK once at the end of the transmission or after receiving a predefined number of packets for sequential data with the sequence number(s) of the missing packet(s). Therefore, only the packets with missing data are resent according to the ACK message.

We evaluated DACK-LoRa's performance in terms of transmission time. In the sensor node, the LoRa module is connected with a low-power MCU using high-speed bus. Therefore, the total image transmission time depends on LoRa TOA, CPU processing time, and ACK delay time (T_{ACK}). Figure 5-3 shows and message flow and the time required for a complete image transmission using three different protocols. As shown in figure 5-3(a), the sensor node waits for ACK from the sink after transmitting every LoRa packet. Figure 5.3(b) shows the message flow for MPLR that sends ACK after a block of multiple LoRa packets. Figure 5-3(c) shows the message flow for the proposed DACK-LoRa. It uses the End of Transmission ACK (ETA) scheme and sends only one ACK after receiving the last LoRa packet.

We can calculate the total time of transmission for these three protocols using equations (4) to (6) and can validate the result with the actual time taken by the implemented system.

$$T_s = (T_i + T)N_P + (T_{AS} + T')N_P + (T_i + T)N_{PL} \quad (4)$$

$$T_M = (T_i + T)N_P + (T_{AM} + T')N_B + (T_i + T)N_{PL} \quad (5)$$

$$T_E = (T_i + T)N_P + (T_{AE} + T') + (T_i + T)N_{PL} \quad (6)$$

T_S : Total time for Stop-wait protocol
T_M : Total time for MPLR protocol
T_E : Total time for ETA protocol
T_i : TOA of LoRa image packet
T : SW Processing time for image packet transfer
T` : SW Processing time for ACK packet transfer
T_{AS} : TOA of ACK for stop-wait protocol
T_{AM} : TOA of ACK for MPLR protocol
T_{AE} : TOA of ACK for ETA protocol
N_P : Number of LoRa image packet

N_{PL} : Number of image packet loss
N_B : Number of block for MPLR protocol (= N_P/P_B)
P_B : Number of LoRa packet per block

$$T_s - T_M = (T_{AS} + T')N_P - (T_{AM} + T')N_B \quad (7)$$
$$T_M - T_E = (T_{AM} + T')N_B - (T_{AE} + T') \quad (8)$$

Time differences between the protocols calculated using (7) and (8) depend on the TOA of the ACK packets, which is directly related to the packet construction of that protocol. TOA itself depends on different LoRa configurations, N_B selection and the software processing time. These three parameters are evaluated in the performance evaluation sections.

5.5 Field trial and performance evaluation

Field trial was performed using the SoilCam [6] as the imaging device. Figure 5-4 shows the functional blocks of the trial setup. The SoilCam generates a 150 Dots Per Inch (DPI) root image of 20cmx50cm. One image consists of 180 snaps of 118x158x8-bit grayscale bitmap images. Every snap generates 18kB data. The transmitting controller acquires images from the camera and sends the data to the LoRa modem. The LoRa-IoT gateway receives the data, checks for missing or lossy packets after receiving the last packet of a snap and sends ACK with the packet index to be resent by the transmitter.

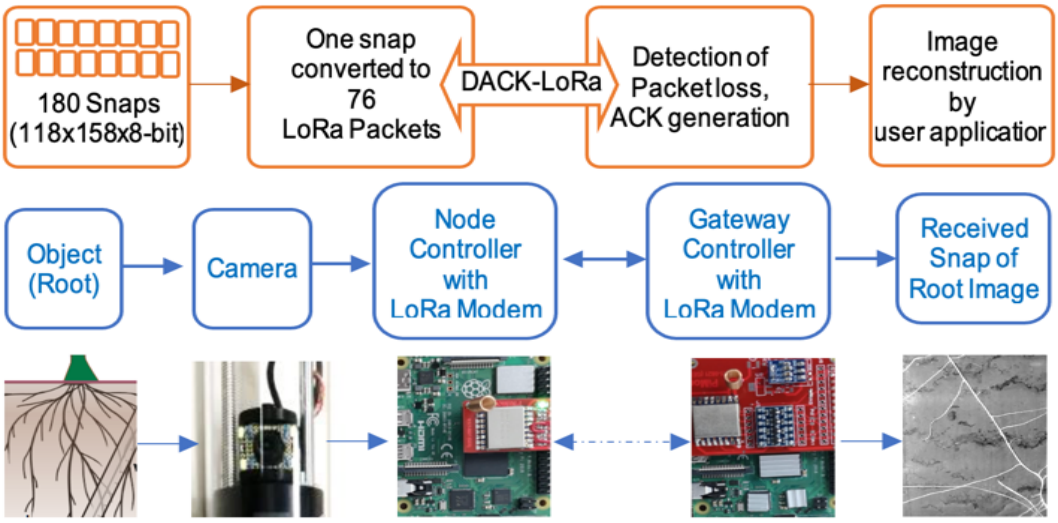

Figure 5-4. Functional blocks of the DACK-LoRa trial setup

LoRa TOA can be calculated for the number of image packet (*Np*) sent and number of lossy packets (N_{PL}) using equation (3), derived from SX1276 datasheet [11] for the LoRa parameters shown in Table 5-1. The required TOAs for the image file sent over LoRa at different SF and BW configurations are shown in Table 5-2.

$$TOA = \frac{2^{SF}}{BW}(4.25 + N_P + N_{PL}) \qquad (9)$$

Table 5-1: LoRa parameters used for DACK-LoRa protocol.

Parameters	**Values**
Image file size	9kB, 18kB, 28kB
SF	7, 8, 9, 10, 11
BW	125 KHz, 250 KHz, 500 KHz
CR	1
CRC	0
D	0
H	0
P_B	10-40
nPR	8 symbols

Table 5-2: Image file size and calculated TOA using DAck-LoRa protocol.

LoRa Parameters		**TOA (Sec)**		
BW	**SF**	**9 kB**	**18 kB**	**28 kB**
500 KHz	7	3.75	7.5	11.64
	8	6.62	13.24	20.56
	9	11.88	23.76	36.88
	10	21.42	42.84	66.52
	11	38.95	77.90	120.95
250 KHz	7	7.50	14.99	23.28
	8	13.24	26.48	41.11
	9	23.76	47.51	73.77
	10	42.84	85.68	133.04
125 KHz	7	14.99	29.98	46.55
	8	26.48	52.96	82.23
	9	47.51	95.02	147.54

For TOA of the ACK message, we need to consider the packet construction based on the

length of the payload. Such as, ACK of Stop-Wait protocol needs 8 bytes for pay-load header and only 1 byte for the status (loos or no-loss) of the received image packet. ACK of MPLR needs 8 bytes for pay-load header and 2 to 16 bytes for the bitmap of the packet received depending on the number of packets transferred in a block (P_B). ACK of ETA protocol needs 8 bytes for pay load header and more than 2 to 16 bytes for the bitmap of the packet received depending on the image size. DACK-LoRa uses ETA for every snaps. The processing time shown in (7) and (8) includes the data transfer time from memory to the LoRa buffer and other fixed (or dynamic) software delay. These processing times are very negligible due to the high bus speed and processer speed of the controller. The fixed/dynamic software delay depends on the algorithm used. So, neglecting these times, (7) and (8) can be written as-

$$T_s - T_M = T_{AS}N_P + T_{AM}N_B \quad (9)$$

$$T_M - T_E = T_{AM}N_B + T_{AE} \quad (10)$$

Figure 5-5 shows the total ACK time required for Stop-Wait, MPLR (with block size 10 bytes and 40 bytes) and DACK-LoRa using ETA. ACK time for MPLR using 10-byte block size is almost 10 times lower than the ACK time required for Stop-Wait protocol, which is 30 times lower using 40-byte blocks. DACK-LoRa requires the lowest ACK time which is 5 to 10 times lower than the MPLR. Our trial data using 18 kB image file also shown the same differences among the protocols. However, total image transfer time was 1.5 to 2.2 times of the calculated transfer time depending on the processor and the software algorithm used.

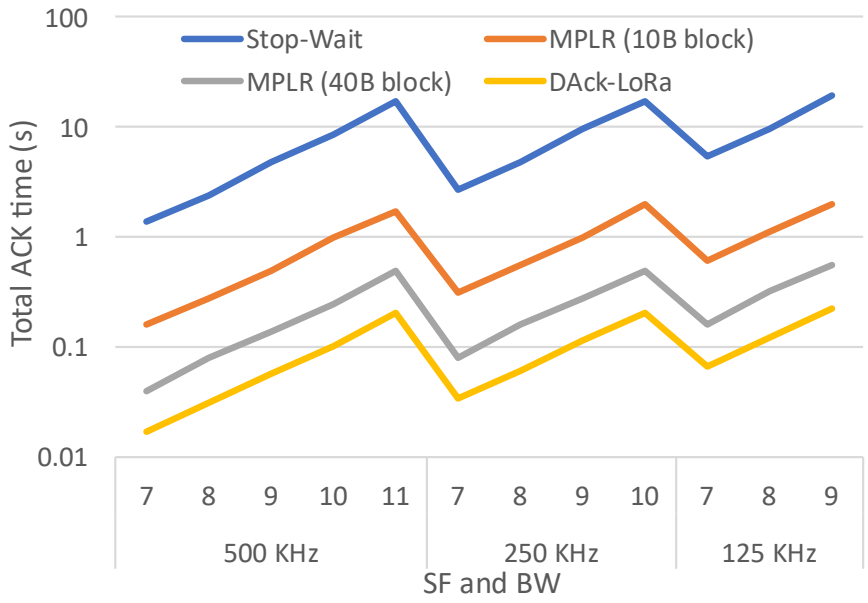

Figure 5-5. Performance comparison of DACK-LoRa with MPLR and Stop-Wait protocols in terms of total ACK time.

5.6 Conclusion

The proposed DACK-LoRa is evaluated using the application-specific grayscale data without any compression to observe the packet loss in detail. Reconstruction of the JPG image with a minimum packet loss was not possible. However, the use of header less JPG images as used in CIRA can improve the goodput of DACK-LoRa by reducing the total image size. An application like SoilCam requires offline image data at one to three days intervals. Practical data and mathematical calculations show that complete SoilCam data can be sent within 13 to 20 minutes, which may reduce the cost involving the manual data collection process.

5.7 References

1. S.Z. Khan, Y. Le Moullec, and M.M. Alam, “An NB-IoT-Based Edge-of-Things Framework for Energy-Efficient Image Transfer” In *MDPI* Sensors, vol. *21*, no., pp. 5929-5961, 2021, doi: 10.3390/s21175929.
2. R. Mugo, R. Waswa, J.W. Nyaga, A. Ndubi, E.C. Adams, and A.I. Flores-Anderson, “Quantifying Land Use Land Cover Changes in the Lake Victoria Basin Using Satellite Remote Sensing: The Trends and Drivers between 1985 and 2014,” In *MDPI Remote Sens.*, vol.12, no., pp. 2829-2861, 2020, doi: 10.3390/rs12172829.
3. C. Pham, "Low-cost Wireless Image Sensor Networks for visual surveillance and intrusion detection applications," 2015 IEEE 12th International Conference on Networking, Sensing and Control, 2015, pp. 376-381, doi: 10.1109/ICNSC.2015.7116066.
4. D. M. Hernandez, G. Peralta, L. Manero, R. Gomez, J. Bilbao and C. Zubia, "Energy and coverage study of LPWAN schemes for Industry 4.0," 2017 IEEE International Workshop of Electronics, Control, Measurement, Signals and their Application to Mechatronics (ECMSM), 2017, pp. 1-6, doi: 10.1109/ECMSM.2017.7945893.
5. G. Callebaut and L. Van der Perre, "Characterization of LoRa Point-to-Point Path Loss: Measurement Campaigns and Modeling Considering Censored Data," in *IEEE Internet of Things Journal,* vol. 7, no. 3, pp. 1910-1918, March 2020, doi: 10.1109/JIOT.2019.2953804.
6. G. Rahman, H. Sohag, R. Chowdhury, K.A. Wahid, A. Dinh, M. Arcand, and S. Vail, “SoilCam: A Fully Automated Minirhizotron using Multispectral Imaging for Root Activity Monitoring,” In *MDPI* Sensors*, vol.20*, no., pp. 787-810, 2020, doi: 10.3390/s20030787.
7. A.H. Jebril, A. Sali, A. Ismail, M.F.A. Rasid, “Overcoming Limitations of LoRa Physical Layer in Image Transmission,” In *MDPI Sensors*, vol. 18, no., pp. 3257-3278, 2018, doi: 10.3390/s18103257.
8. R. Kirichek, VD. Pham, A. Kolechkin, M. Al-Bahri, A. Paramonov, “Transfer of Multimedia Data via LoRa,” Conference on IoT. Springer, 2017, pp. 708-720, doi:10.1007/978-3-319-67380-6_67.
9. G. M. E. Rahman and K. A. Wahid, "LDCA: Lightweight Dynamic Clustering Algorithm for IoT-Connected Wide-Area WSN and Mobile Data Sink Using LoRa," in *IEEE Internet of Things Journal*, vol. 9, no. 2, pp. 1313-1325, 15 Jan.15, 2022, doi: 10.1109/JIOT.2021.3079096.

10. S. García, D.F. Larios, J. Barbancho, E. Personal, J.M. Mora-Merchán, C. León, “Heterogeneous LoRa-Based Wireless Multimedia Sensor Network Multiprocessor Platform for Environmental Monitoring,” in *MDPI Sensors*, vol. 19, no. 16, pp. 3446-1466, 2019, doi:10.3390/s19163446.
11. Semtech SX1276/77/78/79, Accessed: Jan. 10, 2022. [Online]. Available: https://semtech.my.salesforce.com/sfc/p/#E0000000JelG/a/2R0000001Rc1/QnUuV9TviODKUgt_rpBlPz.EZA_PNK7Rpi8HA5..Sbo
12. L. Beltramelli, A. Mahmood, P. Österberg and M. Gidlund, "LoRa Beyond ALOHA: An Investigation of Alternative Random-Access Protocols," in *IEEE Transactions on Industrial Informatics*, vol. 17, no. 5, pp. 3544-3554, May 2021, doi: 10.1109/TII.2020.2977046.
13. C. Wei, P. Su, and S. Chen, "Comparison of the LoRa Image Transmission Efficiency Based on Different Encoding Methods," In *International Journal of Information and Electronics Engineering,* vol. 10, no. 1, pp. 1-4, 2020, doi: 10.18178/IJIEE.2020.10.1.712.
14. C. Pham, "Robust CSMA for long-range LoRa transmissions with image sensing devices," 2018 Wireless Days, 2018, pp. 116-122, doi: 10.1109/WD.2018.8361706.
15. J. Y. Q. Zhang, B. L. Yeung, J. C. Y. Wong, R. C. C. Cheung and A. H. F. Lam, "LoRaWAN-based Camera with (CIRA) Compression and Image Recovery Algorithm," 2021 IEEE 7th World Forum on Internet of Things (WF-IoT), 2021, pp. 136-141, doi: 10.1109/WF-IoT51360.2021.9595674.
16. M. Ji, J. Yoon, J. Choo, M. Jang and A. Smith, "LoRa-based Visual Monitoring Scheme for Agriculture IoT," 2019 IEEE Sensors Applications Symposium (SAS), 2019, pp. 1-6, doi: 10.1109/SAS.2019.8706100.
17. C. Wei, S. Chen and P. Su, "Image Transmission Using LoRa Technology with Various Spreading Factors," 2019 2nd World Symposium on Communication Engineering (WSCE), 2019, pp. 48-52, doi: 10.1109/WSCE49000.2019.9041044.
18. C. Wei, J. Huang, C. Chang, and K. Chang, "The Development of LoRa Image Transmission Based on Time Division Multiplexing," 2020 International Symposium on Computer, Consumer and Control (IS3C), 2020, pp. 323-326, doi: 10.1109/IS3C50286.2020.00090.
19. T. Chen, D. Eager and D. Makaroff, "Efficient Image Transmission Using LoRa Technology In Agricultural Monitoring IoT Systems," International Conference on IoT, 2019, pp. 937-944, doi: 10.1109/iThings/GreenCom/ CPSCom/SmartData.2019.00166.

6. Conclusion and Future Direction

6.1 Summary and conclusion

This research shows that LoRa may not be suitable for wide-area and high-density WSNs needing a higher data rate. WSN using LoRa physical layer can increase the network coverage by applying a LoRa-specific clustering algorithm and multi-hop data transmission protocol. Higher data rate and mobility are also required for some wide-area WSN applications using LoRa, which are yet to be addressed. Present WSN protocols and clustering algorithms are intended for short-range wireless technology with static SNs. The clustering and routing algorithms require high processing resources, energy and are mostly offline, which is better suitable for a heterogeneous WSN. However, heterogeneous WSNs may require extra resources and energy to manage the network for a wide-area and densely populated WSN with mobility. Therefore, this research focused on the lightweight clustering algorithms, using efficient data transmission protocol for the homogenous WSN with mobility utilizing the long-range capability of LoRa. The present data transmission protocol used for LoRa is unsuitable for transmitting data from the clusters to the DS over a multi-hop data link due to its long TOA compared to other wireless technologies like Zigbee. Therefore, this research also focuses on lightweight data transmission protocol for LoRa to support the multi-hop WSN for wider coverage.

The proposed LDAP focuses on efficient data transmission of the wide-area WSN introducing mobile DS in a LoRa network. It considered direct and single-hop data transfer using homogenous SNs to maximize the coverage area for a mobile DS mounted on the UAV by minimizing the data acquisition time. The SN used in this protocol can act as a SN and a repeater node (RN) dynamically as requested by the DS to extend the coverage area. The mathematical model can dimension the WSN size and determine the energy efficiency and coverage area. The energy model shows that the energy efficiency of an LDAP-based WSN is highly dependent on the amount of data transmission through the RN. Energy efficiency can be increased by reducing the data transmission through RN; however, it may reduce the coverage area. The mobility model shows that a mobile DS mounted on a Zypher 7 UAV can accumulate data from at least 147 SNs. Therefore, a minimum distance of 3.5km between the SNs can cover up to 128 km in the direction of the UAV movement and 15 km laterally at 50% data transmission using the RN. Besides the energy efficiency and WSN coverage, the proposed LDAP can reduce the requirement of DS by up to 81%. It can facilitate remote data acquisition without satellite-based communication and reduce costs. However, using single-hop data transmission, a mobile DS may require travelling multiple paths to cover more area laterally. Only six mobile DS can acquire data from a WSN with 1000 SNs covering an area of 12,800km^2 (128 km x 100 km) utilizing the LDAP and proper path planning for the DS.

The proposed LDCA focuses on the mobility of the SNs in a densely populated, wide-area WSN. Unlike the static and offline clustering algorithms, it performs clustering in real time to deal with the ad-hoc nature of a wide-area WSN along with mobility. This clustering algorithm is light enough to be processed using the resource constrained SNs and the DS. The LDCA uses RSSI and SNR of the LoRa link between the SNs and DS along with the residual energy of the SNs to include the environmental effect on the RF channels dynamically and avoid the complicated distance calculation. It uses the LDAP as a single-hop data transmission protocol between the SNs and DS through the CH. This research derives the mathematical models to dimension the WSN capacity and timing model to determine the WSN coverage. The mathematical models can also calculate the clustering algorithm's resource requirement and energy efficiency. The field trial validates using RSSI and SNR as clustering parameters that can be used without calculating the distance between the SNs and DS. Experimental data is used to calculate the energy requirement for the clustering algorithms and hence the clustering efficiency of the proposed LDCA. It shows that the energy efficiency of LDCA is highly dependent on the LoRa TOA and the total clustering time. On the other hand, total clustering time highly depends on the number of candidate CH. Therefore, the clustering efficiency needs to be optimized using the presented mathematical models. It achieves up to 99.59% clustering efficiency and 98.17% for a densely populated WSN. The cluster size calculated is 64 SNs using single-hop routing to minimize the clustering energy and time requirements. This research shows that the proposed LDCA and mobile DS can provide wider coverage and network density using a smaller number of hops and DS (or base station). Using LDCA, two mobile DS can acquire data from a WSN of 600 SNs, forming only two clusters dynamically, compared to 60 clusters required for a WSN with short-range wireless technology like Zigbee and at least 6 clusters using LoRa. Hence, LDCA is better suited for a dynamic WSN with mobile SNs. Similarly, LDCA can provide three times wider coverage using the same number of mobile DS compared to the WSN with static DS.

Multi-hop routing can improve the WSN coverage and capacity. Besides single hop routing and clustering using mobile DS, this research proposes a synchronization algorithm for parallel data transmission using multiple LoRa channels to achieve a higher data rate. A higher data rate may facilitate multi-hop routing in the WSN. This research investigates the quasi-orthogonality features of LoRa and evaluates the possibility of parallel data transmission between two nodes in terms of interference and data rate. Although LoRa is orthogonal in the RF channels, experimental data shows significant co-channel interference, which may not be suitable for long-range parallel data transmission. On the other hand, parallel data transmission using different SF can be used due to LoRa’s quasi-orthogonality nature in SF. This parallel data transmission using different SFs in the same RF channel requires proper synchronization to maintain SINR for a long-range LoRa link. The proposed LSAQ utilizes the existing LoRa modems without changing the modulation technique for easy implementation and to maintain compatibility with the existing LoRa network. However, single-chip modems with parallel

transmission capability can be developed to facilitate long-range data transmission between the CHs and the DS using LSAQ in a multi-hop WSN. According to the mathematical models of LSAQ, the selection of SF for parallel transmission depends on the link range, and the data rate can be improved from 71% to 83% between two sets of consecutive SFs. An optimized selection of SFs can increase the WSN capacity by 10% in a densely populated network and up to 44% for a less populated WSN that requires wider coverage using multiple clusters and hops.

Continuous data transmission using LoRa may suffer inferior goodput due to its small packet size. This is further worsened by frequent ACK messages for long-range links with low RSSI or SNR. This research focuses on the transmission of dynamic ACK messages after receiving a data block of multiple packets that may have missing data to improve the overall goodput. The proposed DACK protocol shows that the goodput highly depends on the number of packets sent in every block. The ACK message consists of a bitmap presentation of the missing data packets. The overhead of the ACK message also contributes to the overall goodput. Therefore, an optimum block size must be determined to maximize the goodput for a specific data volume. DACK and other ACK messaging schemes are evaluated for different data volumes and different block sizes. DACK shows significant improvement in goodput compared to Stop-Wait and MPLR for larger block sizes.

6.2 Future research direction

The proposed protocols and algorithms focused on LoRa WSN coverage, capacity, mobility, and data rate without changing the LoRa physical layer or modulation scheme. The future scope of research and improvement are described below.

Energy efficiency and network coverage of the WSN with mobile DS highly depend on efficient data acquisition at the minimum travel time. Traditional offline path planning may not support mobility in the WSN. Real-time lightweight path planning for the LDAP can further increase the network capacity and coverage area of a LoRa WSN, introducing mobility for the SNs. Dynamic data buffering can reduce the data acquisition cycle hence increasing network lifetime for the WSN, which can further increase WSN coverage by reducing the travel time of the mobile DS. The use of multi-hop data transfer with mobile DS can increase the WSN lateral coverage area and the lifetime of the overall WSN. A real-time multi-hop routing algorithm and DS path planning can be developed to accommodate data efficiently.

The proposed LDCA can further be improved by utilizing more than two dynamic clusters simultaneously. An optimization algorithm can be introduced to reduce data transmission during the clustering phase. The use of multi-hop data transmission during the clustering and transmission phases may reduce clustering time, data acquisition time and travel time for the

mobile DS. The performance of LDCA highly depends on proper stop points to reduce overlapping SNs among the clusters. The offline stop points determination algorithm is unsuitable due to the mobility of the SNs. Lightweight real-time stop points determination algorithm can be introduced. LDCA performs the clustering phase before every data transmission phase to accommodate most of the mobile SNs. Artificial Intelligence (AI) based reclustering algorithm can reduce the number of clustering phases, increasing WSN lifetime. The SNs and the DS perform LDCA without involving the higher control layers to reduce control data flow over the LoRa links or use gateways in a WSN with mobility. WSN lifetime can be improved by reducing clustering overload. WSN virtualization can be introduced along with LDCA to further reduce clustering control data flow in the WSN, where the SNs may perform the clustering without involving the DS. This will further reduce the travel requirement of the mobile DS and increase the mobility of the SNs.

Performance analysis of various dynamic clustering algorithms is mainly done using mathematical models. However, the performance matrices used for the static WSNs may not be suitable for the WSNs with mobility. Existing simulation tools such as NS-3 and Cupcarbon that supports mobility can be used to evaluate clustering algorithms with mobility.

Synchronous transmission using different SFs used in LSAQ can be extended among the nodes or end devices for different LCs using different sets of SFs to accommodate more nodes in a WSN. Similarly, synchronous SF-based clustering can be used instead of asynchronous SF-based clustering algorithms. AI-based dynamic SF selection for LSAQ can be used to increase channel utilization for the densely populated WSN without increasing base stations. The performance of DACK-LoRa can be further improved by introducing efficient image data segmentation and headless packetization.

APPENDIX

Publications:

1. G.M.E. Rahman and K. A. Wahid, "LDAP: Lightweight Dynamic Auto-Reconfigurable Protocol in an IoT-Enabled WSN for Wide-Area Remote Monitoring." Remote Sens., vol. 12, no. 19, pp. 3131-3151, Sep. 2020, doi: 10.3390/rs12193131.
2. G.M.E. Rahman and K. A. Wahid, "LDCA: Lightweight Dynamic Clustering Algorithm for IoT-Connected Wide-Area WSN and Mobile Data Sink Using LoRa," in IEEE Internet of Things Journal, vol. 9, no. 2, pp. 1313-1325, 15 Jan.15, 2022, doi: 10.1109/JIOT.2021.3079096.
3. G.M.E. Rahman and K. A. Wahid, "LSAQ-LoRa: Lightweight Synchronization Algorithm for Quasi-orthogonal LoRa Channels in Wide-area Wireless Sensor Network," submitted and under review at the IEEE Transactions on Industrial Informatics.

Other publications:

1. G.M.E. Rahman, R. I. Chowdhury, A. Dinh and K. A. Wahid, "A Smart Sensor Node with Smartphone based IoMT," 2019 IEEE International Conference on Consumer Electronics - Asia (ICCE-Asia), 2019, pp. 92-95, doi: 10.1109/ICCE-Asia46551.2019.8942205.
2. G. Rahman, H. Sohag, R. Chowdhury, K.A. Wahid, A. Dinh, M. Arcand, S. Vail, "SoilCam: A Fully Automated Minirhizotron using Multispectral Imaging for Root Activity Monitoring" in *MDPI Sensors*, Vol. 20, pp. 787, 2020, doi:10.3390/s20030787
3. G.M.E. Rahman, K.A. Wahid, and A. Dinh, "IoT enabled Low power and Wide range WSN platform for environment monitoring application", 2020 IEEE Region 10 Symposium (TENSYMP), Dhaka, Bangladesh, 2020, pp. 908-911, doi: 10.1109/TENSYMP50017.2020.9230959.
4. S. S. Vedaei, A. Fotovvat, G.M.E. Rahman, K.A. Wahid, P. Babyn, H.R.Marateb, M.Mansourian, and R. Sami, "COVID-SAFE: An IoT-Based System for Automated Health Monitoring and Surveillance in Post-Pandemic Life," in *IEEE Access*, vol. 8, pp. 188538-188551, 2020, doi: 10.1109/ACCESS.2020.3030194.
5. A. Fotovvat, G.M.E. Rahman, S. S. Vedaei and K. A. Wahid, "Comparative Performance Analysis of Lightweight Cryptography Algorithms for IoT Sensor Nodes," in *IEEE Internet of Things Journal*, vol. 8, no. 10, pp. 8279-8290, 2021, doi: 10.1109/JIOT.2020.3044526.
6. S. Mushran, F. Akther, G.M.E. Rahman, M.M. Elahi, R. Mostafa, and K.A. Wahid, "Dimensioning of Wide-Area Alternate Wetting and Drying (AWD) System for IoT-Based Automation" *MDPI Sensors*, vol. 18, pp. 6040, 2021, doi:10.3390/s21186040.